medRxiv preprint doi: https://doi.org/10.1101/2021.11.08.21266020; this version posted July 14, 2022. The copyright holder for this preprint (which was not certified by peer review) is the author/funder, who has granted medRxiv a license to display the preprint in perpetuity. It is made available under a CC-BY-NC-ND 4.0 International license .

Article Title

Sleep EEG in young people with 22q11.2 deletion syndrome: a cross-sectional study of slow-waves, spindles and correlations with memory and neurodevelopmental symptoms

Authors

Donnelly NA[1,2, *]; Bartsch U[3,4, *, #]; Moulding HA[5]; Eaton C[5]; Marston H[4, $]; Hall JE[5]; Hall J[5]; Owen MJ[5]; van den Bree MBM[5]†; Jones MW[3]†

*These authors contributed equally

†These authors contributed equally

Affiliations:

[1] Centre for Academic Mental Health, Population Health Sciences, University of Bristol, Bristol, UK

[2] Avon and Wiltshire Partnership NHS Mental Health Trust, UK

[3] School of Physiology, Pharmacology & Neuroscience, University of Bristol, Bristol, UK

[4] Translational Neuroscience, Eli Lilly & Co Ltd UK, Erl Wood Manor, Windlesham, UK

[5] Medical Research Council Centre for Neuropsychiatric Genetics and Genomics, Division of Psychological Medicine and Clinical Neurosciences, Cardiff University School of Medicine, Cardiff, UK

current address: UK DRI Care Research & Technology at Imperial College London and the University of Surrey, Surrey Sleep Research Centre, University of Surrey, Clinical Research Building, Egerton Road, Guildford, Surrey, GU2 7XP

$ current address: Böhringer Ingelheim Pharma GmbH & Co. KG, Biberach, Germany

Correspondence:

nick.donnelly@bristol.ac.uk

NOTE: This preprint reports new research that has not been certified by peer review and should not be used to guide clinical practice.

medRxiv preprint doi: https://doi.org/10.1101/2021.11.08.21266020; this version posted July 14, 2022. The copyright holder for this preprint (which was not certified by peer review) is the author/funder, who has granted medRxiv a license to display the preprint in perpetuity. It is made available under a CC-BY-NC-ND 4.0 International license .

Abstract

Background

Young people living with 22q11.2 Deletion Syndrome (22q11.2DS) are at increased risk of schizophrenia, intellectual disability, attention-deficit hyperactivity disorder (ADHD) and autism spectrum disorder (ASD). In common with these conditions, 22q11.2DS is also associated with sleep problems. We investigated whether abnormal sleep or sleep-dependent network activity in 22q11.2DS reflects convergent, early signatures of neural circuit disruption also evident in associated neurodevelopmental conditions.

Methods

In a cross-sectional design, we recorded high-density sleep EEG in young people (6-20 years) with 22q11.2DS (n=28) and their unaffected siblings (n=17), quantifying associations between sleep architecture, EEG oscillations (spindles and slow waves) and psychiatric symptoms. We also measured performance on a memory task before and after sleep.

Results

22q11.2DS was associated with significant alterations in sleep architecture, including a greater proportion of N3 sleep and lower proportions of N1 and REM sleep than in siblings. During sleep, deletion carriers showed broadband increases in EEG power with increased slow-wave and spindle amplitudes, increased spindle frequency and density, and stronger coupling between spindles and slow-waves. Spindle and slow-wave amplitudes correlated positively with overnight memory in controls, but negatively in 22q11.2DS. Mediation analyses indicated that genotype effects on anxiety, ADHD and ASD were partially mediated by sleep EEG measures.

Conclusions

This study provides a detailed description of sleep neurophysiology in 22q11.2DS, highlighting alterations in EEG signatures of sleep which have been previously linked to neurodevelopment, some of which were associated with psychiatric symptoms. Sleep EEG features may therefore reflect delayed or compromised neurodevelopmental processes in 22q11.2DS, which could inform

medRxiv preprint doi: https://doi.org/10.1101/2021.11.08.21266020; this version posted July 14, 2022. The copyright holder for this preprint (which was not certified by peer review) is the author/funder, who has granted medRxiv a license to display the preprint in perpetuity. It is made available under a CC-BY-NC-ND 4.0 International license .

our understanding of the neurobiology of this condition and be biomarkers for neuropsychiatric disorders.

Funding

This research was funded by a Lilly Innovation Fellowship Award (UB), the National Institute of Mental Health (NIMH 5UO1MH101724; MvdB), a Wellcome Trust Institutional Strategic Support Fund (ISSF) award (MvdB), the Waterloo Foundation (918-1234; MvdB), the Baily Thomas Charitable Fund (2315/1; MvdB), MRC grant Intellectual Disability and Mental Health: Assessing Genomic Impact on Neurodevelopment (IMAGINE) (MR/L011166/1; JH, MvdB and MO), MRC grant Intellectual Disability and Mental Health: Assessing Genomic Impact on Neurodevelopment 2 (IMAGINE-2) (MR/T033045/1; MvdB, JH and MO); Wellcome Trust Strategic Award 'Defining Endophenotypes From Integrated Neurosciences' Wellcome Trust (100202/Z/12/Z MO, JH).

NAD was supported by a National Institute for Health Research Academic Clinical Fellowship in Mental Health and MWJ by a Wellcome Trust Senior Research Fellowship in Basic Biomedical Science (202810/Z/16/Z). CE and HAM were supported by Medical Research Council Doctoral Training Grants (C.B.E. 1644194, H.A.M MR/K501347/1). HMM and UB were employed by Eli Lilly & Co during the study; HMM is currently an employee of Boehringer Ingelheim Pharma GmbH & Co KG.

The views and opinions expressed are those of the author(s), and not necessarily those of the NHS, the NIHR or the Department of Health funders.

medRxiv preprint doi: https://doi.org/10.1101/2021.11.08.21266020; this version posted July 14, 2022. The copyright holder for this preprint (which was not certified by peer review) is the author/funder, who has granted medRxiv a license to display the preprint in perpetuity. It is made available under a CC-BY-NC-ND 4.0 International license .

Introduction

22q11.2 microdeletion syndrome (22q11.2DS) is caused by a deletion spanning a ~2.6 megabase region on the long arm of chromosome 22. It occurs in ~1:3,000-4,000 births and is associated with increased risk of neuropsychiatric conditions including intellectual disability, autism spectrum disorder (ASD), attention-deficit hyperactivity disorder (ADHD), and epileptic seizures. (Cunningham et al., 2018; Eaton et al., 2019; Moulding et al., 2020; Niarchou et al., 2014). 22q11.2DS is also considered to be one of the largest biological risk factors for schizophrenia, with up to 41% of adults with 22q11.2DS having psychotic disorders (Karayiorgou et al., 1995; Monks et al., 2014; Schneider et al., 2014). However, the neurobiological mechanisms underlying psychiatric symptoms in 22q11.2DS remain unclear. Deep phenotyping of young people with 22q11.2DS may allow their elucidation and therefore enable early detection and/or intervention.

The electroencephalogram (EEG) recorded during non-rapid eye movement (NREM) sleep features spindle and slow-wave (SW) oscillations: highly conserved and non-invasively measurable signatures of neuronal network activity generated by corticothalamic circuits (Adamantidis et al., 2019). The properties and co-ordination of these oscillations are candidate biomarkers of brain dysfunction in neuropsychiatric disorders (Ferrarelli & Tononi, 2017; Gardner et al., 2014; Manoach et al., 2016).

Sleep EEG features are altered across many neurodevelopmental disorders, including schizophrenia, including first episode psychosis, as well as first degree relatives (Chouinard et al., 2004; Cohrs, 2008; Ferrarelli et al., 2007, 2010; Göder et al., 2015; Bartsch et al., 2019; Demanuele et al., 2017; Wamsley et al., 2012; Manoach & Stickgold, 2019; Castelnovo et al., 2017; Keshavan et al., 1998); ADHD (Cortese et al., 2009; Gorgoni et al., 2020; Lunsford-Avery et al., 2016), ASD (although findings have been inconsistent (Gorgoni et al., 2020; Lehoux et al., 2019)) and a range of rare genetic conditions, including Down syndrome, Fragile-X syndrome and Angelman syndrome (Angriman et al., 2015).

We have recently shown that the majority of young people with 22q11.2DS have sleep problems, particularly insomnia and sleep fragmentation, that associate with psychopathology (Moulding et

medRxiv preprint doi: https://doi.org/10.1101/2021.11.08.21266020; this version posted July 14, 2022. The copyright holder for this preprint (which was not certified by peer review) is the author/funder, who has granted medRxiv a license to display the preprint in perpetuity. It is made available under a CC-BY-NC-ND 4.0 International license .

al., 2020). However, this analysis was based on parental report; the neurophysiological properties of sleep in this condition remain unexplored. Furthermore, it has been demonstrated that neuroanatomical features associated with psychopathology in 22q11.2DS significantly converge with those in idiopathic psychiatric disorders (Ching et al., 2020). Therefore studying the sleep EEG in 22q11.2DS may produce insights that can be generalized to broader populations, affording a unique opportunity to clarify the relationship between sleep EEG and psychiatric risk.

We hypothesized that 22q11.2DS would be associated with alterations in sleep EEG features relative to controls, including altered spindle and SW events, and aberrant spindle-SW coupling. We investigated these hypotheses in a cross-sectional study of young people with 22q11.2DS and unaffected sibling controls, combining detailed neuropsychiatric assessments with overnight high-density EEG recordings and a sleep-dependent memory task.

medRxiv preprint doi: https://doi.org/10.1101/2021.11.08.21266020; this version posted July 14, 2022. The copyright holder for this preprint (which was not certified by peer review) is the author/funder, who has granted medRxiv a license to display the preprint in perpetuity. It is made available under a CC-BY-NC-ND 4.0 International license .

Results

Psychopathology and sleep architecture in 22q11.2 DS

Young people living with 22q11.2DS (n = 28) and healthy control siblings (n = 17) completed semi-structured research diagnostic interviews to quantify Full Spectrum Intelligence Quotient (FSIQ), neuropsychiatric symptoms and self- and carer-reported sleep behavioral problems (**Table 1 and Figure 1 – Supplement 1**). Participants with 22q11.2DS had a lower mean FSIQ (reported as Odds Ratio (OR) or group difference (GD) with [95% confidence interval]): FSIQ, GD = -28.70 [-40.48, -16.92], $p < 0.001$), and higher incidence of anxiety (OR = 3.10 [1.93, 4.99], $p < 0.001$), ADHD (OR = 9.46 [5.12 – 17.48], $p < 0.001$) and ASD symptoms (Odds Ratio [OR] = 7.46 [4.76, 11.70], $p < 0.001$), but did not show significantly more psychotic experiences than controls (OR = 4.05 [0.67, 43.67], p = 0.096). Details of the specific psychotic symptoms reported are shown in **Table 2**.

Participants with 22q11.2DS also experienced more sleep problems (OR = 6.27 [2.12, 18.56], p = 0.001); more sleep problems were associated with younger age, 22q11.2DS genotype and anxiety symptoms but not with gender, family income, psychotic experiences, ADHD or ASD symptoms (**Table 3**).

Participants were asked to perform a delayed recall 2D object location task (**Figure 1A**) to test sleep-dependent memory consolidation. Of 42 participants who engaged in the task, those with 22q11.2DS needed more training cycles to reach a 30% performance criterion (Hazard Ratio [95%CI] = 0.328 [0.151, 0.714], p = 0.005, **Figure 1B, Table 4)** and made fewer correct responses in the morning test session (OR = 0.631 [0.45, 0.885], p = 0.008, **Figure 1C, Table 4**). However, there was no difference between groups in overnight change in correct responses between the evening learning session and the morning test session (**Figure 1D, Table 4**). Additionally, there was no association between task performance or accuracy in the morning test session and any psychiatric measure, or FSIQ (**Table 4**).

medRxiv preprint doi: https://doi.org/10.1101/2021.11.08.21266020; this version posted July 14, 2022. The copyright holder for this preprint (which was not certified by peer review) is the author/funder, who has granted medRxiv a license to display the preprint in perpetuity. It is made available under a CC-BY-NC-ND 4.0 International license .

All participants completed one night of full polysomnography with 64-channel high density EEG recorded at their home. After expert sleep scoring, we compared sleep architecture between 22q11.2DS and controls (**Figure 1E** and **Table 1)**. There was no difference in gross measures of sleep such as Total Sleep Time and Sleep Efficiency, suggesting that our EEG recordings did not disrupt sleep differently between groups. However, 22q11.2DS was associated with a reduced percentage of N1 (GD = -2.71 [-5.05, -0.36], p = 0.044) and REM sleep (GD = -4.20 [-7.10, -1.30], p = 0.012) while the percentage of N3 sleep was increased (GD = 5.47 [1.98, 8.96], p = 0.009). There were no significant relationships between sleep architecture metrics and psychiatric measures or FSIQ in 22q11.2DS (**Table 5**).

medRxiv preprint doi: https://doi.org/10.1101/2021.11.08.21266020; this version posted July 14, 2022. The copyright holder for this preprint (which was not certified by peer review) is the author/funder, who has granted medRxiv a license to display the preprint in perpetuity. It is made available under a CC-BY-NC-ND 4.0 International license .

Figure 1: Memory task performance and sleep architecture features of 22q11.2DS

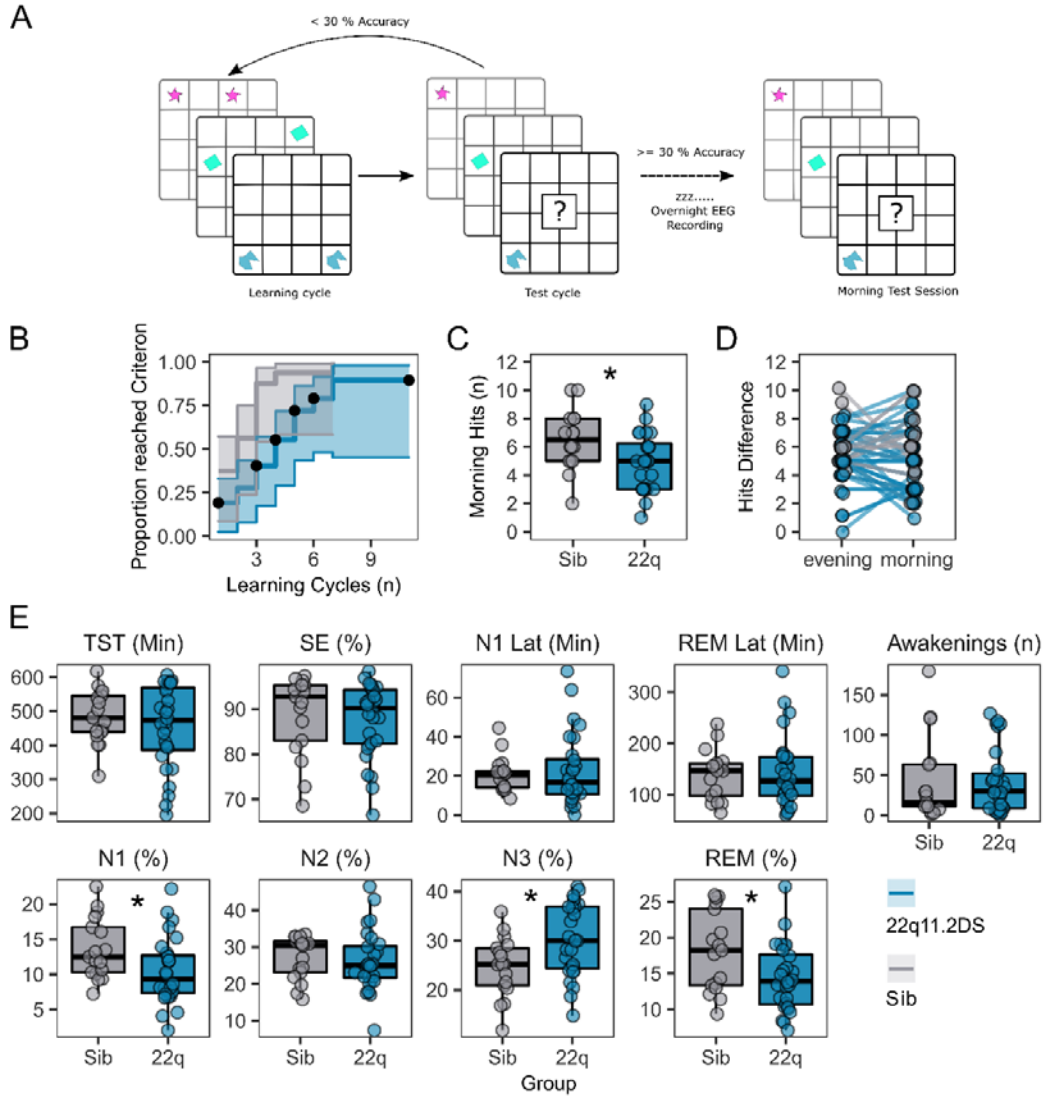

Figure 1 Legend:

A: Schematic of the 2D object location task. The evening before sleep EEG recordings, participants first were sequentially presented with pairs of images on a 5 x 6 grid. In a subsequent test cycle, they were presented with one image of the pair, and were required to select the grid location of the other half of the pair. If the participant did not achieve > 30% accuracy, they would have another learning cycle. In the morning a single test cycle was undertaken.

B: Plot of performance in acquiring the 2D object location task, showing the proportion of participants in each group reaching the 30% performance criterion after each learning cycle.

medRxiv preprint doi: https://doi.org/10.1101/2021.11.08.21266020; this version posted July 14, 2022. The copyright holder for this preprint (which was not certified by peer review) is the author/funder, who has granted medRxiv a license to display the preprint in perpetuity. It is made available under a CC-BY-NC-ND 4.0 International license .

Shaded areas represent the 95% confidence interval. Black dots show when participants were right-censored due to stopping the task prior to reaching the 30% criterion.

*C: Box plots of performance in the morning test session, where participants had one cycle of the memory task. Number of correct responses is out of a possible 15. Asterix indicate the group difference is statistically significant, generalised linear mixed model, $p < 0.05$ (see **Table 2** for full statistics).*

D: Plots of change in performance between the final evening learning session and the morning test session. Each participant is represented as a point, with a line connecting their evening and morning performance. Points have been slightly jittered to illustrate where multiple participants had the same score.

*E: Box and whisker plots showing sleep architecture features: Total sleep time (TST) in minutes, Sleep efficiency (SE) as a percentage, Latency to N1 sleep (minutes), Latency to first REM sleep (minutes), Number of awakenings after sleep onset (n), Percentage of hypnogram in N1 sleep, Percentage of hypnogram in N2 sleep, Percentage of hypnogram in N3 sleep, and Percentage of hypnogram in REM sleep. Asterixes indicate the group difference is statistically significant, linear mixed model, $p < 0.05$ (see **Table 1** for full statistics). Boxes represent the median and IQR, with the whiskers representing 1.5 x the IQR. Individual participant data are shown as individual points. Points have been slightly jittered in the x direction only to illustrate where multiple participants had similar results.*

medRxiv preprint doi: https://doi.org/10.1101/2021.11.08.21266020; this version posted July 14, 2022. The copyright holder for this preprint (which was not certified by peer review) is the author/funder, who has granted medRxiv a license to display the preprint in perpetuity. It is made available under a CC-BY-NC-ND 4.0 International license .

Figure 1: Supplement 1

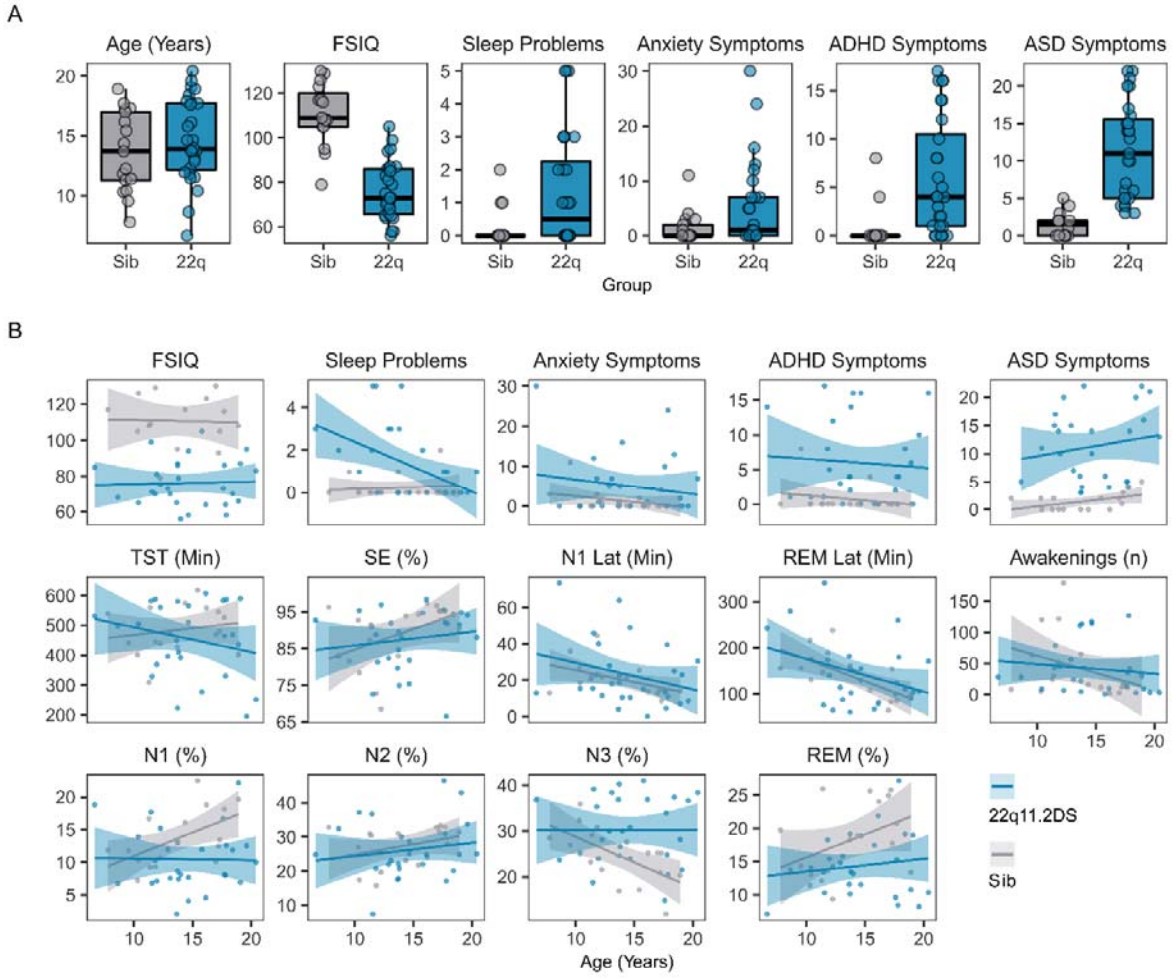

Figure 1 – Supplement 1 Legend:

A. Boxplots and overplotted individual data for participant age, Full Spectrum IQ (FSIQ) and psychiatric symptoms. ADHD = Attention Deficit Hyperactivity Disorder symptoms, from the CAPA interview; ASD = Autism Spectrum Disorder symptoms, from the SCQ interview. Boxes represent the median and IQR, with the whiskers representing 1.5 x the IQR. Individual participant data are shown as individual points. Points have been slightly jittered in the x direction only to illustrate where multiple participants had similar results.

B. Line plots and overplotted individual data for FSIQ, psychiatric and hypnographic measures, plotted against participant age at the time of EEG. Lines of best fit and 95% confidence intervals are derived from linear models. Acronyms: TST = Total Sleep Time (in minutes); SE = Sleep Efficiency (%); N1 Lat = Latency to reach first N1 sleep epoch, (in

medRxiv preprint doi: https://doi.org/10.1101/2021.11.08.21266020; this version posted July 14, 2022. The copyright holder for this preprint (which was not certified by peer review) is the author/funder, who has granted medRxiv a license to display the preprint in perpetuity. It is made available under a CC-BY-NC-ND 4.0 International license .

minutes); REM Lat = Latency to reach first REM sleep epoch (in minutes); N1 = Percentage of night in N1 sleep; N2 = Percentage of night in N2 sleep; N3 = Percentage of night in N3 sleep; REM = Percentage of night in REM sleep.

medRxiv preprint doi: https://doi.org/10.1101/2021.11.08.21266020; this version posted July 14, 2022. The copyright holder for this preprint (which was not certified by peer review) is the author/funder, who has granted medRxiv a license to display the preprint in perpetuity. It is made available under a CC-BY-NC-ND 4.0 International license .

Table 1: Psychiatric Characteristics and Sleep Architecture

Variable	Group		Type	Statistic (95% CI)	p-value
	22q11.2DS, n = 28[a]	**Sibling Control, n = 17[a]**			
Age @ EEG	14.6 (3.4)	13.7 (3.4)	Group Difference (22q - Sib) [b]	0.897 [-1.219, 3.013]	0.397
Sex			Chi-Squared [c]	0	1
Female	14 (50%)	9 (53%)			
Male	14 (50%)	8 (47%)			
Sleep Problem	1.32 (1.70)	0.24 (0.56)	Odds Ratio [d]	6.269 [2.118, 18.556]	**0.001**
FSIQ	76 (13)	105 (27)	Group Difference (22q - Sib) [e]	-28.696 [-40.478, -16.915]	**<0.001**
missing	0	1			
Anxiety Symptoms	5.0 (7.8)	1.4 (2.8)	Odds Ratio [d]	3.101 [1.929, 4.986]	**<0.001**
ADHD Symptoms	6.0 (6.0)	0.7 (2.1)	Odds Ratio [d]	9.456 [5.117, 17.475]	**<0.001**
ASD Symptoms	11 (6)	1 (2)	Odds Ratio [d]	7.463 [4.762, 11.697]	**<0.001**
missing	1	1			
Psychotic Experiences			Odds Ratio [f]	4.047 [0.698, 43.668]	0.096
No PE	18 (64%)	15 (88%)			
PE	10 (36%)	2 (12%)			
N1 (%)	10.4 (4.7)	13.6 (4.3)	Group Difference (22q - Sib) [e]	-2.707 [-5.05, -0.363]	**0.044**
N2 (%)	26.2 (8.2)	27.1 (5.9)	Group Difference (22q - Sib) [e]	-1.089 [-5.146, 2.967]	0.620
N3 (%)	30 (7)	25 (6)	Group Difference (22q - Sib) [e]	5.473 [1.984, 8.962]	**0.009**
REM (%)	14.4 (4.6)	18.2 (5.6)	Group Difference (22q - Sib) [e]	-4.198 [-7.1, -1.296]	**0.012**
N1 Latency (Minutes)	23 (18)	21 (9)	Group Difference (22q - Sib) [e]	3.486 [-5.538, 12.509]	0.470
REM Latency (Minutes)	143 (69)	140 (49)	Group Difference (22q - Sib) [e]	9.368 [-19.312, 38.048]	0.549
Sleep Efficiency (%)	88 (8)	89 (9)	Group Difference (22q - Sib) [e]	-1.845 [-5.826, 2.136]	0.398
Total Sleep Time (Minutes)	456 (122)	485 (79)	Group Difference (22q - Sib) [e]	-27.206 [-88.489, 34.077]	0.413
Awakenings (n)	42 (52)	42 (40)	Group Difference (22q - Sib) [e]	3.097 [-19.732, 25.925]	0.802

[a] Mean (SD); n (%)

[b] Linear Model

[c] Pearson's Chi Squared Test

[d] Generalised Linear Mixed Model

[e] Linear Mixed Model

[f] Fisher's Exact Test

medRxiv preprint doi: https://doi.org/10.1101/2021.11.08.21266020; this version posted July 14, 2022. The copyright holder for this preprint (which was not certified by peer review) is the author/funder, who has granted medRxiv a license to display the preprint in perpetuity. It is made available under a CC-BY-NC-ND 4.0 International license .

Table 1 Legend: *Demographic, psychiatric and sleep architecture of study participants, comparing participants with 22q11.2DS and unaffected sibling controls. Abbreviations: ADHD (Attention Deficit Hyperactivity Disorder), ASD (Autism Spectrum Disorder), EEG (Electroencephalogram), FSIQ (Full Spectrum IQ), PE (Psychotic Experience), REM (Rapid Eye Movement Sleep), SD (standard deviation)*

medRxiv preprint doi: https://doi.org/10.1101/2021.11.08.21266020; this version posted July 14, 2022. The copyright holder for this preprint (which was not certified by peer review) is the author/funder, who has granted medRxiv a license to display the preprint in perpetuity. It is made available under a CC-BY-NC-ND 4.0 International license .

Table 2: Psychotic Experiences Details

Frequency of Specific Psychotic Experiences		
Type of PE	**22q11.2DS**	**Sibling**
Unusual thought content/Delusional ideas	8	1
Suspiciousness/Persecutory ideas	5	0
Grandiose Ideas	3	2
Perceptual Abnormalities/Hallucinations	8	2
Disorganised communication	4	0
Count of total distinct types of Psychotic Experience		
Number of PE	**22q11.2DS**	**Sibling**
0	18	15
1	2	0
2	2	1
3	2	1
4	4	0

Table 2 Legend: *Details of psychotic experiences reported by participants with 22q11.2DS and unaffected sibling controls in the CAPA interview.*

medRxiv preprint doi: https://doi.org/10.1101/2021.11.08.21266020; this version posted July 14, 2022. The copyright holder for this preprint (which was not certified by peer review) is the author/funder, who has granted medRxiv a license to display the preprint in perpetuity. It is made available under a CC-BY-NC-ND 4.0 International license .

Table 3: CAPA Sleep Problem Adjusted Model

Term		**Odds Ratio**	**p-value**
Genotype	Sibling	*Reference*	
	22q11.2DS	7.867 [1.71, 36.186]	0.008
Gender	Female	*Reference*	
	Male	1.557 [0.486, 4.986]	0.456
Age @ EEG		0.757 [0.622, 0.921]	0.005
Family Income (£PA)	<19999	*Reference*	
	20000-39999	0.38 [0.068, 2.13]	0.271
	40000-59999	0.227 [0.034, 1.505]	0.124
	> 60000	0.297 [0.043, 2.058]	0.219
Anxiety Symptoms[a]		1.117 [1.031, 1.21]	0.007
ADHD Symptoms[a]		1.025 [0.945, 1.112]	0.546
ASD Symptoms[a]		0.964 [0.869, 1.07]	0.488
Psychotic Experiences (PEs)	No PEs	*Reference*	
	PEs	1.369 [0.646, 2.9]	0.413
[a]Continuous variables (no reference category)			

Table 3 Legend: *Associations between CAPA sleep problem count and group, demographic, family and psychiatric covariates, modeled with a generalized linear mixed model, with a poisson distribution and family identity as a random (varying) intercept. Data shown are odds ratios and the 95% confidence interval.*

medRxiv preprint doi: https://doi.org/10.1101/2021.11.08.21266020; this version posted July 14, 2022. The copyright holder for this preprint (which was not certified by peer review) is the author/funder, who has granted medRxiv a license to display the preprint in perpetuity. It is made available under a CC-BY-NC-ND 4.0 International license .

222 Table 4: Memory Task Acquisition and Test Session Performance

Cycles to Criterion Cox Model			
Term		**Hazard Ratio**	**p-value**
Group	Control	*Reference*	
	22q11.2DS	0.328 [0.151, 0.714]	**0.005**
Gender	Female	*Reference*	
	Male	1.389 [0.642, 3.005]	0.400
Age @ EEG		1.029 [0.91, 1.164]	0.650
Cycles to Criterion Cox Model – Adjusted for Psychiatric Measures - 22q11.2DS Only			
Term		**Hazard Ratio**	**p-value**
Gender	Female	*Reference*	
	Male	2.314 [0.542, 9.882]	0.257
Psychotic Experiences	No PEs	*Reference*	
	PEs	0.203 [0.041, 1.012]	0.052
Age @ EEG		1.139 [0.933, 1.390]	0.200
FSIQ		1.026 [0.972, 1.082]	0.355
Anxiety Symptoms		0.992 [0.879, 1.120]	0.900
ADHD Symptoms		0.915 [0.760, 1.102]	0.349
ASD Symptoms		1.027 [0.926, 1.139]	0.616
Morning Accuracy Binomial Model			
Term		**OR**	**p-value**
Group	Control	*Reference*	
	22q11.2DS	0.631 [0.45, 0.885]	**0.008**
Gender	Female	*Reference*	
	Male	1.083 [0.762, 1.538]	0.657
Age @ EEG		0.997 [0.945, 1.051]	0.900
Morning Accuracy Binomial Model - Adjusted for Psychiatric Measures - 22q11.2DS Only			
Term		**OR**	**p-value**
Gender	Female	*Reference*	
	Male	1.623 [0.807, 3.268]	0.174
Psychotic Experiences	No PEs	*Reference*	

medRxiv preprint doi: https://doi.org/10.1101/2021.11.08.21266020; this version posted July 14, 2022. The copyright holder for this preprint (which was not certified by peer review) is the author/funder, who has granted medRxiv a license to display the preprint in perpetuity. It is made available under a CC-BY-NC-ND 4.0 International license .

	PEs	0.556 [0.296, 1.032]	0.065
Age @ EEG		1.012 [0.924, 1.108]	0.803
FSIQ		1.004 [0.982, 1.027]	0.716
Anxiety Symptoms		1.028 [0.969, 1.091]	0.353
ADHD Symptoms		0.973 [0.924, 1.023]	0.288
ASD Symptoms		1.018 [0.973, 1.066]	0.441
Evening – Morning Difference			
Term		**Group Difference**	**p-value**
Group	Control	*Reference*	
	22q11.2DS	-0.424 [-1.923, 1.074]	0.565
Gender	Female	*Reference*	
	Male	-0.5 [-2.036, 1.035]	0.512
Age @ EEG		-0.023 [-0.256, 0.21]	0.839

Table 4 Legend: *Associations between genotype group, sex, age and psychiatric symptoms and performance in the 2D object location task.*

medRxiv preprint doi: https://doi.org/10.1101/2021.11.08.21266020; this version posted July 14, 2022. The copyright holder for this preprint (which was not certified by peer review) is the author/funder, who has granted medRxiv a license to display the preprint in perpetuity. It is made available under a CC-BY-NC-ND 4.0 International license .

227 Table 5: Regression of sleep architecture features in 22q11.2DS

Measure	Variable	Beta (95% CI)	Adjusted P-value (BH)
N1 (%)	Sex	-0.059 [-5.21, 5.092]	0.981
	Age @ EEG	0.101 [-0.808, 1.01]	0.963
	CAPA Sleep Problems	0.003 [-1.632, 1.639]	0.963
	FSIQ	0.135 [-0.044, 0.313]	0.963
	Anxiety Symptoms	0.158 [-0.38, 0.696]	0.963
	ADHD Symptoms	-0.288 [-0.682, 0.105]	0.963
	ASD Symptoms	0.33 [-0.006, 0.666]	0.963
	Psychotic Experiences	-2.758 [-6.921, 1.404]	0.963
N2 (%)	Sex	2.183 [-8.465, 12.831]	0.963
	Age @ EEG	0.097 [-1.782, 1.976]	0.915
	CAPA Sleep Problems	-0.407 [-3.787, 2.974]	0.915
	FSIQ	0.195 [-0.174, 0.564]	0.915
	Anxiety Symptoms	0.254 [-0.859, 1.366]	0.915
	ADHD Symptoms	-0.691 [-1.505, 0.123]	0.915
	ASD Symptoms	0.28 [-0.414, 0.974]	0.915
	Psychotic Experiences	-3.603 [-12.208, 5.002]	0.915
N3 (%)	Sex	-0.849 [-10.545, 8.847]	0.915
	Age @ EEG	0.675 [-1.037, 2.386]	0.915
	CAPA Sleep Problems	1.399 [-1.68, 4.477]	0.997
	FSIQ	-0.062 [-0.398, 0.273]	0.997
	Anxiety Symptoms	-0.43 [-1.442, 0.583]	0.816
	ADHD Symptoms	0.359 [-0.382, 1.1]	0.816
	ASD Symptoms	-0.05 [-0.682, 0.582]	0.997
	Psychotic Experiences	3.852 [-3.984, 11.688]	0.816
REM (%)	Sex	2.516 [-2.744, 7.775]	0.816
	Age @ EEG	-0.682 [-1.61, 0.246]	0.816
	CAPA Sleep Problems	-1.168 [-2.837, 0.502]	0.816
	FSIQ	0.138 [-0.044, 0.32]	0.235
	Anxiety Symptoms	0.732 [0.182, 1.281]	0.421
	ADHD Symptoms	-0.295 [-0.697, 0.107]	0.788
	ASD Symptoms	-0.054 [-0.397, 0.288]	0.235
	Psychotic Experiences	-0.404 [-4.655, 3.847]	0.719
N1 Latency (Minutes)	Sex	-8.061 [-32.213, 16.092]	0.235
	Age @ EEG	-1.225 [-5.487, 3.037]	0.235
	CAPA Sleep Problems	0.484 [-7.184, 8.152]	0.947

medRxiv preprint doi: https://doi.org/10.1101/2021.11.08.21266020; this version posted July 14, 2022. The copyright holder for this preprint (which was not certified by peer review) is the author/funder, who has granted medRxiv a license to display the preprint in perpetuity. It is made available under a CC-BY-NC-ND 4.0 International license .

	FSIQ	-0.237 [-1.073, 0.6]	0.235
	Anxiety Symptoms	-0.62 [-3.143, 1.902]	0.638
	ADHD Symptoms	0.143 [-1.703, 1.989]	0.638
	ASD Symptoms	-0.194 [-1.769, 1.38]	0.638
	Psychotic Experiences	1.894 [-17.625, 21.414]	0.107
REM Latency (Minutes)	Sex	-30.174 [-110.781, 50.433]	0.638
	Age @ EEG	1.517 [-12.707, 15.741]	0.638
	CAPA Sleep Problems	10.761 [-14.83, 36.353]	0.638
	FSIQ	-2.491 [-5.283, 0.301]	0.638
	Anxiety Symptoms	-2.763 [-11.183, 5.656]	0.638
	ADHD Symptoms	3.909 [-2.251, 10.069]	0.254
	ASD Symptoms	-2.116 [-7.371, 3.139]	0.254
	Psychotic Experiences	-14.904 [-80.048, 50.24]	0.363
Sleep Efficiency (%)	Sex	1.813 [-8.177, 11.802]	0.254
	Age @ EEG	-0.099 [-1.862, 1.663]	0.872
	CAPA Sleep Problems	-0.979 [-4.151, 2.192]	0.256
	FSIQ	0.286 [-0.06, 0.632]	0.254
	Anxiety Symptoms	0.587 [-0.456, 1.63]	0.254
	ADHD Symptoms	-0.671 [-1.435, 0.092]	0.256
	ASD Symptoms	0.444 [-0.207, 1.096]	0.483
	Psychotic Experiences	-1.347 [-9.42, 6.726]	0.736
Total Sleep Time (Minutes)	Sex	76.874 [-63.554, 217.302]	0.87
	Age @ EEG	-14.689 [-39.469, 10.092]	0.87
	CAPA Sleep Problems	-13.13 [-57.714, 31.453]	0.87
	FSIQ	0.156 [-4.708, 5.021]	0.736
	Anxiety Symptoms	9.132 [-5.536, 23.799]	0.507
	ADHD Symptoms	-10.338 [-21.069, 0.394]	0.87
	ASD Symptoms	-0.955 [-10.11, 8.2]	0.507
	Psychotic Experiences	-121.448 [-234.938, -7.958]	0.772
Awakenings (n)	Sex	5.695 [-44.381, 55.77]	0.772
	Age @ EEG	0.932 [-7.904, 9.769]	0.772
	CAPA Sleep Problems	4.938 [-10.96, 20.836]	0.844
	FSIQ	-1.403 [-3.138, 0.332]	0.844
	Anxiety Symptoms	-2.383 [-7.613, 2.848]	0.844
	ADHD Symptoms	2.443 [-1.383, 6.27]	0.844
	ASD Symptoms	-2.331 [-5.596, 0.933]	0.336
	Psychotic Experiences	-15.59 [-56.06, 24.879]	0.772

medRxiv preprint doi: https://doi.org/10.1101/2021.11.08.21266020; this version posted July 14, 2022. The copyright holder for this preprint (which was not certified by peer review) is the author/funder, who has granted medRxiv a license to display the preprint in perpetuity. It is made available under a CC-BY-NC-ND 4.0 International license .

Table 5 Legend: *Associations between sleep architecture measures (proportion of N1, N2, N3 and REM sleep, latency to N1 and REM sleep, Sleep Efficiency, Total Sleep Time and total Awakenings), sex, age and psychiatric and cognitive (FSIQ) covariates, in participants with 22q11.2DS. Regression models were fit with linear mixed models, with family identity as a random (varying) intercept. Data presented are regression beta coefficients with 95% confidence intervals.*

medRxiv preprint doi: https://doi.org/10.1101/2021.11.08.21266020; this version posted July 14, 2022. The copyright holder for this preprint (which was not certified by peer review) is the author/funder, who has granted medRxiv a license to display the preprint in perpetuity. It is made available under a CC-BY-NC-ND 4.0 International license .

Altered Spectral Properties of the Sleep EEG in 22q11.2DS

Given the above evidence for an altered overall distribution of sleep stages in 22q11.2DS, we next used spectral analyses to quantify sleep EEG oscillations in our sample.

Before analyzing all 60 EEG electrodes, we calculated power spectral density (PSD) across frequencies from 0.5 – 20 Hz for controls and in 22q11.2DS for electrode Cz, as both spindle and slow wave oscillations can be reliable detected at this location (**Figure 2A**). We found that power in lower frequencies appeared to be increased in 22q11.2DS across N2 and N3 as well as across a range of frequencies during REM sleep (cluster-corrected $p < 0.05$).

To investigate potential changes in specific oscillatory components of the EEG (particularly at the sigma and SO frequency bands), we first z-scored raw EEG recordings in the time domain to eliminate broadband power differences between recordings, and again compared the PSD (**Figure 2B**). This analysis revealed reduced relative power in the sigma frequency band in 22q11.2DS in N2 and N3 sleep (cluster-corrected $p < 0.05$).

Next, we used irregular-resampling auto-spectral analysis (Hahn et al., 2020; Wen & Liu, 2016) to separate the oscillatory and fractal (1/f) components of the EEG. This analysis demonstrated that the power of the fractal component of the PSD was increased in 22q11.2DS across a wide range of frequencies in N2, N3 and REM sleep (**Figure 2C**). However, in the oscillatory component of the EEG we found that power in the sigma band appeared to be reduced in 22q11.2DS (**Figure 2D**) but to have a higher peak frequency. Every participant had a distinct peak in oscillatory activity in the sigma frequency band (**Figure 2 – Supplement 1A**).

We then focused on a set of PSD derived measures from N2 and N3 sleep: power in the slow delta (< 1.25 Hz) and sigma (10 – 16 Hz) bands, and peak sigma frequency. Additionally, we calculated the y-intercept (cons) and the negative exponent (beta) of a 1/f line fit to the fractal component of the signal to allow comparison of non-oscillatory activity between groups, for N2, N3 and REM epochs. We extracted these measures across all 60 EEG electrodes and fitted generalized additive mixed models to the data from all electrodes for each measure. **Table 6** shows all spectral EEG measures calculated. A detailed topographical analysis revealed that 22q11.2DS showed lower

medRxiv preprint doi: https://doi.org/10.1101/2021.11.08.21266020; this version posted July 14, 2022. The copyright holder for this preprint (which was not certified by peer review) is the author/funder, who has granted medRxiv a license to display the preprint in perpetuity. It is made available under a CC-BY-NC-ND 4.0 International license .

sigma power, but higher sigma frequency during N2 and N3 sleep in central regions, and higher total power, as indexed by the 1/f intercept measure across N2, N3 and REM sleep, particularly in fronto-lateral regions (**Figure 2E-G**). In contrast, there were no substantial differences in slow delta power or 1/f slope between groups.

Individual data and group boxplots for this set of spectral measures extracted at electrode Cz are shown in **Figure 2 – Supplement 1B**, and plots of spectral measures with age are shown in **Figure 2 – Supplement 1C**, demonstrating clear positive relationships between age and sigma frequency, and negative relationships between age and the overall PSD power (constant) and slope (beta), as previously demonstrated (Hahn et al., 2020).

medRxiv preprint doi: https://doi.org/10.1101/2021.11.08.21266020; this version posted July 14, 2022. The copyright holder for this preprint (which was not certified by peer review) is the author/funder, who has granted medRxiv a license to display the preprint in perpetuity. It is made available under a CC-BY-NC-ND 4.0 International license .

Figure 2: Increased PSD power and Sigma Frequency in 22q11.2DS

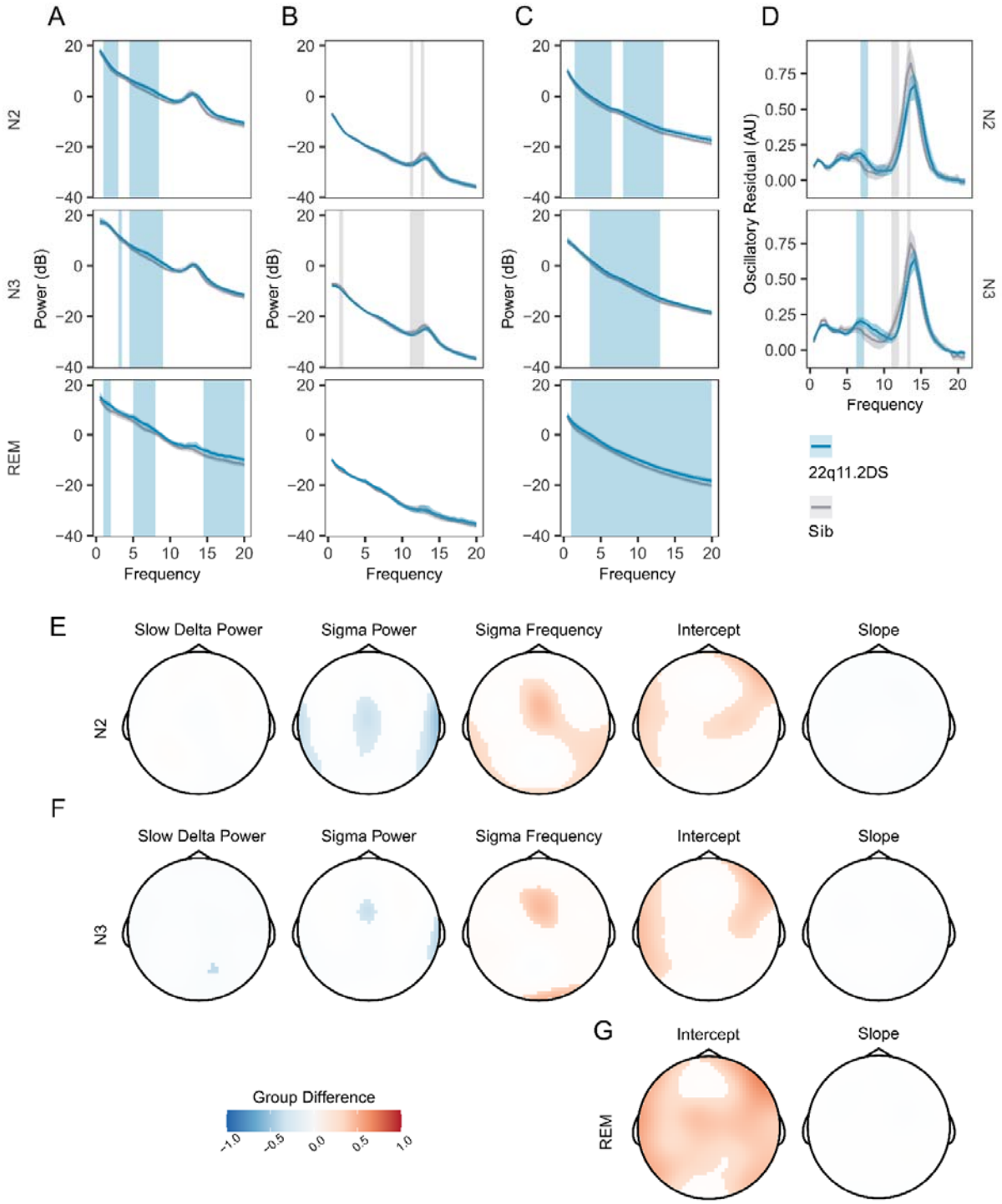

Figure 2 Legend:

A. *Raw Welch Power Spectral Density (PSD, in decibels, 10 * $\log_{10}$ of the PSD) on electrode Cz across Stage N2, N2 and REM sleep. Lines show group mean power (blue =*

medRxiv preprint doi: https://doi.org/10.1101/2021.11.08.21266020; this version posted July 14, 2022. The copyright holder for this preprint (which was not certified by peer review) is the author/funder, who has granted medRxiv a license to display the preprint in perpetuity. It is made available under a CC-BY-NC-ND 4.0 International license .

22q11.2DS, gray = Sibling), with bootstrapped 95% confidence intervals of the mean. Patches show regions of significant (cluster corrected) difference between groups (blue = 22q11.2DS > Sibling; grey = 22q11.2DS < Sibling), with 22q11.2DS being associated with increased power at lower frequencies.

B. Welch PSD of Z-Scored EEG signals on electrode Cz, as in (A); with 22q11.2DS being associated with lower power in the sigma frequency band (10 – 16 Hz)

C. Fractal (1/f) component of EEG signal processed using the IRASA method on electrode Cz, conventions as (A). Higher power across a wide frequency range in 22q11.2DS.

D. Oscillatory component of the EEG signal processed using the IRASA method on electrode Cz, conventions as (A).

E. Topoplots of group difference calculated from multilevel generalized additive models fit to the full 60 channel dataset for the five measures (mean Slow Delta power, mean Sigma power and peak Sigma frequency, 1/f Intercept and 1/f Slope) recorded in N2 sleep. Positive differences represent z score group differences indicate 22q11.2DS > Sibling (red colors); negative group differences (blue colors) indicate 22q11.2DS < Sibling. Only regions were where the probability of direction statistic for group difference was > 0.995 are colored.

F. As in (E), for N3 sleep.

G. As in (F), for REM sleep. Note as REM sleep lacks prominent oscillatory activity, we have not calculated models for SD or sigma related measures in REM as these would not be meaningful.

medRxiv preprint doi: https://doi.org/10.1101/2021.11.08.21266020; this version posted July 14, 2022. The copyright holder for this preprint (which was not certified by peer review) is the author/funder, who has granted medRxiv a license to display the preprint in perpetuity. It is made available under a CC-BY-NC-ND 4.0 International license .

Figure 2: Supplement 1

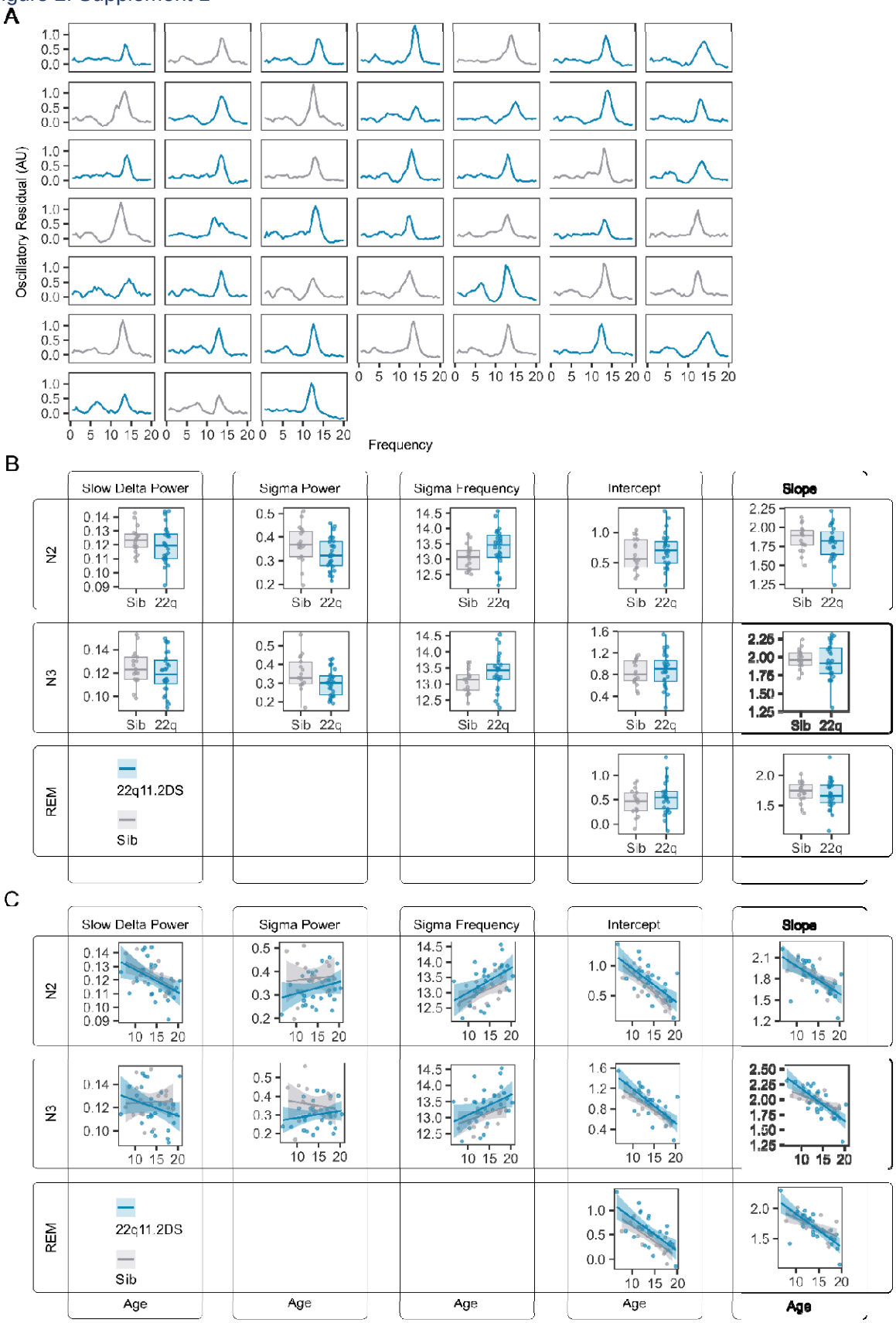

medRxiv preprint doi: https://doi.org/10.1101/2021.11.08.21266020; this version posted July 14, 2022. The copyright holder for this preprint (which was not certified by peer review) is the author/funder, who has granted medRxiv a license to display the preprint in perpetuity. It is made available under a CC-BY-NC-ND 4.0 International license .

Figure 2 – Supplement 1 Legend:

A. Plots of the oscillatory signal component of the EEG for each individual in stage N2 (each plot is the average PSD for a single participant). Plots are colored by genotype; grey = sibling, blue = 22q11.2DS.

B. Boxplots and overplotted individual data for spectral measures derived from N2, N3 and REM epochs. Boxes represent the median and IQR, with the whiskers representing 1.5 x the IQR. Individual participant data are shown as individual points. Points have been slightly jittered in the x direction only to illustrate where multiple participants had similar results.

C. Line plots and overplotted individual data for spectral measures derived from N2, N3 and REM epochs, plotted against participant age at the time of EEG. Lines of best fit and 95% confidence intervals are derived from linear models.

medRxiv preprint doi: https://doi.org/10.1101/2021.11.08.21266020; this version posted July 14, 2022. The copyright holder for this preprint (which was not certified by peer review) is the author/funder, who has granted medRxiv a license to display the preprint in perpetuity. It is made available under a CC-BY-NC-ND 4.0 International license .

Figure 2: Supplement 2

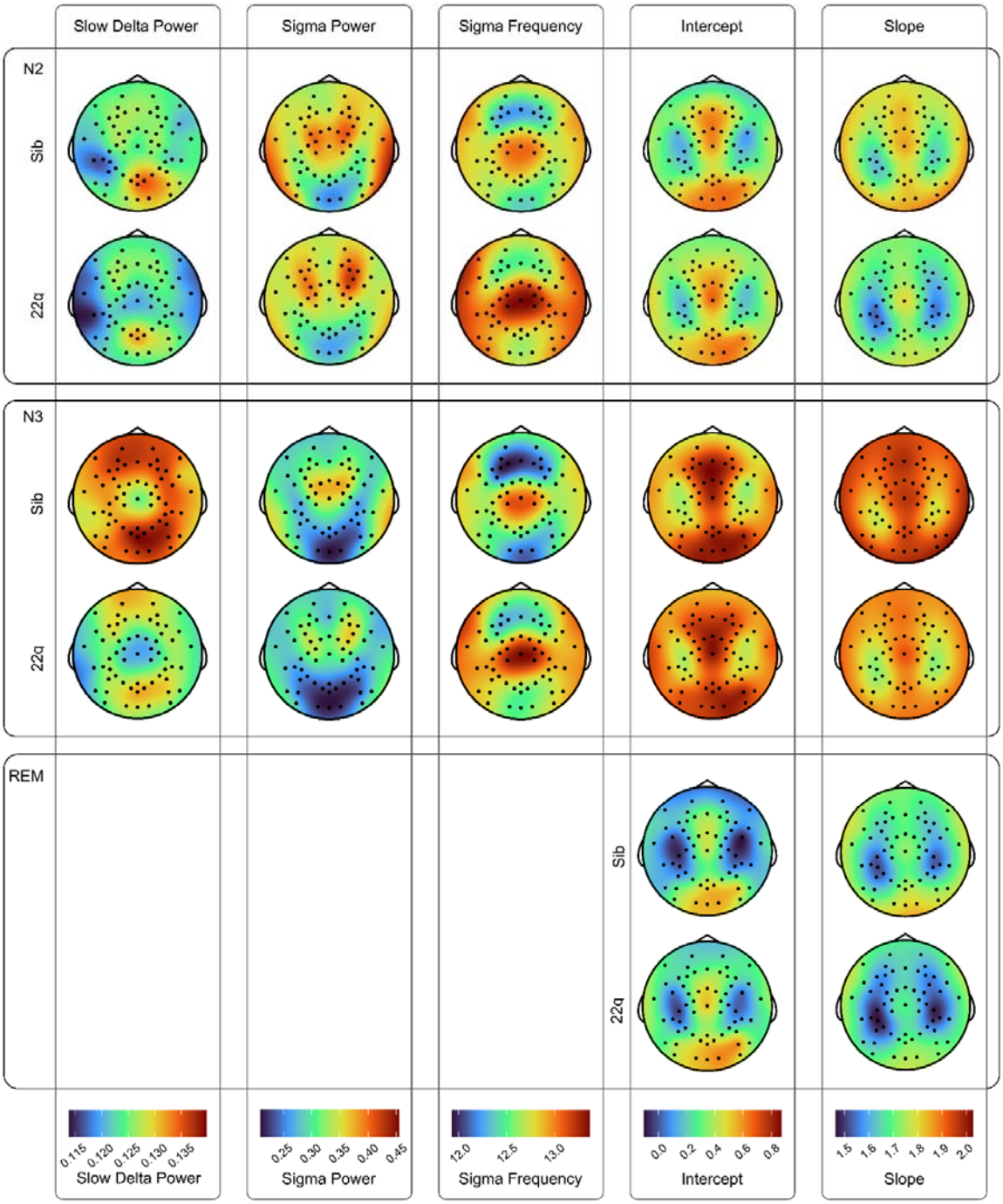

Figure 2 – Supplement 2 Legend:

Topoplots of group average values for spectral EEG measures (slow delta power, sigma power, peak sigma frequency, 1/f signal component intercept and 1/f signal component slope), across N2, N3, and REM epochs. Topoplots in the same column are on the same color scale (color scale shown at the bottom of each column).

medRxiv preprint doi: https://doi.org/10.1101/2021.11.08.21266020; this version posted July 14, 2022. The copyright holder for this preprint (which was not certified by peer review) is the author/funder, who has granted medRxiv a license to display the preprint in perpetuity. It is made available under a CC-BY-NC-ND 4.0 International license .

Table 6: EEG Measure Summary

Measure Group	Measure Details	Sleep Stage
Spectral	Mean Slow Delta Power	N2
Spectral	Mean Slow Delta Power	N3
Spectral	Mean Sigma Power	N2
Spectral	Mean Sigma Power	N3
Spectral	Peak Sigma Frequency	N2
Spectral	Peak Sigma Frequency	N3
Spectral	Aperiodic Signal Slope	N2
Spectral	Aperiodic Signal Slope	N3
Spectral	Aperiodic Signal Slope	REM
Spectral	Aperiodic Signal Intercept	N2
Spectral	Aperiodic Signal Intercept	N3
Spectral	Aperiodic Signal Intercept	REM
Spindle	Density	N2 + N3
Spindle	Amplitude	N2 + N3
Spindle	Frequency	N2 + N3
Slow Wave	Density	N2 + N3
Slow Wave	Amplitude	N2 + N3
Slow Wave	Duration	N2 + N3
Spindle – Slow Wave Coupling	Spindle – Slow Wave Overlap (z-scored against shuffled data)	N2 + N3
Spindle – Slow Wave Coupling	Spindle – Slow Wave Mean Resultant Length (z-scored against shuffled data)	N2 + N3
Spindle – Slow Wave Coupling	Spindle – Slow Wave Mean Coupling Angle	N2 + N3

medRxiv preprint doi: https://doi.org/10.1101/2021.11.08.21266020; this version posted July 14, 2022. The copyright holder for this preprint (which was not certified by peer review) is the author/funder, who has granted medRxiv a license to display the preprint in perpetuity. It is made available under a CC-BY-NC-ND 4.0 International license .

Table 6 Legend: *All derived EEG measures, grouped by signal type (spectral, derived from the PSD; spindle, derived from individual detected spindle events; slow wave, derived from individual detected slow wave events and measures derived from spindle – slow wave coupling*

medRxiv preprint doi: https://doi.org/10.1101/2021.11.08.21266020; this version posted July 14, 2022. The copyright holder for this preprint (which was not certified by peer review) is the author/funder, who has granted medRxiv a license to display the preprint in perpetuity. It is made available under a CC-BY-NC-ND 4.0 International license .

Spindles and Slow Waves in 22q11.2DS

To further interrogate the thalamocortical oscillations underlying genotype-dependent alterations in spectral power and frequency, we quantified individual spindle and slow wave (SW) events using automated detection algorithms. For spindle detection, for each participant and each electrode, we individualized the frequency used for spindle detection, using the peak sigma band frequency from our spectral analysis.

Figure 3A and B show example spectrograms from electrode Cz for a pair of siblings; one control (**Figure 3A**), one with 22q11.2DS (**Figure 3B**), with detected spindle and SW events overlaid. As expected, these plots clearly indicate the presence of co-occurring spindle and SW events during NREM sleep.

The average waveforms of spindle and SW events detected on electrode Cz are shown in **Figure 3C and Figure 3D**, exemplifying group differences in spindle and SW properties: participants with 22q11.2DS showed increased spindle amplitude across fronto-lateral regions, with accompanying increases in spindle density and frequency across smaller regions (**Figure 3E**). SW amplitude was also increased in central, frontal and lateral areas, but there were no differences in SW density or duration between groups (**Figure 3F**). Individual data from all participants for the measured spindle and SW properties are presented in **Figure 3 – Supplement 1**, and group topoplots for each property in **Figure 3 – Supplement 2**.

medRxiv preprint doi: https://doi.org/10.1101/2021.11.08.21266020; this version posted July 14, 2022. The copyright holder for this preprint (which was not certified by peer review) is the author/funder, who has granted medRxiv a license to display the preprint in perpetuity. It is made available under a CC-BY-NC-ND 4.0 International license .

Figure 3: Spindles and Slow Waves in 22q11.2DS

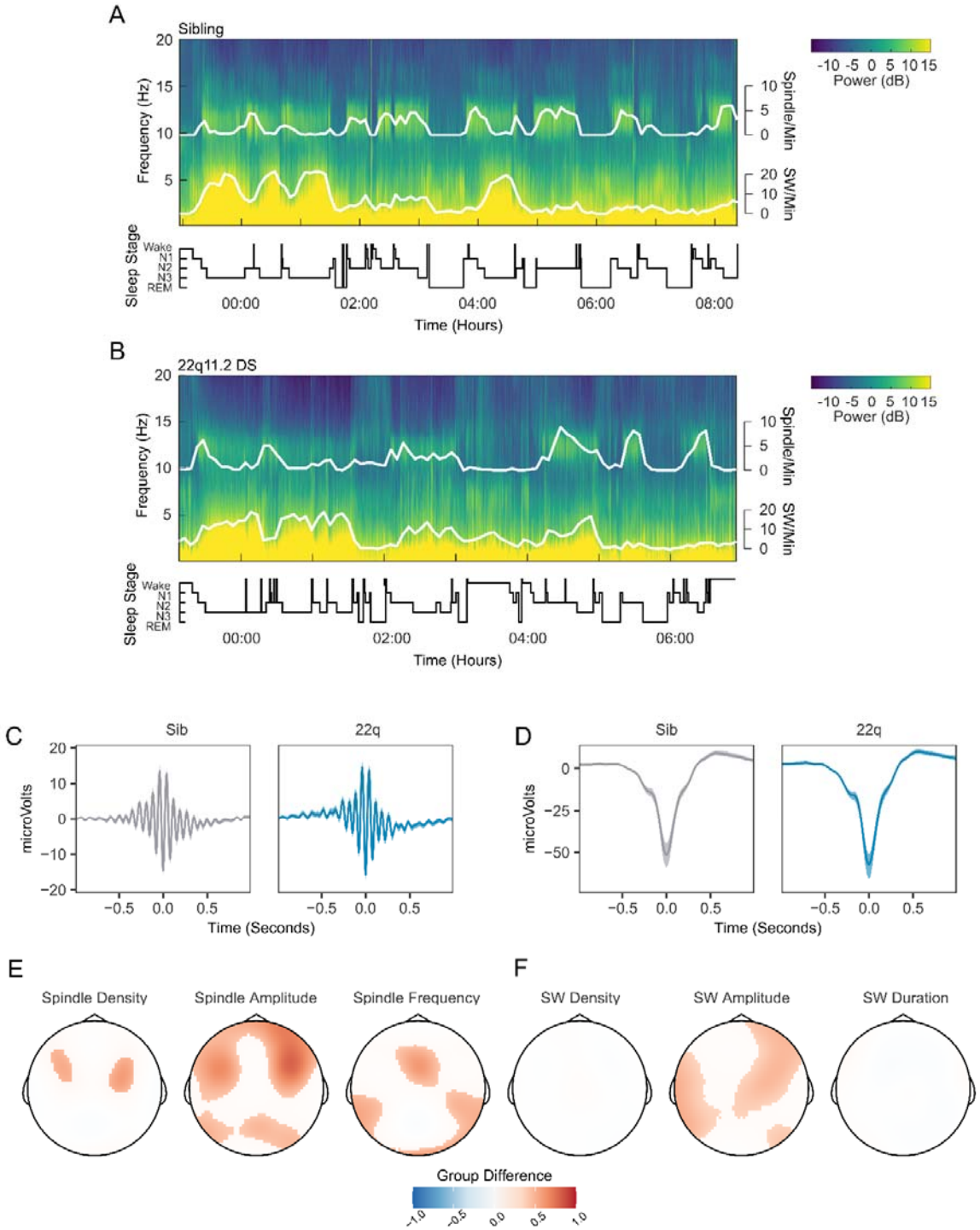

Figure 3 Legend:

A. Example spectrogram of a whole night EEG recording from electrode Cz for an example sibling. The associated hypnogram is displayed below the spectrogram in black, detected

medRxiv preprint doi: https://doi.org/10.1101/2021.11.08.21266020; this version posted July 14, 2022. The copyright holder for this preprint (which was not certified by peer review) is the author/funder, who has granted medRxiv a license to display the preprint in perpetuity. It is made available under a CC-BY-NC-ND 4.0 International license .

spindle and slow wave events are overplotted in white. The co-occurrence of spindle events with epochs of N2 sleep, and of SW events and N3 sleep can be observed.

B. *Example spectrogram of a whole night EEG recording from electrode Cz for an example participant with 22q11.2DS, sibling of the participant illustrated in A*

C. *Average spindle waveforms detected on electrode Cz for siblings (left, gray), and 22q11.2DS (right, blue). For each individual the average spindle waveform at Cz was calculated, these averaged waveforms were then calculated for all siblings or all participants with 22q11.2DS. Shaded areas highlight the bootstrapped 95% confidence interval of the mean.*

D. *Average SW waveforms detected on electrode Cz, same conventions as C*

E. *Topoplots of group differences in spindle density, amplitude and frequency, Z-transformed, across all 60 electrodes, from GAMM analyses. Only regions with significant group differences are highlighted. Red colors indicate values of the parameter of interest are greated in 22q11.2DS; blue color that the parameter of interest is greater in siblings*

F. *Topoplots of group differences in SW density, amplitude and duration, conventions as in E*

medRxiv preprint doi: https://doi.org/10.1101/2021.11.08.21266020; this version posted July 14, 2022. The copyright holder for this preprint (which was not certified by peer review) is the author/funder, who has granted medRxiv a license to display the preprint in perpetuity. It is made available under a CC-BY-NC-ND 4.0 International license .

Figure 3: Supplement 1

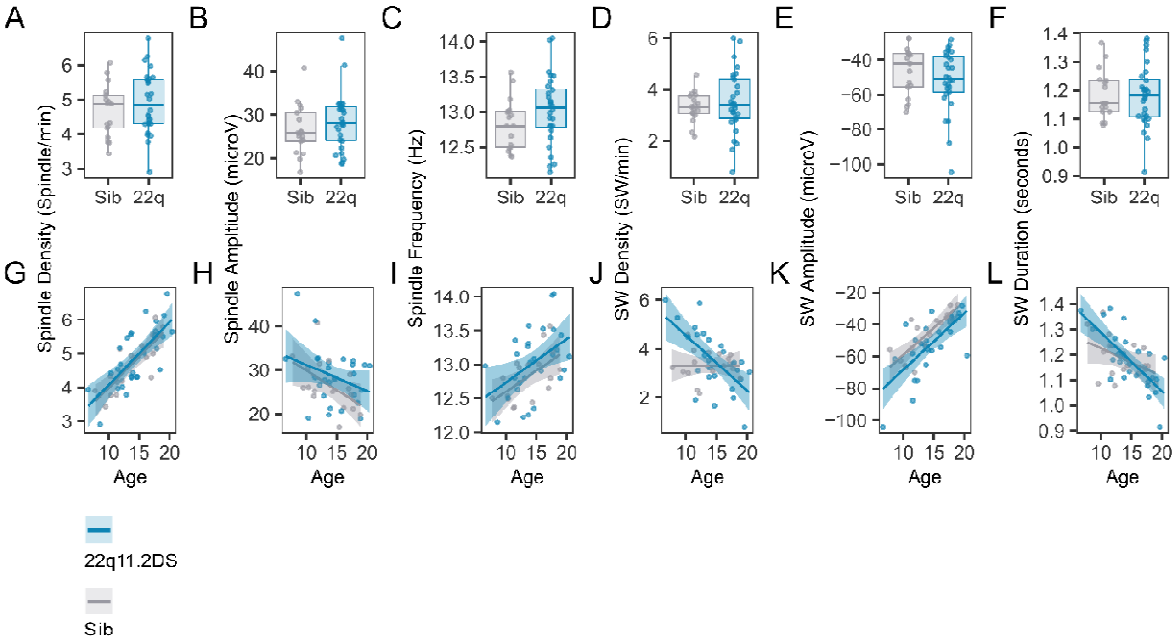

Figure 3 – Supplement 1 Legend:

A. Boxplots and overplotted individual data for spindle and SW measures. Boxes represent the median and IQR, with the whiskers representing 1.5 x the IQR. Individual participant data are shown as individual points. Points have been slightly jittered in the x direction only to illustrate where multiple participants had similar results.

B. Line plots and overplotted individual data for spindle and SW measures, plotted against participant age at the time of EEG. Lines of best fit and 95% confidence intervals are derived from linear models.

medRxiv preprint doi: https://doi.org/10.1101/2021.11.08.21266020; this version posted July 14, 2022. The copyright holder for this preprint (which was not certified by peer review) is the author/funder, who has granted medRxiv a license to display the preprint in perpetuity. It is made available under a CC-BY-NC-ND 4.0 International license .

Figure 3: Supplement 2

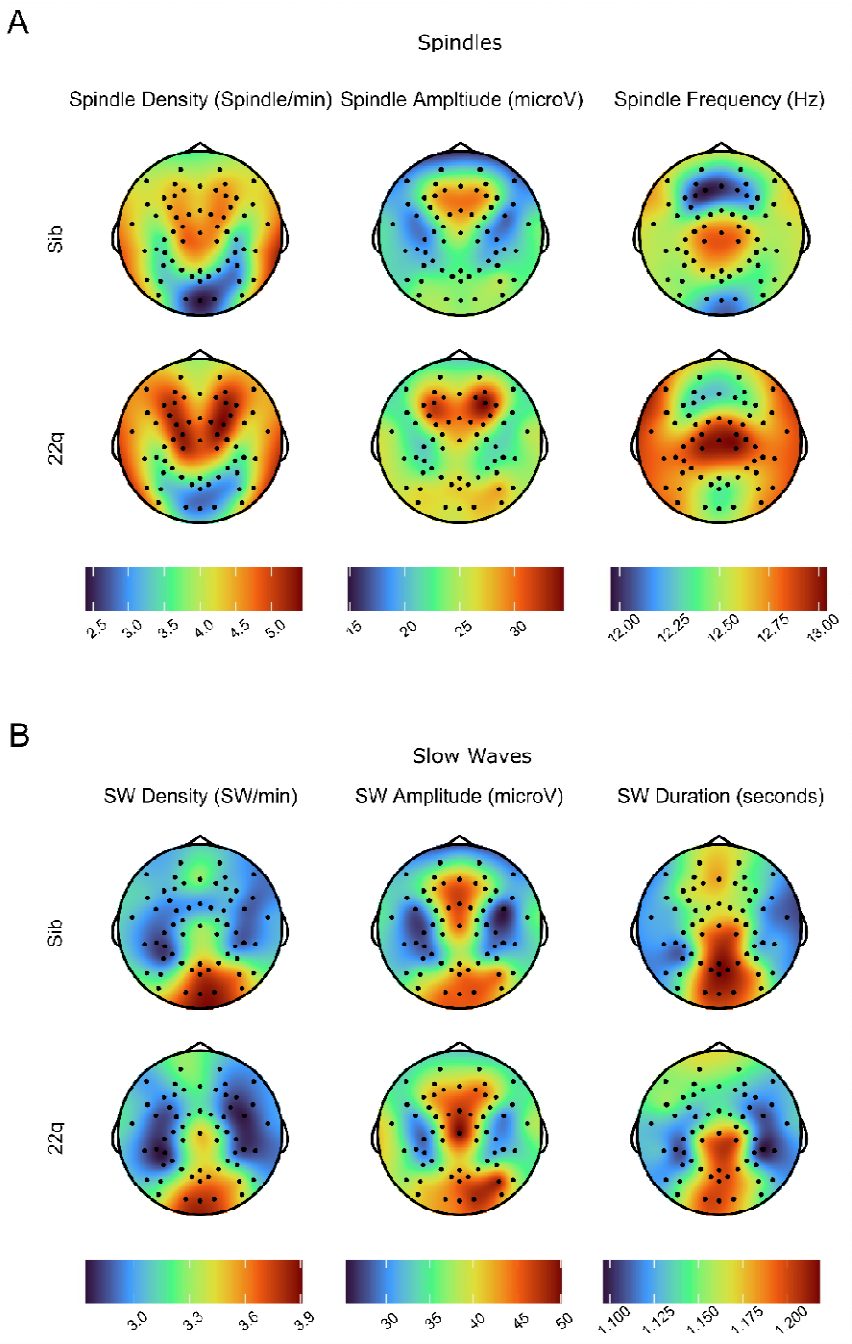

Figure 3 – Supplement 2 Legend:

A. Topoplots of group average values for spindle measures (density, amplitude and frequency). Topoplots in the same column are on the same color scale (color scale shown at the bottom of each column).

medRxiv preprint doi: https://doi.org/10.1101/2021.11.08.21266020; this version posted July 14, 2022. The copyright holder for this preprint (which was not certified by peer review) is the author/funder, who has granted medRxiv a license to display the preprint in perpetuity. It is made available under a CC-BY-NC-ND 4.0 International license .

B. Topoplots of group average values for SW measures (density, amplitude and duration). Topoplots in the same column are on the same color scale (color scale shown at the bottom of each column).

medRxiv preprint doi: https://doi.org/10.1101/2021.11.08.21266020; this version posted July 14, 2022. The copyright holder for this preprint (which was not certified by peer review) is the author/funder, who has granted medRxiv a license to display the preprint in perpetuity. It is made available under a CC-BY-NC-ND 4.0 International license .

Increased Spindle-SW Coupling in 22q11.2DS

The relative timing of spindle and SW events is coupled during NREM sleep, and thought to reflect limbic-thalamic-cortical interactions (Bartsch et al., 2019; Demanuele et al., 2017; Djonlagic et al., 2020; Helfrich et al., 2018; Latchoumane et al., 2017). An illustrative example of an overlapping spindle and SW detection is shown in **Figure 4A**. To investigate whether 22q11.2DS was associated with alterations in spindle-SW coupling, we first calculated the proportion of spindles that overlapped a detected SW (where a spindle peak fell within +/- 1.5 seconds of a detected SW negative peak). We then calculated the SW phase angle at the point of peak amplitude in each spindle, and the mean resultant length (MRL, a measure of the circular concentration of phase angles, with greater values indicating a more consistent spindle-SW phase relationship (Djonlagic et al., 2020)) at the peak of each spindle.

The mean angle of spindle-SW coupling showed a non-uniform distribution, confirming that spindles tended to consistently occur at particular SW phases (**Figure 4B** shows coupling angles for spindles detected at electrode Cz); at electrode Cz both control and 22q11.2DS participants had significantly non-uniform distributions of spindle-SW coupling phase angles (siblings: mean angle = 27.6^{o}, SD = 0.959, Rayleigh Test for non—uniformity statistic = 0.632, $p < 0.001$; 22q11.2DS: mean angle = 9.51^{o}, SD = 0.769, Rayleigh test statistic 0.744, $p < 0.001$), but no difference in coupling angle was observed between groups: Watson Williams test $F_{1,43} = 1.341$, $p = 0.253$.

We then compared coupling between groups across all electrodes. Compared to siblings, 22q11.2DS was not associated with any change in the proportion of spindles overlapping SW, but was associated with increased MRL across a central region, indicating less variable spindle-SW phase coupling (**Figure 4C)**. There were only minor differences in preferred coupling angle in 22q11.2DS (**Figure 4D**). Per participant data for the overlap and MRL measures recorded on electrode Cz are presented in **Figure 4 – Supplement 1** and group topoplots in **Figure 4 – Supplement 2**.

medRxiv preprint doi: https://doi.org/10.1101/2021.11.08.21266020; this version posted July 14, 2022. The copyright holder for this preprint (which was not certified by peer review) is the author/funder, who has granted medRxiv a license to display the preprint in perpetuity. It is made available under a CC-BY-NC-ND 4.0 International license .

Figure 4: Increased Spindle-SW Coupling in 22q11.2DS

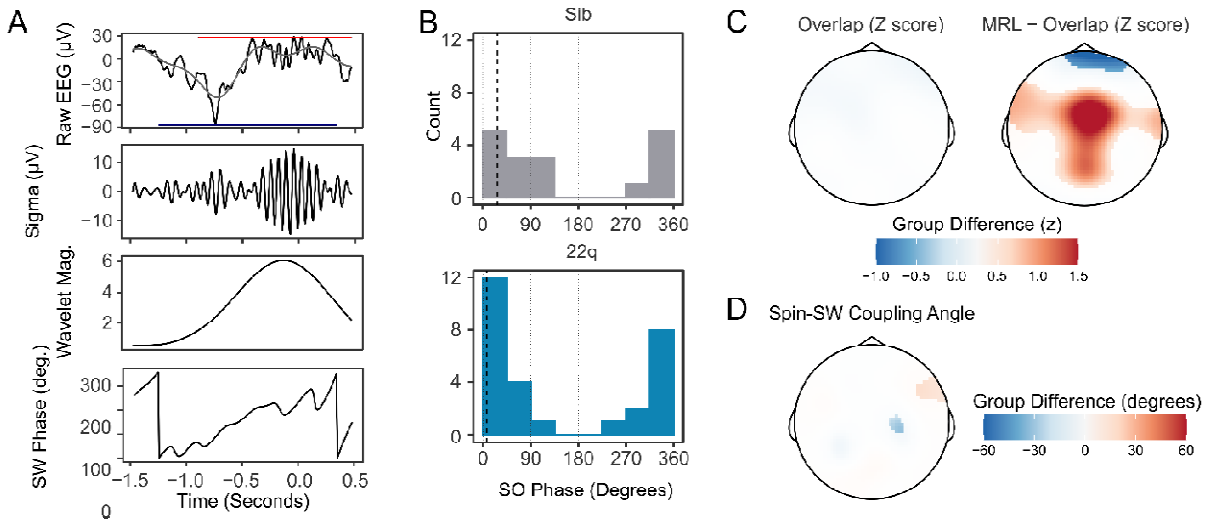

Figure 4 Legend:

A. *Illustrative plot of a single spindle and SW recorded at electrode Cz in a control sibling. From top to bottom, panels show the raw EEG (black) with Slow-Wave frequency (0.25 – 4 Hz) filtered data superimposed (gray) and with the detected boundaries of the spindle and SW highlighted with a red and blue horizontal bar, the sigma-filtered raw signal (10 – 16 Hz); the magnitude of the continuous wavelet transform of the signal (center frequency 13 Hz); and the SW phase (in degrees).*

B. *Histograms of the mean SW phase angle of spindles detected overlapping an SW for all participants at electrode Cz. The SO phase angles are as defined in (A). Black vertical dashed lines indicate the mean coupling phase angle for each group*

C. *Topoplots of group difference in spindle-SW coupling properties: z-transformed spindle-SW overlap (left), and z-transformed mean resultant length (right). The color represents the difference in z-score between groups where a multilevel generalized additive model fit to each dataset predicts a difference between group.*

D. *Topoplots of mean Spindle-SW coupling phase angle, where a multilevel generalized additive model fit to each dataset predicts a difference in coupling phase angle between groups.*

medRxiv preprint doi: https://doi.org/10.1101/2021.11.08.21266020; this version posted July 14, 2022. The copyright holder for this preprint (which was not certified by peer review) is the author/funder, who has granted medRxiv a license to display the preprint in perpetuity. It is made available under a CC-BY-NC-ND 4.0 International license .

Figure 4: Supplement 1

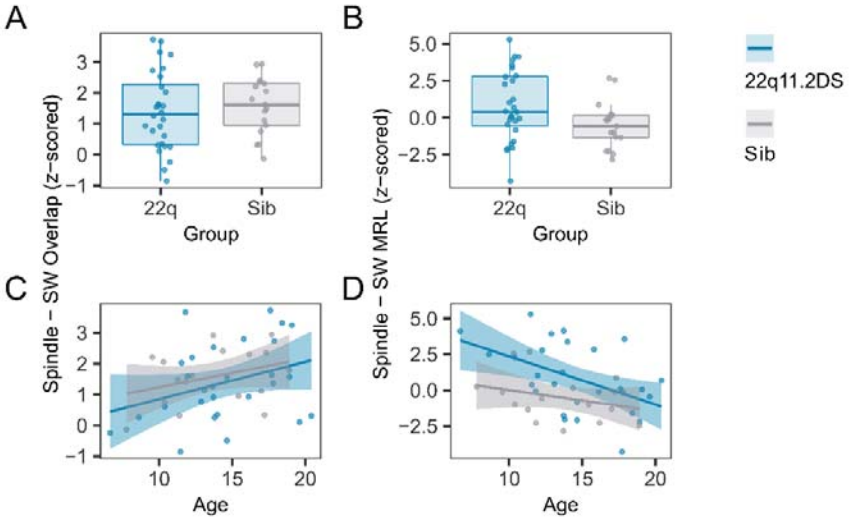

Figure 4 – Supplement 1 Legend:

A. *Boxplots and overplotted individual data for spindle - SW overlap. Boxes represent the median and IQR, with the whiskers representing 1.5 x the IQR. Individual participant data are shown as individual points. Points have been slightly jittered in the x direction only to illustrate where multiple participants had similar results.*
B. *Boxplots and overplotted individual data for spindle - SW MRL, conventions as A*
C. *Line plots and overplotted individual data for spindle - SW overlap, plotted against participant age at the time of EEG. Lines of best fit and 95% confidence intervals are derived from linear models.*
D. *Line plots and overplotted individual data for spindle - SW MRL, conventions as C*

medRxiv preprint doi: https://doi.org/10.1101/2021.11.08.21266020; this version posted July 14, 2022. The copyright holder for this preprint (which was not certified by peer review) is the author/funder, who has granted medRxiv a license to display the preprint in perpetuity. It is made available under a CC-BY-NC-ND 4.0 International license .

Figure 4: Supplement 2

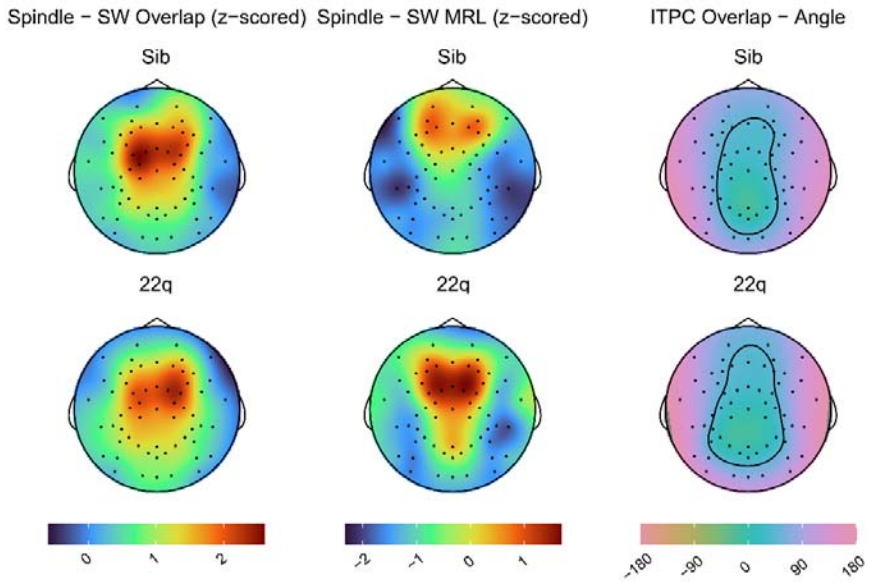

Figure 4 – Supplement 2 Legend:

Topoplots of group average values for spindle – SW coupling measures (overlap, MRL and mean angle). Topoplots in the same column are on the same color scale (color scale shown at the bottom of each column), note the Angle Measure is in degrees.

medRxiv preprint doi: https://doi.org/10.1101/2021.11.08.21266020; this version posted July 14, 2022. The copyright holder for this preprint (which was not certified by peer review) is the author/funder, who has granted medRxiv a license to display the preprint in perpetuity. It is made available under a CC-BY-NC-ND 4.0 International license .

Sleep Feature Associations with Memory Recall

Next, we tested whether features of the sleep EEG which demonstrated significant group differences (REM 1/f intercept, spindle amplitude, SW amplitude and spindle-SW MRL), interacted with group effects on accuracy in the morning test session. As there were no group differences in change in task performance overnight, but groups differed in morning test performance, we focused on number of correct responses in the morning memory test session. For features extracted at electrode Cz (**Figure 5A**), significant features x genotype interactions were observed (all $p < 0.05$). Applying the same analysis across all recording electrodes (**Figure 5B**), we found significant clusters of negative interactions between group and REM intercept, spindle and SW amplitude across multiple central and posterior electrodes: higher spindle and SW amplitudes were associated with higher accuracy in controls; in 22q11.2DS, higher amplitudes were associated with lower accuracy. We did not observe any interaction between spindle-SW MRL and task performance.

medRxiv preprint doi: https://doi.org/10.1101/2021.11.08.21266020; this version posted July 14, 2022. The copyright holder for this preprint (which was not certified by peer review) is the author/funder, who has granted medRxiv a license to display the preprint in perpetuity. It is made available under a CC-BY-NC-ND 4.0 International license .

Figure 5: EEG Signatures of Sleep Dependent Memory Consolidation

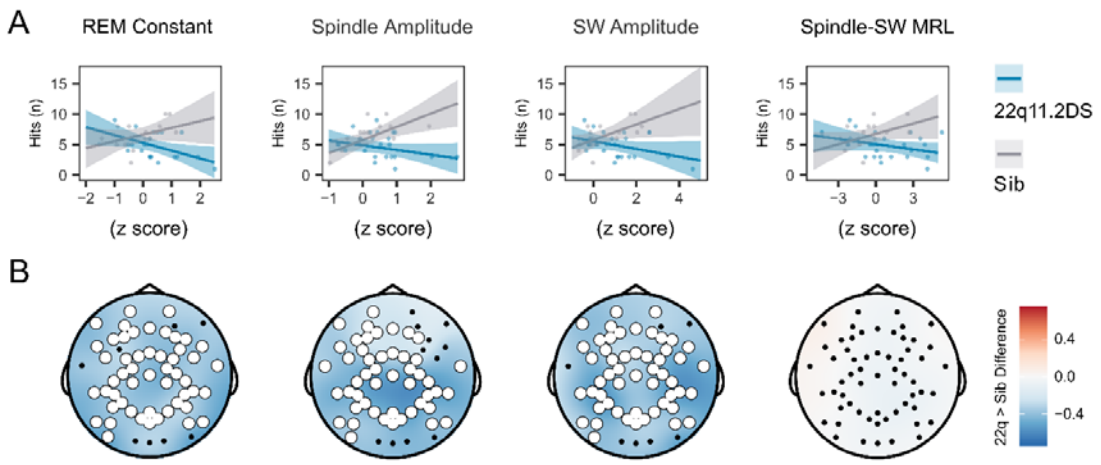

Figure 5 Legend:

A. Scatter plot of the relationship between EEG measures (recorded on electrode Cz) and hits in the memory task test session, by group. Lines represent predicted mean values, with 95% confidence interval, from linear mixed model).

*B. Topoplots of the value of the group*EEG feature interaction term, for models fit to hits in the morning test session. Electrodes highlighted in white indicate a significant interaction for an EEG measure detected on that channel, after correction for multiple comparisons. Note all topoplots are on the same color scale.*

medRxiv preprint doi: https://doi.org/10.1101/2021.11.08.21266020; this version posted July 14, 2022. The copyright holder for this preprint (which was not certified by peer review) is the author/funder, who has granted medRxiv a license to display the preprint in perpetuity. It is made available under a CC-BY-NC-ND 4.0 International license .

Mediation of Genotype Effects on Psychiatric Symptoms by EEG Features

Finally, we used mediation models to investigate whether the effects of 22q11.2DS genotype on psychiatric symptoms and FSIQ were potentially mediated via sleep EEG measures (**Figure 6A**); such mediation would support the potential role for quantitative sleep EEG measures serving as biomarkers for psychiatric disorders e.g. (Manoach & Stickgold, 2019). We calculated the total effect of genotype on psychiatric measures and IQ, the indirect (mediated) effect of EEG measures, and the proportion of the total effect that may be mediated by EEG measures, correcting for multiple comparisons using cluster-based permutation testing. The largest effects were of mediation of genotype effects on anxiety and ADHD symptoms by SW amplitude and spindle – SW coupling, with mediation of genotype effects on ADHD symptoms by REM constant, and genotype effect on ASD symptoms by spindle amplitude (**Figure 6B and Table 7**). There was little evidence for consistent mediation of genotype effects on sleep problems, psychotic experiences or FSIQ.

medRxiv preprint doi: https://doi.org/10.1101/2021.11.08.21266020; this version posted July 14, 2022. The copyright holder for this preprint (which was not certified by peer review) is the author/funder, who has granted medRxiv a license to display the preprint in perpetuity. It is made available under a CC-BY-NC-ND 4.0 International license .

Figure 6: Mediation of Psychiatric Symptoms and FSIQ by Sleep EEG Features

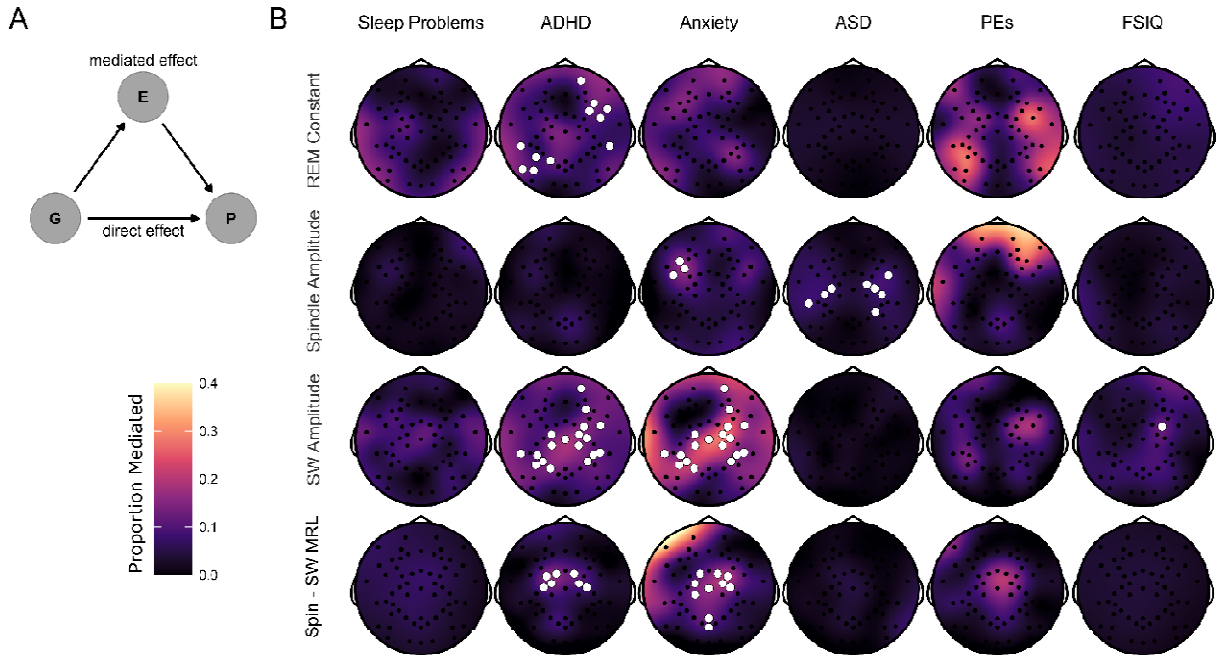

Figure 6 Legend:

A. Directed acyclic graph describing the mediation model fit to EEG data. The effect of Group (G) on psychiatric measures and FSIQ (P) was hypothesized to be mediated by (E) – sleep EEG features.

B. Topoplots of the proportion of the effect of genotype on psychiatric measures and FSIQ mediated by one of four NREM sleep EEG features (REM constant spindle amplitude, SW amplitude and spindle-SW MRL). Fill color represents the Proportion Mediated. Electrodes are highlighted in white where a mediation model fit on data from that electrode had a significant mediated effect and a significant total effect, corrected for multiple comparisons by the cluster method.

medRxiv preprint doi: https://doi.org/10.1101/2021.11.08.21266020; this version posted July 14, 2022. The copyright holder for this preprint (which was not certified by peer review) is the author/funder, who has granted medRxiv a license to display the preprint in perpetuity. It is made available under a CC-BY-NC-ND 4.0 International license .

Table 7: Average proportions of genotype effects on psychiatric measures and IQ mediated by sleep EEG measures

Measure	**Mediator**	**Proportion Mediated**
ADHD Symptoms	REM Constant	0.11 (0.02)
ADHD Symptoms	SW Amplitude	0.14 (0.03)
ADHD Symptoms	Spin - SW MRL	0.16 (0.03)
Anxiety Symptoms	Spindle Amplitude	0.17 (0)
Anxiety Symptoms	SW Amplitude	0.21 (0.05)
Anxiety Symptoms	Spin - SW MRL	0.19 (0.07)
ASD Symptoms	Spindle Amplitude	0.08 (0.02)
FSIQ	SW Amplitude	0.18

***Table 7 Legend**: Proportions of genotype effect on psychiatric measures and FSIQ mediated (Measure) by select sleep EEG features (Mediator) of for all electrodes in significant clusters. Data shown are mean (SD). Note FSIQ does not have an SD as there was only one electrode in a significant cluster.*

medRxiv preprint doi: https://doi.org/10.1101/2021.11.08.21266020; this version posted July 14, 2022. The copyright holder for this preprint (which was not certified by peer review) is the author/funder, who has granted medRxiv a license to display the preprint in perpetuity. It is made available under a CC-BY-NC-ND 4.0 International license .

Discussion

Summary of Findings

We performed an analysis of sleep EEG characteristics in 22q11.2DS, correlating these with psychiatric symptoms, sleep architecture and performance in a memory task.

Our previous results, based on primary carer reports, discovered sleep disruption, particularly insomnia and restless sleep in 22q11.2DS (Moulding et al., 2020), which was associated with psychopathology. We extend these findings to show that, compared to unaffected control siblings, 22q11.2DS is associated with decreased N1 and REM sleep, increased N3 sleep, increased overall EEG power and altered power and frequency in the sigma band during NREM sleep.

These finding were accompanied by changes in NREM sleep-related events: increased spindle amplitude, density, and frequency; increased SW amplitude; and increased spindle-SW phase coupling. The relationship between spindle and SW features and performance of a spatial memory task differed by group, with a positive correlation between spindle and SW amplitude and performance in controls, but a negative relationship in 22q11.2DS. Finally, group differences in anxiety, ADHD and ASD symptoms were mediated by several EEG measures, particularly SW amplitude and spindle – SW coupling, across multiple electrodes.

Relationship to previous findings – Spindles and Spindle Slow Wace-coupling

We observed increased spindle amplitude, frequency, and density in 22q11.2DS, accompanied by increased spindle-SW coupling, and evidence that spindle amplitude and spindle - SW coupling mediated genotype effects on anxiety, ADHD and ASD symptoms.

The clinical presentation of 22q11.2DS is heterogenous (Cunningham et al., 2018), including anxiety, ADHD and ASD symptoms, reduced IQ and increased risk of psychotic disorders (Schneider et al., 2014). Adult schizophrenia is consistently associated with reduced spindle activity (Ferrarelli et al., 2007, 2010; Lai et al., 2022), a finding replicated in a study of early onset schizophrenia (Gerstenberg et al., 2020), and meta-analytic evidence suggests spindle deficits increase with higher symptom burden and longer illness duration (Lai et al., 2022). However,

medRxiv preprint doi: https://doi.org/10.1101/2021.11.08.21266020; this version posted July 14, 2022. The copyright holder for this preprint (which was not certified by peer review) is the author/funder, who has granted medRxiv a license to display the preprint in perpetuity. It is made available under a CC-BY-NC-ND 4.0 International license .

increased spindle amplitudes and densities have been observed in healthy adolescents with raised polygenic risk scores for schizophrenia (Merikanto et al., 2019). In contrast, no clear differences in spindle properties have been found in other 22q11.2DS-associated neurodevelopmental disorders such as ADHD (Prehn-Kristensen et al., 2011) and ASD (Maski et al., 2015).

Spindle properties and spindle – SW relationships change across the lifespan (Djonlagic et al., 2020; Hahn et al., 2020, 2022; Purcell et al., 2017; Zhang et al., 2021): spindle density, power and frequency increases from childhood to adolescence alongside spindle-SW coupling, while power in lower frequency declines (Hahn et al., 2020; Jenni & Carskadon, 2004; Tarokh & Carskadon, 2010). Our findings could therefore be interpreted in the context of alterations in developmental processes in 22q11.2DS: higher spindle amplitude, density and frequency in young, at-risk populations for psychosis could mark an aberrant maturational state, which leads to reduced spindle activity in adulthood for individuals who go on to develop psychotic disorders, with higher symptom burden and illness duration linked to greater reductions in spindle activity.

Relationship to previous findings – Slow Waves

We observed increased SW amplitude in 22q11.2DS and mediation of genotype differences in anxiety and ADHD symptoms by SW amplitude (and spindle-SW coupling). A previous study found delta frequency (<4 Hz) EEG activity to be reduced in ADHD patients not using psychostimulant medication (Furrer et al., 2019); the authors related their finding to reduced cortical grey matter, and delays in its maturation in ADHD (Nakao et al., 2011; Shaw et al., 2006, 2010). In contrast, imaging studies have suggested increased cortical grey matter thickness in 22q11.2DS, alongside changes in corticothalamic networks (Lin et al., 2017; Sønderby et al., 2021; Sun et al., 2020), which may reduce across adolescence (Schaer et al., 2009). This could therefore explain our finding of increased SW amplitude in 22q11.2DS, and its relationship with ADHD symptoms, as it has been previously demonstrated (in adults) that greater SW amplitude is associated with greater cortical thickness (Dubé et al., 2015).

Anxiety and ADHD symptoms in late childhood (~ age 10) are associated with subsequent psychotic symptoms in 22q11.2DS (Chawner et al., 2019; Niarchou et al., 2019), although ASD

medRxiv preprint doi: https://doi.org/10.1101/2021.11.08.21266020; this version posted July 14, 2022. The copyright holder for this preprint (which was not certified by peer review) is the author/funder, who has granted medRxiv a license to display the preprint in perpetuity. It is made available under a CC-BY-NC-ND 4.0 International license .

symptoms are not. Brain imaging studies have demonstrated that individuals with 22q11.2DS who developed psychotic symptoms had a trajectory of thicker frontal cortex in childhood and early adolescence, which then more rapidly thinned during adolescence, than individuals with 22q11.2DS who did not develop psychotic symptoms (Bagautdinova et al., 2021; Ramanathan et al., 2017). Therefore, increased spindle and SW amplitude in 22q11.2DS in childhood/adolescence could reflect aberrant cortical development processes which clinically associate with ADHD and/or anxiety symptoms in this age group, but then progress to thinner frontal cortex, increased risk of psychotic disorders and potentially decreased spindle/SW density in adulthood.

Relationship to previous findings – Aperiodic Signal Component

We discovered increased broadband EEG power in 22q11.2DS during sleep, particularly in REM. Furthermore, the intercept of the aperiodic signal component in REM was observed to be a mediator of genotype effects on ADHD symptoms. One possibility is that the increased power is related to the increased cortical grey matter thickness observed in 22q11.2DS, as has been observed in brain imaging studies (Lin et al., 2017; Sønderby et al., 2021; Sun et al., 2020).

We also observed that the slope and intercept of the aperiodic part of the signal reduced with age, similar to previously reported findings in awake resting state EEG in children and adolescents (Hill et al., 2022), and aging adults (Voytek et al., 2015). The slope of the 1/f component of the EEG has also been associated with changes in level of arousal across different sleep stages, with REM being associated with the steepest slopes (Kozhemiako et al., 2021; Lendner et al., 2020). However, we did not observe any differences between groups in 1/f slope.

Mechanisms of sleep EEG changes in 22q11.2DS

Our EEG findings together suggest a complex picture of sleep neurophysiology in 22q11.2DS. On the one hand, increased intercept of the aperiodic component of the signal and increased SW amplitude is associated with a younger developmental age in controls; on the other hand, higher spindle frequency and higher spindle-SW coupling is associated with an older developmental age. Furthermore, we found partial mediation of genotype effects on anxiety, ADHD and ASD symptoms by several EEG measures, in addition to opposing relationships between EEG measures and

medRxiv preprint doi: https://doi.org/10.1101/2021.11.08.21266020; this version posted July 14, 2022. The copyright holder for this preprint (which was not certified by peer review) is the author/funder, who has granted medRxiv a license to display the preprint in perpetuity. It is made available under a CC-BY-NC-ND 4.0 International license .

memory task performance in 22q11.2DS, again suggesting a complex relationship between sleep physiology and cognition in carriers of this genotype.

Although the physiological bases of 22q11.2DS-associated changes in sleep architecture are unknown, genes in the deleted region of chromosome 22 have been implicated in sleep regulation, potentially via a role in sleep promoting GABA-ergic signaling (Maurer et al., 2020). GABA signaling is also integral to the mechanisms of spindle and slow wave oscillations (Feld et al., 2013; Feld & Born, 2020; Ulrich et al., 2018). Although a study using magnetic resonance spectroscopy did not demonstrate gross changes in GABA levels in the anterior cingulate cortex in 22q11.2DS (Vingerhoets et al., 2020), a mouse model of 22q11.2DS does harbor a reduction in GABA-ergic parvalbumin containing cortical interneurons in 22q11.2DS (Al-Absi et al., 2020). Therefore, a potential mechanism of altered sleep and sleep-associated EEG oscillations may involve neurodevelopmental changes to cortical structure and GABAergic signaling in cortical inhibitory networks in 22q11.2DS.

Limitations and Future Directions

In this study we made a single overnight EEG recording. Although there were no differences between groups in terms of total sleep time, or awakenings overnight – indicating minimal disruption by the EEG recording setup – it is possible that the recording protocol caused undetected effects that differed between groups, contributing to our EEG findings. A future study which included a baseline night where participants become familiar with the recording equipment would help to address this possibility.

We used mediation analyses to infer associations between genotype, psychiatric measures or FSIQ, and a wide range of sleep EEG measures. Although we corrected for multiple comparisons, these initial findings should be replicated and used for generating hypotheses for future studies. Sleep architecture is heterogenous in young people with ADHD and ASD, as it is in adult schizophrenia patients (Chouinard et al., 2004; Cohrs, 2008); it therefore may be unlikely that sleep macrostructure alone (i.e. percentages of different sleep stages, sleep efficiency etc.) will prove a useful biomarker or prognostic indicator of later neurodevelopmental diagnoses in

medRxiv preprint doi: https://doi.org/10.1101/2021.11.08.21266020; this version posted July 14, 2022. The copyright holder for this preprint (which was not certified by peer review) is the author/funder, who has granted medRxiv a license to display the preprint in perpetuity. It is made available under a CC-BY-NC-ND 4.0 International license .

22q11.2DS. However, our results suggest that the use of quantitative measurements of sleep microstructure, such as of spindles, SWs and their coupling could be mediators of genotype effects on psychiatric symptoms and therefore be useful as biomarkers of neurodevelopmental disorders in future studies (Manoach & Stickgold, 2019).

As expected, age had a large influence on EEG properties in our between-subject, cross-sectional study (Hahn et al., 2020; Markovic et al., 2020; Purcell et al., 2017). It has previously been demonstrated that psychopathology changes with age in 22q11.2DS, including that ADHD symptoms decline with age (Chawner et al., 2019). Therefore, a longitudinal cohort study of sleep EEG biomarkers in 22q11.2DS from childhood and adolescence into adulthood is an important extension of the present study, to elucidate developmental trajectories, as has been achieved with brain imaging (Bagautdinova et al., 2021; Ramanathan et al., 2017). Further, a retrospective cohort study of EEGs for those with 22q11.DS who go on to develop schizophrenia-spectrum disorders could dissociate which EEG features relate to the development of psychosis.

Conclusion

In conclusion, in this study quantifying sleep neurophysiology in 22q11.2DS, we highlight differences that could serve as potential biomarkers for 22q11.2DS-associated neurodevelopmental syndromes. Future longitudinal studies should clarify the relationship between psychiatric symptoms, sleep EEG measures, and development in 22q11.2DS, with a view to establishing mechanistic biomarkers of circuit dysfunction that may inform patient stratification and treatment.

medRxiv preprint doi: https://doi.org/10.1101/2021.11.08.21266020; this version posted July 14, 2022. The copyright holder for this preprint (which was not certified by peer review) is the author/funder, who has granted medRxiv a license to display the preprint in perpetuity. It is made available under a CC-BY-NC-ND 4.0 International license .

Methods and Materials

Participants and study recruitment

Participants were recruited as part of the previously described, ongoing Experiences of Children with cOpy number variants (ECHO) study (Moulding et al., 2020). Where available, a sibling (n = 17) without the deletion closest in age to the participant with 22q11.2DS (n = 28) was invited to participate as a control. As this study was an exploratory cross-sectional study of a rare neurodevelopmental copy number variant, our sample size was taken as the maximum number of participants who agreed to have an EEG recording.

The presence or absence of the deletion was confirmed by a Medical Genetics laboratory and/or microarray analysis in the MRC Centre for Neuropsychiatric Genetics and Genomics laboratory at Cardiff University.

Prior to recruitment, primary carers consented for all participants and additional consent was obtained from participants aged ≥16 years with capacity. The protocols used in this study were approved by the NHS Southeast Wales Research Ethics Committee.

Age and sex characteristics of the study sample are shown in **Table 1**. Of participants with 22q.11.2DS, four were prescribed melatonin, one was prescribed methylphenidate (Medikinet) for ADHD and one was prescribed sertraline for “mood”. No controls were prescribed psychiatric medication. No study participant reported a diagnosis of epilepsy or seizure disorder.

All data were collected during study team visits to participants’ family home. Data collection, including EEG recordings from sets of siblings were carried out on the same visit, which were typically on weekends or school holidays.

Psychiatric characteristics and IQ

Psychopathology and subjective sleep quality was measured by the research diagnostic Child and Adolescent Psychiatric Assessment (CAPA) interview (Angold et al., 1995) with either the participant or primary carer. Interviews were carried out during the same visit as EEG recordings.

medRxiv preprint doi: https://doi.org/10.1101/2021.11.08.21266020; this version posted July 14, 2022. The copyright holder for this preprint (which was not certified by peer review) is the author/funder, who has granted medRxiv a license to display the preprint in perpetuity. It is made available under a CC-BY-NC-ND 4.0 International license .

Participants were also screened for Autism-Spectrum Disorder (ASD) symptoms using the Social Communication Questionnaire (SCQ, (Rutter et al., 2003)), completed by the primary carer. Full-Scale IQ (FSIQ) was measured using the Wechsler Abbreviated Scale of Intelligence (Wechsler, 1999), as the combination of all subscores.

Sleep-dependent memory consolidation task

The effect of sleep on participants' memory performance was evaluated using a 2D object location task (Wilhelm et al., 2008) implemented in *E-Prime*. Participants completed a learning and test session the evening before the EEG recording, and a recall session the next morning. In the task, a 5 x 6 grid of covered square "cards" was presented on a laptop screen. During learning, successive pairs (n = 15) of cards were revealed for 3 seconds, showing matching images of everyday objects and animals. During recall, one of each pair was uncovered, and subjects were required to select the covered location of the matching pair.

In the evening, learning and recall sessions alternated until participants reached a performance criterion of 30% accuracy. The next morning a test session was carried out with a single recall session.

Polysomnography data acquisition

High-density EEG and video recordings were acquired with a 60 channel Geodesic Net (Electrical Geodesics, Inc. Eugene, Oregon, USA) and a BE Plus LTM amplifier running the Galileo acquisition software suite (EBNeuro S.p.A, Florence, Italy). Additional polysomnography channels including EOG, EMG, ECG, respiratory inductance plethysmography, pulse oximetry and nasal airflow were recorded with an Embla Titanium ambulatory amplifier. PSG signals were acquired at 512 Hz sampling rate with a 0.1 Hz high pass filter. The online references was electrode Cz.

On recording visits, a member of the study team came to the participant's home, set up the EEG and PSG recording systems and left; participants went to be at their normal bedtime, slept in their own beds, and as the system was ambulatory, were able to move freely during recordings e.g. to

medRxiv preprint doi: https://doi.org/10.1101/2021.11.08.21266020; this version posted July 14, 2022. The copyright holder for this preprint (which was not certified by peer review) is the author/funder, who has granted medRxiv a license to display the preprint in perpetuity. It is made available under a CC-BY-NC-ND 4.0 International license .

use the bathroom overnight. The experimenter returned the following morning to end the recordings, collect equipment and carry out the morning memory task test session.

Sleep scoring

Sleep scoring was performed by an experienced scorer on a standard PSG montage (6 EEG + all PSG channels) according to Academy of American Sleep Medicine criteria. Artefact and Wake epochs of EEG were discarded from further analysis. Sleep architecture was quantified using standard derived variables: total sleep time, sleep efficiency, latencies to N1 and REM sleep and proportion of time spent in N1, N2, N3 and REM sleep.

EEG data analysis

All pre-processing, spectral analysis and event detection algorithms employ methods validated in previously published sleep EEG studies, using the same MATLAB code where available.

Pre-processing

Following acquisition and prior to analysis, EEG data was pre-processed using the following steps: EEG *.edf* files were imported into MATLAB (Mathworks, Nantick, MA, USA) using the *EEGLAB* toolbox (Delorme & Makeig, 2004). Next, signals were downsampled to 128 Hz and processed: detrended with a high pass filter (cut off 0.25 Hz), 50 Hz line noise removed using the *EEGLAB PREP* plugin (Bigdely-Shamlo et al., 2015), artefacts were removed with the Artifact Subspace Reconstruction method (Mullen et al., 2015) implemented in the clean_rawdata EEGLAB plugin and re-referenced to a common average. Two additional automated artefact removal steps were then applied. Firstly, full 60 channel recordings were decomposed with independent components analysis (ICA) using the AMICA EEGLAB plugin (Delorme et al., 2012) and non-brain components were removed using the ICLabel plugin, including ECG, EMG and EOG artifacts (Pion-Tonachini et al., 2019).

Second, we applied an automated iterative epoch-level artefact removal process to N2 and N3 epochs (pooled together) using two sets of criteria, similar to that described by (Purcell et al., 2017): firstly, we applied the method described by (Buckelmüller et al., 2006), removing epochs

medRxiv preprint doi: https://doi.org/10.1101/2021.11.08.21266020; this version posted July 14, 2022. The copyright holder for this preprint (which was not certified by peer review) is the author/funder, who has granted medRxiv a license to display the preprint in perpetuity. It is made available under a CC-BY-NC-ND 4.0 International license .

where the beta (16 – 25 Hz, 2 SD) or delta (1 – 4 Hz, 2.5 SD) power exceeded a threshold of 2 or 2.5 SD relative to the flanking 14 epochs (7 before and 7 after). The resulting set of epochs were then further filtered based on whether an epoch had > 5% clipped signals (e.g., >5% of values in the epoch equal to the minimum or maximum possible value) and then a three-cycle iterative process of removing epochs based on their having a signal RMS or score on the first 3 Hjorth parameters (Hjorth, 1970) that exceeded 2 SD of the whole-signal SD. These processes appeared to remove epochs randomly across the night, although may have removed N3 epochs more than N2. There were no group differences in the proportion of N2 or N3 sleep removed from each recording (mixed models fit to proportion of epochs in N2 and N3 separately, with group as independent variable and gender and age as covariates, both $p > 0.05$). This process was applied to each channel independently as this study did not investigate any cross-channel EEG measures. Sleep montages were then prepared for sleep scoring, and thirty second epochs containing artefacts were flagged for removal after manual review.

Time-frequency Analysis

We calculated whole-night spectrograms using the multitaper method (Bokil et al., 2010) with a 30 second window advanced in steps of 10 seconds and a bandwidth of 1 Hz. The EEG power spectral density (PSD) was calculated for frequencies between 0.25 and 20 Hz using Welch's periodogram (MATLAB function *pwelch* with a 4 second Hanning window advanced in 2 second steps, then averaged over time to give one value per frequency per epoch) and converted to decibels ($10*\log_{10}$ (microvolts^2)). We then repeated this analysis with EEG signals after z-scoring in signals in the time domain (subtracting the overall signal mean and dividing by the signal standard deviation).

Next we used the Irregular Resampling Auto-Spectral Analysis (IRASA) method (Wen & Liu, 2016) to decompose EEG signals into oscillatory and aperiodic (also known as 1/f or fractal) components, using the MATLAB code published by the method's authors. In brief, this method consists of sequentially resampling time domain signals to odd numbered sampling rates and calculating the PSD for this set of stretched or compressed data. The sum of these resampled datasets cancels

medRxiv preprint doi: https://doi.org/10.1101/2021.11.08.21266020; this version posted July 14, 2022. The copyright holder for this preprint (which was not certified by peer review) is the author/funder, who has granted medRxiv a license to display the preprint in perpetuity. It is made available under a CC-BY-NC-ND 4.0 International license .

out oscillatory activity, but the aperiodic component is retained. The oscillatory component of the signal can then be recovered by subtracting the aperiodic component from the full PSD in the frequency domain. We calculated differences in PSD between groups through linear mixed models fit at each frequency, and corrected p-values for multiple comparisons using cluster-based correction (where adjacent frequencies were considered to be neighbors (Maris & Oostenveld, 2007), with 500 permutation iterations) .

From the oscillatory component of the signal, we calculated average power in slow delta (< 1.5 Hz) and sigma bands (10 – 16 Hz), and the sigma-band frequency with maximum power, averaging over all epochs in N2 and N3 sleep separately for each subject. From the aperiodic component of the signal we calculated two measures – a slope and an intercept measure, from fitting an exponential of $y = e^{-slope}$ + intercept to the aperiodic data in the frequency domain. We calculated these measures from all N2, N3 and REM epochs separately for all individuals. This gave a total of 12 spectral measures per electrode per subject (**Table 7**).

medRxiv preprint doi: https://doi.org/10.1101/2021.11.08.21266020; this version posted July 14, 2022. The copyright holder for this preprint (which was not certified by peer review) is the author/funder, who has granted medRxiv a license to display the preprint in perpetuity. It is made available under a CC-BY-NC-ND 4.0 International license .

Spindle Detection

Sleep spindles were automatically detected from artefact-free epochs of N2 and N3 sleep EEG data using a relative-threshold detector based on previously reported methods using the continuous wavelet transform (Djonlagic et al., 2020; Purcell et al., 2017). To enhance spindle detection signal-noise ratio a Complex-Frequency B-Spline wavelet was used in the place of the more typical Complex Morlet wavelet (Bandarabadi et al., 2020).

We determined the wavelet frequency to use for spindle detection from the peak sigma frequency calculated using the IRASA method, for each individual. As we observed almost all participants to have unimodal distributions of sigma power (**Figure 1 - Supplement 1**), and as has been previously suggested in a study of similarly aged participants (Hahn et al., 2020), we did not differentiate between “fast” and “slow” spindles. Therefore, for spindle detection, we used a single wavelet with an individualized centre frequency, a bandwidth parameter of 2, and an order parameter of 2.

Putative spindle cores were identified from the magnitude of the continuous wavelet transform of the EEG signal (smoothed with a 0.1 second moving average), with a main threshold of 3 x the median (calculated over the whole signal) and a secondary threshold of 1.5 x the median. We took putative spindles to be crossings of the main threshold flanked with secondary threshold crossings with a minimum event duration of 0.5 seconds and a maximum duration of 3 seconds. Further, putative spindles had to be separated by at least 0.5 seconds; events closer than this were merged unless their combined duration exceeded 3 seconds.

Putative spindles were further selected based on a quality metric where the power increase in the sigma band (10-16 Hz) during the putative spindle event (calculated as the FFT of the signal, relative to the whole-night baseline PSD) had to exceed the average increase in the delta, theta and beta bands during the same period, relative to their whole-night baselines.

From each putative spindle we extracted the amplitude (maximum peak-to-trough voltage difference in the sigma filtered-EEG, filtered using a least-squares linear-phase FIR filter using MATLAB’s *firls* command with 10 – 16 Hz passband filter, an order of 960, and transition frequency

medRxiv preprint doi: https://doi.org/10.1101/2021.11.08.21266020; this version posted July 14, 2022. The copyright holder for this preprint (which was not certified by peer review) is the author/funder, who has granted medRxiv a license to display the preprint in perpetuity. It is made available under a CC-BY-NC-ND 4.0 International license .

width of 0.5 Hz) and frequency (reciprocal of the mean time difference between positive voltage peaks within the spindle). We also calculated the average density of spindles over the whole duration of all epochs investigated in each participant, in events per minute, giving a total of 3 spindle-related measures per electrode per subject (**Table 7**).

Slow-Wave Detection

Slow waves were detected from epochs of N2 and N3 sleep using a previously validated method (Djonlagic et al., 2020) as follows: first the EEG signal was band-pass filtered between 0.25 and 4 Hz using a Hamming windowed sinc FIR filter (*pop_eegfiltnew* from the EEGLAB toolbox), Next, negative half-waves were detected from positive-to-negative zero crossings and selected as putative SWs if: the putative SW had an amplitude greater 2 x the signal median for all negative half-waves, a minimum length of 0.5 seconds and a maximum length of 2 seconds. These were liberal criteria which detected large numbers of negative half waves; this approach was chosen as we wished to investigate SW-spindle interactions, and therefore wished to maximise our sample of putative SWs. Furthermore, as it has been observed that the overall power of the EEG signal decreases from childhood to adolescence (Hahn et al., 2020), the use of an absolute threshold for SW detection could introduce bias in detections based on participant age. We therefore considered a relative threshold most appropriate for our dataset.

From each SW we extracted the amplitude (as the peak negative deflection), the duration (the time between the initial positive-to-negative zero crossing to the negative-to-positive zero crossing), and from the total set of SWs calculated the average SW density in events per minute, giving a total of 3 SW-related measures per electrode per subject (**Table 7**).

Spindle–SW Coupling

Spindle - SW coupling was measured using three metrics. First, we calculated the simple proportion of detected spindles whose peaks overlapped with any detected SWs, where overlap was defined as spindles whose peak sample fell within a window of +/- 1.5 seconds of the negative peak of a detected SW. Second, we calculated the mean resultant length (MRL) vector of the phase of the slow oscillation at the time of peak spindle amplitude, for spindles which overlapped

medRxiv preprint doi: https://doi.org/10.1101/2021.11.08.21266020; this version posted July 14, 2022. The copyright holder for this preprint (which was not certified by peer review) is the author/funder, who has granted medRxiv a license to display the preprint in perpetuity. It is made available under a CC-BY-NC-ND 4.0 International license .

an SW. The MRL metric was calculated as follows: the phase angle of the filtered slow oscillation signal was calculated using the Hilbert transform (where 0 degrees was the first positive-to-negative crossing of the SW). The phase value at the index of each spindle peak was taken, and the overall MRL for that signal was calculated as *mrl = abs(mean(exp(1i*phase)))*, where phase is a vector of all spindle peak phase values in a recording. Third, we took the mean angle of the SW phase at the peak of all SW-overlapping spindles where angle = *angle(mean(exp(1i*phase)))*. For the overlap and MRL measures, we converted the raw measure to a z-score relative to a resampling distribution calculated by randomly shuffling each spindle peak either within its local 30 second epoch (overlap measure) or shuffling only within the overlapping detected SW (MRL measure). This resampling procedure was repeated 1,000 times to create a null distribution from which the mean and standard deviation was calculated for deriving the z-score for each signal. We then calculated these three measures for each electrode, for each subject (**Supplementary Table 4**).

Statistical analysis

Following acquisition, preprocessing and feature identification and extraction, summary data were exported into R 4.1.0 (R Development Core Team, 2017) for statistical analysis.

Psychiatric, Sleep Architecture and Memory Data

Psychiatric and sleep architecture data were analyzed using a mixed model approach, with subject family entered into models as a random (varying) intercept, to account for the shared genetic and environmental influences within sibling pairs. Mixed models are also robust to missing data.

For memory task data, the number of learning cycles to reach the 30% performance criterion were modeled using mixed effects Cox Proportional Hazard Regression (*coxme* in the *coxme* package), with right censoring as some participants (22q11.2DS n = 6, siblings n = 0) completed numerous training cycles but never reached criterion before stopping the task.

Accuracy in the morning memory test was measured using a binomial model (*glmer* with *family = binomial(link = "logit")* in the *lme4 package* (Bates, 2010)) with the number of hits from the 15 trials

medRxiv preprint doi: https://doi.org/10.1101/2021.11.08.21266020; this version posted July 14, 2022. The copyright holder for this preprint (which was not certified by peer review) is the author/funder, who has granted medRxiv a license to display the preprint in perpetuity. It is made available under a CC-BY-NC-ND 4.0 International license .

as the dependent variable. In both models, genotype was the independent variable and age and sex were included as covariates, with family as a random intercept.

High-Density Sleep EEG Data

Our EEG dataset consisted of 21 EEG measures across 60 channels recorded in 45 participants (**Table 7**). As we used a high-density electrode array, we used multilevel generalized additive models (GAMM) applied to EEG data from all 60 electrodes in one model. The generalized additive model can model non-linear relationships, including spatial relationships, between variables using splines or other smoothers (Wood, 2004, 2017) and can, for example, be used to model complex or spatial relationships in models that also include covariates and random effects structures (Pedersen et al., 2019). In the case of EEG data, this allowed the estimation of a model than included the value of an EEG measure of interest (e.g., spindle density) at all 60 electrodes, with genotype, gender and age as a covariates and participant identity nested in their family identity as a random intercept, giving overall statistics for group differences.

This approach represents an extension of traditional EEG topographical plots, which present a smoothed interpolation of an EEG measure onto a 2D grid representing the head, by allowing the modelling of the relationship between multiple independent variables (and random effects) across the 2D representation of the head.

In order to fit these computationally intensive models consistently, we adopted a Bayesian approach, fitting the models using Hamiltonian Monte Carlo using the R *BRMS* package and Stan (Bürkner, 2017; Carpenter et al., 2017), with 4000 iterations (1000 warm up) on 4 chains, and regularizing priors (in keeping with (McElreath, 2018)). All model posterior information was inspected manually, and all Gelman-Rubin statistics (measures of model convergence) were close to 1.00, which is considered the optimal value. The formula used for all models (except for angular data) was *value ~ s(x, y, by = group, bs = "tp", k = 20, m = 2) + gender + age_eeg + group + (1|family) + (1|family:subject)*, where *value* was a placeholder for each EEG feature of interest, and *x* and *y* represented the 2D-projected x and y co-ordinate for each EEG electrode. This model fits an isotropic smooth with thin plate regression splines to the EEG measure across electrodes, with

medRxiv preprint doi: https://doi.org/10.1101/2021.11.08.21266020; this version posted July 14, 2022. The copyright holder for this preprint (which was not certified by peer review) is the author/funder, who has granted medRxiv a license to display the preprint in perpetuity. It is made available under a CC-BY-NC-ND 4.0 International license .

a separate smooth being estimated for 22q11.2DS and sibling controls. The model was fit was a normal distribution and an identity link function.

This approach allowed us to generate topographic plots of group differences by taking draws from the posterior fitted values of each model across a grid of spatial locations, for both 22q11.2DS and Siblings. From these posterior samples, we then calculated the genotype difference distribution, and from this, calculated the probability of direction statistic (Makowski et al., 2019), selecting spatial locations where the value of the statistic was less than 0.05 for further plotting.

Spindle-SW Coupling Angle Model

We modelled Spindle-SW Coupling angle (in radians) with a GAMM with a von Mises distribution (equivalent to a normal distribution on the circle) and a half tan link function. We modelled both the mean angle and kappa (the circular concentration parameter) to improve model fitting. The formula used for the angle model was: *overlap_angle ~ 0 + group + gender + age_eeg + s(x,y,by = group, bs = "tp", k = 20, m = 2) + (1|family) + (1|family:subject)*, *kappa ~ 0 + group + gender + age_eeg + s(x,y,by = group, bs = "tp", k = 20, m = 2) + (1|family) + (1|family:subject)*. We plot both the mean angle for coupling across the scalp, and model estimated angle differences between groups on topoplots with a circular color scale.

Memory Task – EEG Correlation Models

We analyzed the correlation between Sleep EEG measures and performance in the test session of our behavioral task the next morning. For each EEG measure and EEG electrode, we fit a generalized linear mixed model, with number of hits in the morning session as dependent variable, the interaction between an EEG measure and genotype as independent variable, and gender and age as covariates, with family identity as a random intercept, and a binomial distribution with logit link function. We then took p-values for the interaction term, corrected using a cluster-correction permutation testing approach with 500 permutations (Maris & Oostenveld, 2007), and plotted those electrodes where the EEG measure * genotype interaction was significant (cluster-corrected $p < 0.05$).

medRxiv preprint doi: https://doi.org/10.1101/2021.11.08.21266020; this version posted July 14, 2022. The copyright holder for this preprint (which was not certified by peer review) is the author/funder, who has granted medRxiv a license to display the preprint in perpetuity. It is made available under a CC-BY-NC-ND 4.0 International license .

EEG Mediation Models

We analyzed whether genotype effects on psychiatric symptoms or FSIQ were mediated by EEG measures using mediation models (Imai et al., 2010). Mediation analysis is a statistical technique which allows the estimation of whether the effect of one exposure (genotype) on an outcome (here a psychiatric measure or FSIQ) occurs via an effect of the exposure on a third variable (known as the mediator, here an EEG measure) or via a direct effect on the exposure. These models can be estimated by the combination of two statistical models predicting (1) the outcome from the exposure, mediator, and other covariates (including random effects) and (2) the mediator from the exposure, other covariates and random effects.

In our mediation analysis, we fit models for each pair of a psychiatric measure or IQ (ADHD, anxiety, ASD symptoms, psychotic experiences, CAPA sleep problems or FSIQ) and an EEG measure (focusing on the 4 measures where we observed raw group differences: REM constant, spindle amplitude, SW amplitude and spindle-SW MRL): one linear mixed model predicting the EEG measure from genotype, age and gender as covariates, and family as a random intercept; and one model predicting the psychiatric measure/IQ from genotype, EEG measure, age and gender, and family as a random intercept. The link function of the second model depended on the measure; poisson count models were used for symptom count data (ADHD, anxiety and ASD), a binomial model for psychotic experiences, or a linear model for FSIQ. These models were fit using the *lme4* package as above, then combined in a mediation analysis using the *mediate* function in the *R mediation* package (Imai et al., 2010). From each model we extracted the estimated direct and mediated effects, and the proportion mediated (the proportion of the total effect of genotype on the psychiatric measure/FSIQ mediated via the EEG measure) and constructed topographic plots of the proportion mediated. We derived p-values from mediation models using the cluster correction method by generating 500 shuffled datasets at each electrode, where group identity was permuted, and refit the models to each. We then plotted those electrodes where there was a cluster-corrected significant mediated effect by the given measure *and* a significant total effect on the same electrode.

medRxiv preprint doi: https://doi.org/10.1101/2021.11.08.21266020; this version posted July 14, 2022. The copyright holder for this preprint (which was not certified by peer review) is the author/funder, who has granted medRxiv a license to display the preprint in perpetuity. It is made available under a CC-BY-NC-ND 4.0 International license .

Source Data and Source Code File Legends

This manuscript contains the following source data and source code files:

- eLife Submission Data.zip
- eLife Submission Scripts.zip

These zip files contain data and R scripts which will reproduce the analysis and figures presented in the manuscript. Note that data files are in the .rds file format, which can be opened using the free open source R statistic programming language.

eLife Submission Data

The .zip file "eLife Submission Data.zip" contains data files which produce the analyses contains the following files:

- **sleep_study_beh_psych_demographic_data.rds:** Contains data for participant performance on the memory task, psychiatric and cognitive assessments and demographic data
- **sleep_study_eeg_coupling_example.rds**: Contains EEG data of an example spindle-SW interaction event, used to construct **Figure 4A**
- **sleep_study_eeg_locations.rds:** Contains the standardized locations of the EEG electrodes used throughout the study
- **sleep_study_eeg_neighbours.rds:** Contains the neighboring electrode for all 60 electrodes in the recording system used in our study, used in the cluster correction statistics utilized in **Figure 5B** and **Figure 6B**
- **sleep_study_eeg_spectrogram_example.rds:** Contains example whole night spectrograms for a sibling pair, with hypnogram and spindle and SW detection counts over the night, used in **Figure 3A-B**
- **sleep_study_eeg_summary_data.rds:** Contains summary EEG measures (one value per measure per electrode per participant) for the measures in **Table 7**. Data are in their own standard units.

medRxiv preprint doi: https://doi.org/10.1101/2021.11.08.21266020; this version posted July 14, 2022. The copyright holder for this preprint (which was not certified by peer review) is the author/funder, who has granted medRxiv a license to display the preprint in perpetuity. It is made available under a CC-BY-NC-ND 4.0 International license .

- **sleep_study_eeg_summary_data_z.rds:** Contains summary EEG measures (one value per measure per electrode per participant) for the measures in **Table 7**. Data are z scored.
- **sleep_study_epoch_removal.rds:** Contains data on the number of epochs removed by our artefact removal process (See **Methods and Materials/EEG data analysis/Pre-processing**)
- **sleep_study_example_so_waveforms_bootci.rds:** Contains example slow wave waveforms and bootstrapped 95% confidence intervals, used in **Figure 3D**
- **sleep_study_example_spindle_waveforms_bootci.rds:** Contains example spindle waveforms and bootstrapped 95% confidence intervals, used in **Figure 3C**
- **sleep_study_interaction_clusters.rds:** Contains the electrode locations and statistics for clusters of significant group*EEG measure interactions, used in **Figure 5B**
- **sleep_study_interaction_models.rds:** Contains fitted mixed models for group*EEG measure interactions, used in **Figure 5B**
- **sleep_study_mediation_plot.rds:** Contains cluster-corrected mediation models, used in **Figure 6B**
- **sleep_study_psd_bootci.rds:** Contains power spectral density plot data, with bootstrapped 95% confidence intervals, used in **Figure 2A-D**
- **sleep_study_psd_clusters.rds:** Contains the location of clusters of frequencies with significant group differences, used in **Figure 2A-D**
- **sleep_study_psd_data.rds:** Contains PSD data used to calculate group differences and for cluster correction, to derive the data in **sleep_study_psd_bootci.rds** and **sleep_study_psd_clusters.rds**
- **sleep_study_topoplot_angle_data.rds:** Contains posterior samples from the GAMM model fit to the coupling angle data. Used to construct the topoplot found in **Figure 4D**
- **sleep_study_topoplot_posterior_data.rds:** Contains posterior samples from the GAMM models used to construct group difference topoplots for the EEG measures in **Table 7** (except angular data, which is found in **sleep_study_topoplot_angle_data.rds.** Used to construct the topoplots found in **Figure 2E-G**, **Figure 3E-F** and **Figure 4C**

medRxiv preprint doi: https://doi.org/10.1101/2021.11.08.21266020; this version posted July 14, 2022. The copyright holder for this preprint (which was not certified by peer review) is the author/funder, who has granted medRxiv a license to display the preprint in perpetuity. It is made available under a CC-BY-NC-ND 4.0 International license .

eLife Submission Scripts

The .zip file "eLife Submission Data.zip" contains R scripts to reproduce the main figures and analysis. Scripts beginning with the prefix "Analysis" run computations which produce data used in tables and figures (and may run slowly); scripts beginning with the prefix "Figure" produce the figures themselves

The following files are included:

- **Analysis-Artefact-Removal.R**: Code to analyze the effect of artefact removal (See **Methods and Materials/EEG data analysis/Pre-processing**)
- **Analysis-Common-Utilities.R**: Code that contains common variables and functions used in the paper
- **Analysis-fitGAMMs.R**: Code that fits the Bayesian GAMMs and extracts posterior samples which produce the topoplots of group differences in **Figure 2E-G**, **Figure 3E-F** and **Figure 4C**
- **Analysis-fitMediationModels.R**: Code that fits the mediation models and performs cluster-based correction for multiple comparisons, producing data used to plot **Figure 6B**
- **Analysis-Interaction-Clusters.R**: Code that fits the EEG*genotype interaction models and performs cluster-based correction for multiple comparisons, producing data used to plot **Figure 5B**
- **Analysis-PSD-Clusters.R**: Code that fits models to the PSD data across multiple frequencies, and performs cluster-based correction for multiple comparisons, producing the data used to plot **Figure 2A-D**
- **Analysis-Tables-1-5.R**: Code that produces T**ables 1-5**, including the statistical tests presented in those tables
- **Figure-1-Revised.R**: Code to produce the elements of **Figure 1** and associated figure supplements
- **Figure-2-Revised.R**: Code to produce the elements of **Figure 2** and associated figure supplements
- **Figure-3-Revised.R:** Code to produce the elements of **Figure 3** and associated figure supplements
- **Figure-4-Revised.R:** Code to produce the elements of **Figure 4** and associated figure supplements
- **Figure-5-Revised.R R**: Code to produce the elements of **Figure 5**

medRxiv preprint doi: https://doi.org/10.1101/2021.11.08.21266020; this version posted July 14, 2022. The copyright holder for this preprint (which was not certified by peer review) is the author/funder, who has granted medRxiv a license to display the preprint in perpetuity. It is made available under a CC-BY-NC-ND 4.0 International license .

- **Figure-6-Revised.R R**: Code to produce the elements of **Figure 6** and **Table 7**

Acknowledgements

We are extremely grateful to all the families that participated in this study as well as to support charities Max Appeal, The 22Crew and Unique for their help and support. We thank the core laboratory team of the Division of Psychological Medicine and Clinical Neurosciences laboratory at Cardiff University for DNA sample management and genotyping, and the National Centre for Mental Health, a collaboration between Cardiff, Swansea and Bangor Universities, for their support. The authors would also like to thank Dr Ines Wilhelm for kindly donating the 2D object location task implementation.

medRxiv preprint doi: https://doi.org/10.1101/2021.11.08.21266020; this version posted July 14, 2022. The copyright holder for this preprint (which was not certified by peer review) is the author/funder, who has granted medRxiv a license to display the preprint in perpetuity. It is made available under a CC-BY-NC-ND 4.0 International license .

Disclosures

MO and MvdB report a research grant from Takeda pharmaceuticals outside the scope of the current study. UB and HM were full-time employees of Lilly UK during this study. The other authors report no financial interests or potential conflicts of interest.

This research was funded in part by the Wellcome Trust (grants listed above). For the purpose of Open Access, the authors have applied a CC BY public copyright license to any Author Accepted Manuscript version arising from this submission.

medRxiv preprint doi: https://doi.org/10.1101/2021.11.08.21266020; this version posted July 14, 2022. The copyright holder for this preprint (which was not certified by peer review) is the author/funder, who has granted medRxiv a license to display the preprint in perpetuity. It is made available under a CC-BY-NC-ND 4.0 International license .

References

Adamantidis, A. R., Gutierrez Herrera, C., & Gent, T. C. (2019). Oscillating circuitries in the sleeping brain. *Nature Reviews. Neuroscience*, *20*(12), 746–762. https://doi.org/10.1038/s41583-019-0223-4

Al-Absi, A.-R., Qvist, P., Okujeni, S., Khan, A. R., Glerup, S., Sanchez, C., & Nyengaard, J. R. (2020). Layers II/III of Prefrontal Cortex in Df(h22q11)/+ Mouse Model of the 22q11.2 Deletion Display Loss of Parvalbumin Interneurons and Modulation of Neuronal Morphology and Excitability. *Molecular Neurobiology*, *57*(12), 4978–4988. https://doi.org/10.1007/s12035-020-02067-1

Angold, A., Prendergast, M., Cox, A., Harrington, R., Simonoff, E., & Rutter, M. (1995). The Child and Adolescent Psychiatric Assessment (CAPA). *Psychological Medicine*, *25*(4), 739–753. https://doi.org/10.1017/s003329170003498x

Angriman, M., Caravale, B., Novelli, L., Ferri, R., & Bruni, O. (2015). Sleep in Children with Neurodevelopmental Disabilities. *Neuropediatrics*, *46*(03), 199–210. https://doi.org/10.1055/s-0035-1550151

Bagautdinova, J., Zöller, D., Schaer, M., Padula, M. C., Mancini, V., Schneider, M., & Eliez, S. (2021). Altered cortical thickness development in 22q11.2 deletion syndrome and association with psychotic symptoms. *Molecular Psychiatry*, *26*(12), 7671–7678. https://doi.org/10.1038/s41380-021-01209-8

Bandarabadi, M., Herrera, C. G., Gent, T. C., Bassetti, C., Schindler, K., & Adamantidis, A. R. (2020). A role for spindles in the onset of rapid eye movement sleep. *Nature Communications, 11*. https://doi.org/10.1038/s41467-020-19076-2

Bartsch, U., Simpkin, A. J., Demanuele, C., Wamsley, E., Marston, H. M., & Jones, M. W. (2019). Distributed slow-wave dynamics during sleep predict memory consolidation and its impairment in schizophrenia. *NPJ Schizophrenia*, *5*(1), 18. https://doi.org/10.1038/s41537-019-0086-8

Bates, D. M. (2010). *lme4: Mixed-effects modeling with R*. http://lme4.r-forge.r-project.org/lMMwR/lrgprt.pdf

medRxiv preprint doi: https://doi.org/10.1101/2021.11.08.21266020; this version posted July 14, 2022. The copyright holder for this preprint (which was not certified by peer review) is the author/funder, who has granted medRxiv a license to display the preprint in perpetuity. It is made available under a CC-BY-NC-ND 4.0 International license .

Bigdely-Shamlo, N., Mullen, T., Kothe, C., Su, K.-M., & Robbins, K. A. (2015). The PREP pipeline: Standardized preprocessing for large-scale EEG analysis. *Frontiers in Neuroinformatics*, *9*. https://doi.org/10.3389/fninf.2015.00016

Bokil, H., Andrews, P., Kulkarni, J. E., Mehta, S., & Mitra, P. P. (2010). Chronux: A platform for analyzing neural signals. *Journal of Neuroscience Methods*, *192*(1), 146–151. https://doi.org/10.1016/j.jneumeth.2010.06.020

Buckelmüller, J., Landolt, H.-P., Stassen, H. H., & Achermann, P. (2006). Trait-like individual differences in the human sleep electroencephalogram. *Neuroscience*, *138*(1), 351–356. https://doi.org/10.1016/j.neuroscience.2005.11.005

Bürkner, P.-C. (2017). brms: An R Package for Bayesian Multilevel Models Using Stan. *Journal of Statistical Software*, *80*(1), 1–28. https://doi.org/10.18637/jss.v080.i01

Carpenter, B., Gelman, A., Hoffman, M. D., Lee, D., Goodrich, B., Betancourt, M., Brubaker, M., Guo, J., Li, P., & Riddell, A. (2017). Stan: A Probabilistic Programming Language. *Journal of Statistical Software*, *76*(1), 1–32. https://doi.org/10.18637/jss.v076.i01

Castelnovo, A., Graziano, B., Ferrarelli, F., & D'Agostino, A. (2017). Sleep spindles and slow waves in schizophrenia and related disorders: Main findings, challenges and future perspectives. *The European Journal of Neuroscience*. https://doi.org/10.1111/ejn.13815

Chawner, S. J. R. A., Niarchou, M., Doherty, J. L., Moss, H., Owen, M. J., & van den Bree, M. B. M. (2019). The emergence of psychotic experiences in the early adolescence of 22q11.2 Deletion Syndrome. *Journal of Psychiatric Research*, *109*, 10–17. https://doi.org/10.1016/j.jpsychires.2018.11.002

Ching, C. R. K., Gutman, B. A., Sun, D., Villalon Reina, J., Ragothaman, A., Isaev, D., Zavaliangos-Petropulu, A., Lin, A., Jonas, R. K., Kushan, L., Pacheco-Hansen, L., Vajdi, A., Forsyth, J. K., Jalbrzikowski, M., Bakker, G., van Amelsvoort, T., Antshel, K. M., Fremont, W., Kates, W. R., … Bearden, C. E. (2020). Mapping Subcortical Brain Alterations in 22q11.2 Deletion Syndrome: Effects of Deletion Size and Convergence With Idiopathic Neuropsychiatric Illness. *The American Journal of Psychiatry*, *177*(7), 589–600. https://doi.org/10.1176/appi.ajp.2019.19060583

medRxiv preprint doi: https://doi.org/10.1101/2021.11.08.21266020; this version posted July 14, 2022. The copyright holder for this preprint (which was not certified by peer review) is the author/funder, who has granted medRxiv a license to display the preprint in perpetuity. It is made available under a CC-BY-NC-ND 4.0 International license .

Chouinard, S., Poulin, J., Stip, E., & Godbout, R. (2004). Sleep in untreated patients with schizophrenia: A meta-analysis. *Schizophrenia Bulletin*, *30*(4), 957–967. https://doi.org/10.1093/oxfordjournals.schbul.a007145

Cohrs, S. (2008). Sleep disturbances in patients with schizophrenia: Impact and effect of antipsychotics. *CNS Drugs*, *22*(11), 939–962. https://doi.org/10.2165/00023210-200822110-00004

Cortese, S., Faraone, S. V., Konofal, E., & Lecendreux, M. (2009). Sleep in children with attention-deficit/hyperactivity disorder: Meta-analysis of subjective and objective studies. *Journal of the American Academy of Child and Adolescent Psychiatry*, *48*(9), 894–908. https://doi.org/10.1097/CHI.0b013e3181ac09c9

Cunningham, A. C., Delport, S., Cumines, W., Busse, M., Linden, D. E. J., Hall, J., Owen, M. J., & van den Bree, M. B. M. (2018). Developmental coordination disorder, psychopathology and IQ in 22q11.2 deletion syndrome. *The British Journal of Psychiatry: The Journal of Mental Science*, *212*(1), 27–33. https://doi.org/10.1192/bjp.2017.6

Delorme, A., & Makeig, S. (2004). EEGLAB: An open source toolbox for analysis of single-trial EEG dynamics including independent component analysis. *Journal of Neuroscience Methods*, *134*(1), 9–21. https://doi.org/10.1016/j.jneumeth.2003.10.009

Delorme, A., Palmer, J., Onton, J., Oostenveld, R., & Makeig, S. (2012). Independent EEG Sources Are Dipolar. *PLOS ONE*, *7*(2), e30135. https://doi.org/10.1371/journal.pone.0030135

Demanuele, C., Bartsch, U., Baran, B., Khan, S., Vangel, M. G., Cox, R., Hämäläinen, M., Jones, M. W., Stickgold, R., & Manoach, D. S. (2017). Coordination of Slow Waves With Sleep Spindles Predicts Sleep-Dependent Memory Consolidation in Schizophrenia. *Sleep*, *40*(1). https://doi.org/10.1093/sleep/zsw013

Djonlagic, I., Mariani, S., Fitzpatrick, A. L., Van Der Klei, V. M. G. T. H., Johnson, D. A., Wood, A. C., Seeman, T., Nguyen, H. T., Prerau, M. J., Luchsinger, J. A., Dzierzewski, J. M., Rapp, S. R., Tranah, G. J., Yaffe, K., Burdick, K. E., Stone, K. L., Redline, S., & Purcell, S. M. (2020). Macro and micro sleep

medRxiv preprint doi: https://doi.org/10.1101/2021.11.08.21266020; this version posted July 14, 2022. The copyright holder for this preprint (which was not certified by peer review) is the author/funder, who has granted medRxiv a license to display the preprint in perpetuity. It is made available under a CC-BY-NC-ND 4.0 International license .

architecture and cognitive performance in older adults. *Nature Human Behaviour*. https://doi.org/10.1038/s41562-020-00964-y

Dubé, J., Lafortune, M., Bedetti, C., Bouchard, M., Gagnon, J. F., Doyon, J., Evans, A. C., Lina, J.-M., & Carrier, J. (2015). Cortical thinning explains changes in sleep slow waves during adulthood. *The Journal of Neuroscience: The Official Journal of the Society for Neuroscience*, *35*(20), 7795–7807. https://doi.org/10.1523/JNEUROSCI.3956-14.2015

Eaton, C. B., Thomas, R. H., Hamandi, K., Payne, G. C., Kerr, M. P., Linden, D. E. J., Owen, M. J., Cunningham, A. C., Bartsch, U., Struik, S. S., & van den Bree, M. B. M. (2019). Epilepsy and seizures in young people with 22q11.2 deletion syndrome: Prevalence and links with other neurodevelopmental disorders. *Epilepsia*, *60*(5), 818–829. https://doi.org/10.1111/epi.14722

Feld, G. B., & Born, J. (2020). Neurochemical mechanisms for memory processing during sleep: Basic findings in humans and neuropsychiatric implications. *Neuropsychopharmacology: Official Publication of the American College of Neuropsychopharmacology*, *45*(1), 31–44. https://doi.org/10.1038/s41386-019-0490-9

Feld, G. B., Wilhelm, I., Ma, Y., Groch, S., Binkofski, F., Mölle, M., & Born, J. (2013). Slow wave sleep induced by GABA agonist tiagabine fails to benefit memory consolidation. *Sleep*, *36*(9), 1317–1326. https://doi.org/10.5665/sleep.2954

Ferrarelli, F., Huber, R., Peterson, M. J., Massimini, M., Murphy, M., Riedner, B. A., Watson, A., Bria, P., & Tononi, G. (2007). Reduced sleep spindle activity in schizophrenia patients. *The American Journal of Psychiatry*, *164*(3), 483–492. https://doi.org/10.1176/ajp.2007.164.3.483

Ferrarelli, F., Peterson, M. J., Sarasso, S., Riedner, B. A., Murphy, M. J., Benca, R. M., Bria, P., Kalin, N. H., & Tononi, G. (2010). Thalamic dysfunction in schizophrenia suggested by whole-night deficits in slow and fast spindles. *The American Journal of Psychiatry*, *167*(11), 1339–1348. https://doi.org/10.1176/appi.ajp.2010.09121731

medRxiv preprint doi: https://doi.org/10.1101/2021.11.08.21266020; this version posted July 14, 2022. The copyright holder for this preprint (which was not certified by peer review) is the author/funder, who has granted medRxiv a license to display the preprint in perpetuity. It is made available under a CC-BY-NC-ND 4.0 International license .

Ferrarelli, F., & Tononi, G. (2017). Reduced sleep spindle activity point to a TRN-MD thalamus-PFC circuit dysfunction in schizophrenia. *Schizophrenia Research*, *180*, 36–43. https://doi.org/10.1016/j.schres.2016.05.023

Furrer, M., Jaramillo, V., Volk, C., Ringli, M., Aellen, R., Wehrle, F. M., Pugin, F., Kurth, S., Brandeis, D., Schmid, M., Jenni, O. G., & Huber, R. (2019). Sleep EEG slow-wave activity in medicated and unmedicated children and adolescents with attention-deficit/hyperactivity disorder. *Translational Psychiatry*, *9*(1), 324. https://doi.org/10.1038/s41398-019-0659-3

Gardner, R. J., Kersanté, F., Jones, M. W., & Bartsch, U. (2014). Neural oscillations during non-rapid eye movement sleep as biomarkers of circuit dysfunction in schizophrenia. *The European Journal of Neuroscience*, *39*(7), 1091–1106. https://doi.org/10.1111/ejn.12533

Gerstenberg, M., Furrer, M., Tesler, N., Franscini, M., Walitza, S., & Huber, R. (2020). Reduced sleep spindle density in adolescent patients with early-onset schizophrenia compared to major depressive disorder and healthy controls. *Schizophrenia Research*, *221*, 20–28. https://doi.org/10.1016/j.schres.2019.11.060

Göder, R., Graf, A., Ballhausen, F., Weinhold, S., Baier, P. C., Junghanns, K., & Prehn-Kristensen, A. (2015). Impairment of sleep-related memory consolidation in schizophrenia: Relevance of sleep spindles? *Sleep Medicine*, *16*(5), 564–569. https://doi.org/10.1016/j.sleep.2014.12.022

Gorgoni, M., Scarpelli, S., Reda, F., & De Gennaro, L. (2020). Sleep EEG oscillations in neurodevelopmental disorders without intellectual disabilities. *Sleep Medicine Reviews*, *49*, 101224. https://doi.org/10.1016/j.smrv.2019.101224

Hahn, M. A., Bothe, K., Heib, D., Schabus, M., Helfrich, R. F., & Hoedlmoser, K. (2022). Slow oscillation-spindle coupling strength predicts real-life gross-motor learning in adolescents and adults. *ELife*, *11*, e66761. https://doi.org/10.7554/eLife.66761

Hahn, M. A., Heib, D., Schabus, M., Hoedlmoser, K., & Helfrich, R. F. (2020). Slow oscillation-spindle coupling predicts enhanced memory formation from childhood to adolescence. *ELife*, *9*. https://doi.org/10.7554/eLife.53730

medRxiv preprint doi: https://doi.org/10.1101/2021.11.08.21266020; this version posted July 14, 2022. The copyright holder for this preprint (which was not certified by peer review) is the author/funder, who has granted medRxiv a license to display the preprint in perpetuity. It is made available under a CC-BY-NC-ND 4.0 International license .

Helfrich, R. F., Mander, B. A., Jagust, W. J., Knight, R. T., & Walker, M. P. (2018). Old Brains Come Uncoupled in Sleep: Slow Wave-Spindle Synchrony, Brain Atrophy, and Forgetting. *Neuron*, *97*(1), 221-230.e4. https://doi.org/10.1016/j.neuron.2017.11.020

Hill, A. T., Clark, G. M., Bigelow, F. J., Lum, J. A. G., & Enticott, P. G. (2022). Periodic and aperiodic neural activity displays age-dependent changes across early-to-middle childhood. *Developmental Cognitive Neuroscience*, *54*, 101076. https://doi.org/10.1016/j.dcn.2022.101076

Hjorth, B. (1970). EEG analysis based on time domain properties. *Electroencephalography and Clinical Neurophysiology*, *29*(3), 306–310. https://doi.org/10.1016/0013-4694(70)90143-4

Imai, K., Keele, L., & Tingley, D. (2010). A general approach to causal mediation analysis. *Psychological Methods*, *15*(4), 309–334. https://doi.org/10.1037/a0020761

Jenni, O. G., & Carskadon, M. A. (2004). Spectral analysis of the sleep electroencephalogram during adolescence. *Sleep*, *27*(4), 774–783.

Karayiorgou, M., Morris, M. A., Morrow, B., Shprintzen, R. J., Goldberg, R., Borrow, J., Gos, A., Nestadt, G., Wolyniec, P. S., & Lasseter, V. K. (1995). Schizophrenia susceptibility associated with interstitial deletions of chromosome 22q11. *Proceedings of the National Academy of Sciences of the United States of America*, *92*(17), 7612–7616.

Keshavan, M. S., Reynolds, C. F., Miewald, M. J., Montrose, D. M., Sweeney, J. A., Vasko, R. C., & Kupfer, D. J. (1998). Delta sleep deficits in schizophrenia: Evidence from automated analyses of sleep data. *Archives of General Psychiatry*, *55*(5), 443–448. https://doi.org/10.1001/archpsyc.55.5.443

Kozhemiako, N., Mylonas, D., Pan, J. Q., Prerau, M. J., Redline, S., & Purcell, S. M. (2021). *Sources of variation in the spectral slope of the sleep EEG* (p. 2021.11.08.467763). https://doi.org/10.1101/2021.11.08.467763

Lai, M., Hegde, R., Kelly, S., Bannai, D., Lizano, P., Stickgold, R., Manoach, D. S., & Keshavan, M. (2022). Investigating sleep spindle density and schizophrenia: A meta-analysis. *Psychiatry Research*, *307*, 114265. https://doi.org/10.1016/j.psychres.2021.114265

medRxiv preprint doi: https://doi.org/10.1101/2021.11.08.21266020; this version posted July 14, 2022. The copyright holder for this preprint (which was not certified by peer review) is the author/funder, who has granted medRxiv a license to display the preprint in perpetuity. It is made available under a CC-BY-NC-ND 4.0 International license .

Latchoumane, C.-F. V., Ngo, H.-V. V., Born, J., & Shin, H.-S. (2017). Thalamic Spindles Promote Memory Formation during Sleep through Triple Phase-Locking of Cortical, Thalamic, and Hippocampal Rhythms. *Neuron*, *95*(2), 424-435.e6. https://doi.org/10.1016/j.neuron.2017.06.025

Lehoux, T., Carrier, J., & Godbout, R. (2019). NREM sleep EEG slow waves in autistic and typically developing children: Morphological characteristics and scalp distribution. *Journal of Sleep Research*, *28*(4), e12775. https://doi.org/10.1111/jsr.12775

Lendner, J. D., Helfrich, R. F., Mander, B. A., Romundstad, L., Lin, J. J., Walker, M. P., Larsson, P. G., & Knight, R. T. (2020). An electrophysiological marker of arousal level in humans. *ELife*, *9*, e55092. https://doi.org/10.7554/eLife.55092

Lin, A., Ching, C. R. K., Vajdi, A., Sun, D., Jonas, R. K., Jalbrzikowski, M., Kushan-Wells, L., Pacheco Hansen, L., Krikorian, E., Gutman, B., Dokoru, D., Helleman, G., Thompson, P. M., & Bearden, C. E. (2017). Mapping 22q11.2 Gene Dosage Effects on Brain Morphometry. *Journal of Neuroscience*, *37*(26), 6183–6199.

Lunsford-Avery, J. R., Krystal, A. D., & Kollins, S. H. (2016). Sleep disturbances in adolescents with ADHD: A systematic review and framework for future research. *Clinical Psychology Review*, *50*, 159–174. https://doi.org/10.1016/j.cpr.2016.10.004

Makowski, D., Ben-Shachar, M. S., & Lüdecke, D. (2019). bayestestR: Describing Effects and their Uncertainty, Existence and Significance within the Bayesian Framework. *Journal of Open Source Software*, *4*(40), 1541. https://doi.org/10.21105/joss.01541

Manoach, D. S., Pan, J. Q., Purcell, S. M., & Stickgold, R. (2016). Reduced Sleep Spindles in Schizophrenia: A Treatable Endophenotype That Links Risk Genes to Impaired Cognition? *Biological Psychiatry*, *80*(8), 599–608. https://doi.org/10.1016/j.biopsych.2015.10.003

Manoach, D. S., & Stickgold, R. (2019). Abnormal Sleep Spindles, Memory Consolidation, and Schizophrenia. *Annual Review of Clinical Psychology*, *15*, 451–479. https://doi.org/10.1146/annurev-clinpsy-050718-095754

medRxiv preprint doi: https://doi.org/10.1101/2021.11.08.21266020; this version posted July 14, 2022. The copyright holder for this preprint (which was not certified by peer review) is the author/funder, who has granted medRxiv a license to display the preprint in perpetuity. It is made available under a CC-BY-NC-ND 4.0 International license .

Maris, E., & Oostenveld, R. (2007). Nonparametric statistical testing of EEG- and MEG-data. *Journal of Neuroscience Methods*, *164*(1), 177–190. https://doi.org/10.1016/j.jneumeth.2007.03.024

Markovic, A., Kaess, M., & Tarokh, L. (2020). Gender differences in adolescent sleep neurophysiology: A high-density sleep EEG study. *Scientific Reports*, *10*. https://doi.org/10.1038/s41598-020-72802-0

Maski, K., Holbrook, H., Manoach, D., Hanson, E., Kapur, K., & Stickgold, R. (2015). Sleep Dependent Memory Consolidation in Children with Autism Spectrum Disorder. *Sleep*, *38*(12), 1955–1963. https://doi.org/10.5665/sleep.5248

Maurer, G. W., Malita, A., Nagy, S., Koyama, T., Werge, T. M., Halberg, K. A., Texada, M. J., & Rewitz, K. (2020). Analysis of genes within the schizophrenia-linked 22q11.2 deletion identifies interaction of night owl/LZTR1 and NF1 in GABAergic sleep control. *PLOS Genetics*, *16*(4), e1008727. https://doi.org/10.1371/journal.pgen.1008727

McElreath, R. (2018). Statistical Rethinking: A Bayesian Course with Examples in R and Stan. In *Statistical Rethinking: A Bayesian Course with Examples in R and Stan* (p. 469). https://doi.org/10.1201/9781315372495

Merikanto, I., Utge, S., Lahti, J., Kuula, L., Makkonen, T., Lahti-Pulkkinen, M., Heinonen, K., Räikkönen, K., Andersson, S., Strandberg, T., & Pesonen, A.-K. (2019). Genetic risk factors for schizophrenia associate with sleep spindle activity in healthy adolescents. *Journal of Sleep Research*, *28*(1), e12762. https://doi.org/10.1111/jsr.12762

Monks, S., Niarchou, M., Davies, A. R., Walters, J. T. R., Williams, N., Owen, M. J., van den Bree, M. B. M., & Murphy, K. C. (2014). Further evidence for high rates of schizophrenia in 22q11.2 deletion syndrome. *Schizophrenia Research*, *153*(1), 231–236. https://doi.org/10.1016/j.schres.2014.01.020

Moulding, H. A., Bartsch, U., Hall, J., Jones, M. W., Linden, D. E., Owen, M. J., & van den Bree, M. B. M. (2020). Sleep problems and associations with psychopathology and cognition in young people with 22q11.2 deletion syndrome (22q11.2DS). *Psychological Medicine*, *50*(7), 1191–1202. https://doi.org/10.1017/S0033291719001119

medRxiv preprint doi: https://doi.org/10.1101/2021.11.08.21266020; this version posted July 14, 2022. The copyright holder for this preprint (which was not certified by peer review) is the author/funder, who has granted medRxiv a license to display the preprint in perpetuity. It is made available under a CC-BY-NC-ND 4.0 International license .

Mullen, T. R., Kothe, C. A. E., Chi, Y. M., Ojeda, A., Kerth, T., Makeig, S., Jung, T.-P., & Cauwenberghs, G. (2015). Real-Time Neuroimaging and Cognitive Monitoring Using Wearable Dry EEG. *IEEE Transactions on Bio-Medical Engineering*, *62*(11), 2553–2567. https://doi.org/10.1109/TBME.2015.2481482

Nakao, T., Radua, J., Rubia, K., & Mataix-Cols, D. (2011). Gray matter volume abnormalities in ADHD: Voxel-based meta-analysis exploring the effects of age and stimulant medication. *The American Journal of Psychiatry*, *168*(11), 1154–1163. https://doi.org/10.1176/appi.ajp.2011.11020281

Niarchou, M., Chawner, S. J. R. A., Fiksinski, A., Vorstman, J. A. S., Maeder, J., Schneider, M., Eliez, S., Armando, M., Pontillo, M., Vicari, S., McDonald-McGinn, D. M., Emanuel, B. S., Zackai, E. H., Bearden, C. E., Shashi, V., Hooper, S. R., Owen, M. J., Gur, R. E., Wray, N. R., … International 22q11.2 Deletion Syndrome Brain and Behavior Consortium. (2019). Attention deficit hyperactivity disorder symptoms as antecedents of later psychotic outcomes in 22q11.2 deletion syndrome. *Schizophrenia Research*, *204*, 320–325. https://doi.org/10.1016/j.schres.2018.07.044

Niarchou, M., Zammit, S., van Goozen, S. H. M., Thapar, A., Tierling, H. M., Owen, M. J., & van den Bree, M. B. M. (2014). Psychopathology and cognition in children with 22q11.2 deletion syndrome. *The British Journal of Psychiatry: The Journal of Mental Science*, *204*(1), 46–54. https://doi.org/10.1192/bjp.bp.113.132324

Pedersen, E. J., Miller, D. L., Simpson, G. L., & Ross, N. (2019). Hierarchical generalized additive models in ecology: An introduction with mgcv. *PeerJ*, *7*, e6876. https://doi.org/10.7717/peerj.6876

Pion-Tonachini, L., Kreutz-Delgado, K., & Makeig, S. (2019). ICLabel: An automated electroencephalographic independent component classifier, dataset, and website. *NeuroImage*, *198*, 181–197. https://doi.org/10.1016/j.neuroimage.2019.05.026

Prehn-Kristensen, A., Göder, R., Fischer, J., Wilhelm, I., Seeck-Hirschner, M., Aldenhoff, J., & Baving, L. (2011). Reduced sleep-associated consolidation of declarative memory in attention-deficit/hyperactivity disorder. *Sleep Medicine*, *12*(7), 672–679. https://doi.org/10.1016/j.sleep.2010.10.010

medRxiv preprint doi: https://doi.org/10.1101/2021.11.08.21266020; this version posted July 14, 2022. The copyright holder for this preprint (which was not certified by peer review) is the author/funder, who has granted medRxiv a license to display the preprint in perpetuity. It is made available under a CC-BY-NC-ND 4.0 International license .

Purcell, S. M., Manoach, D. S., Demanuele, C., Cade, B. E., Mariani, S., Cox, R., Panagiotaropoulou, G., Saxena, R., Pan, J. Q., Smoller, J. W., Redline, S., & Stickgold, R. (2017). Characterizing sleep spindles in 11,630 individuals from the National Sleep Research Resource. *Nature Communications*, *8*. https://doi.org/10.1038/ncomms15930

R Development Core Team. (2017). R: A Language and environment for statistical computing. *Vienna, Austria: R Foundation for Statistical Computing*.

Ramanathan, S., Mattiaccio, L. M., Coman, I. L., Botti, J.-A. C., Fremont, W., Faraone, S. V., Antshel, K. M., & Kates, W. R. (2017). Longitudinal trajectories of cortical thickness as a biomarker for psychosis in individuals with 22q11.2 deletion syndrome. *Schizophrenia Research*, *188*, 35–41. https://doi.org/10.1016/j.schres.2016.11.041

Rutter, M., Bailey, A., & Lord, C. (2003). *The Social Communication Questionnaire – Manual*. Western Psychological Services.

Schaer, M., Debbané, M., Bach Cuadra, M., Ottet, M.-C., Glaser, B., Thiran, J.-P., & Eliez, S. (2009). Deviant trajectories of cortical maturation in 22q11.2 deletion syndrome (22q11DS): A cross-sectional and longitudinal study. *Schizophrenia Research*, *115*(2–3), 182–190. https://doi.org/10.1016/j.schres.2009.09.016

Schneider, M., Debbané, M., Bassett, A. S., Chow, E. W. C., Fung, W. L. A., van den Bree, M., Owen, M., Murphy, K. C., Niarchou, M., Kates, W. R., Antshel, K. M., Fremont, W., McDonald-McGinn, D. M., Gur, R. E., Zackai, E. H., Vorstman, J., Duijff, S. N., Klaassen, P. W. J., Swillen, A., … International Consortium on Brain and Behavior in 22q11.2 Deletion Syndrome. (2014). Psychiatric disorders from childhood to adulthood in 22q11.2 deletion syndrome: Results from the International Consortium on Brain and Behavior in 22q11.2 Deletion Syndrome. *The American Journal of Psychiatry*, *171*(6), 627–639. https://doi.org/10.1176/appi.ajp.2013.13070864

Shaw, P., Gogtay, N., & Rapoport, J. (2010). Childhood psychiatric disorders as anomalies in neurodevelopmental trajectories. *Human Brain Mapping*, *31*(6), 917–925. https://doi.org/10.1002/hbm.21028

medRxiv preprint doi: https://doi.org/10.1101/2021.11.08.21266020; this version posted July 14, 2022. The copyright holder for this preprint (which was not certified by peer review) is the author/funder, who has granted medRxiv a license to display the preprint in perpetuity. It is made available under a CC-BY-NC-ND 4.0 International license .

Shaw, P., Lerch, J., Greenstein, D., Sharp, W., Clasen, L., Evans, A., Giedd, J., Castellanos, F. X., & Rapoport, J. (2006). Longitudinal mapping of cortical thickness and clinical outcome in children and adolescents with attention-deficit/hyperactivity disorder. *Archives of General Psychiatry*, *63*(5), 540–549. https://doi.org/10.1001/archpsyc.63.5.540

Sønderby, I. E., Ching, C. R. K., Thomopoulos, S. I., van der Meer, D., Sun, D., Villalon-Reina, J. E., Agartz, I., Amunts, K., Arango, C., Armstrong, N. J., Ayesa-Arriola, R., Bakker, G., Bassett, A. S., Boomsma, D. I., Bülow, R., Butcher, N. J., Calhoun, V. D., Caspers, S., Chow, E. W. C., … ENIGMA 22q11.2 Deletion Syndrome Working Group. (2021). Effects of copy number variations on brain structure and risk for psychiatric illness: Large-scale studies from the ENIGMA working groups on CNVs. *Human Brain Mapping*. https://doi.org/10.1002/hbm.25354

Sun, D., Ching, C. R. K., Lin, A., Forsyth, J. K., Kushan, L., Vajdi, A., Jalbrzikowski, M., Hansen, L., Villalon-Reina, J. E., Qu, X., Jonas, R. K., van Amelsvoort, T., Bakker, G., Kates, W. R., Antshel, K. M., Fremont, W., Campbell, L. E., McCabe, K. L., Daly, E., … Bearden, C. E. (2020). Large-scale mapping of cortical alterations in 22q11.2 deletion syndrome: Convergence with idiopathic psychosis and effects of deletion size. *Molecular Psychiatry*, *25*(8), 1822–1834. https://doi.org/10.1038/s41380-018-0078-5

Tarokh, L., & Carskadon, M. A. (2010). Developmental Changes in the Human Sleep EEG During Early Adolescence. *Sleep*, *33*(6), 801–809.

Ulrich, D., Lalanne, T., Gassmann, M., & Bettler, B. (2018). GABAB receptor subtypes differentially regulate thalamic spindle oscillations. *Neuropharmacology*, *136*, 106–116. https://doi.org/10.1016/j.neuropharm.2017.10.033

Vingerhoets, C., Tse, D. H., van Oudenaren, M., Hernaus, D., van Duin, E., Zinkstok, J., Ramaekers, J. G., Jansen, J. F., McAlonan, G., & van Amelsvoort, T. (2020). Glutamatergic and GABAergic reactivity and cognition in 22q11.2 deletion syndrome and healthy volunteers: A randomized double-blind 7-Tesla pharmacological MRS study. *Journal of Psychopharmacology (Oxford, England)*, *34*(8), 856–863. https://doi.org/10.1177/0269881120922977

medRxiv preprint doi: https://doi.org/10.1101/2021.11.08.21266020; this version posted July 14, 2022. The copyright holder for this preprint (which was not certified by peer review) is the author/funder, who has granted medRxiv a license to display the preprint in perpetuity. It is made available under a CC-BY-NC-ND 4.0 International license .

Voytek, B., Kramer, M. A., Case, J., Lepage, K. Q., Tempesta, Z. R., Knight, R. T., & Gazzaley, A. (2015). Age-Related Changes in 1/f Neural Electrophysiological Noise. *The Journal of Neuroscience: The Official Journal of the Society for Neuroscience*, *35*(38), 13257–13265. https://doi.org/10.1523/JNEUROSCI.2332-14.2015

Wamsley, E. J., Tucker, M. A., Shinn, A. K., Ono, K. E., McKinley, S. K., Ely, A. V., Goff, D. C., Stickgold, R., & Manoach, D. S. (2012). Reduced sleep spindles and spindle coherence in schizophrenia: Mechanisms of impaired memory consolidation? *Biological Psychiatry*, *71*(2), 154–161. https://doi.org/10.1016/j.biopsych.2011.08.008

Wechsler, D. (1999). *Wechsler Abbreviated Scale of Intelligence*. Psychological Corporation.

Wen, H., & Liu, Z. (2016). Separating Fractal and Oscillatory Components in the Power Spectrum of Neurophysiological Signal. *Brain Topography*, *29*(1), 13–26. https://doi.org/10.1007/s10548-015-0448-0

Wilhelm, I., Diekelmann, S., & Born, J. (2008). Sleep in children improves memory performance on declarative but not procedural tasks. *Learning & Memory*, *15*(5), 373–377. https://doi.org/10.1101/lm.803708

Wood, S. N. (2004). Stable and Efficient Multiple Smoothing Parameter Estimation for Generalized Additive Models. *Journal of the American Statistical Association*, *99*(467), 673–686.

Wood, S. N. (2017). *Generalized Additive Models: An Introduction with R, Second Edition*. Routledge & CRC Press. https://www.routledge.com/Generalized-Additive-Models-An-Introduction-with-R-Second-Edition/Wood/p/book/9781498728331

Zhang, Z. Y., Campbell, I. G., Dhayagude, P., Espino, H. C., & Feinberg, I. (2021). Longitudinal Analysis of Sleep Spindle Maturation from Childhood through Late Adolescence. *The Journal of Neuroscience: The Official Journal of the Society for Neuroscience*, *41*(19), 4253–4261. https://doi.org/10.1523/JNEUROSCI.2370-20.2021

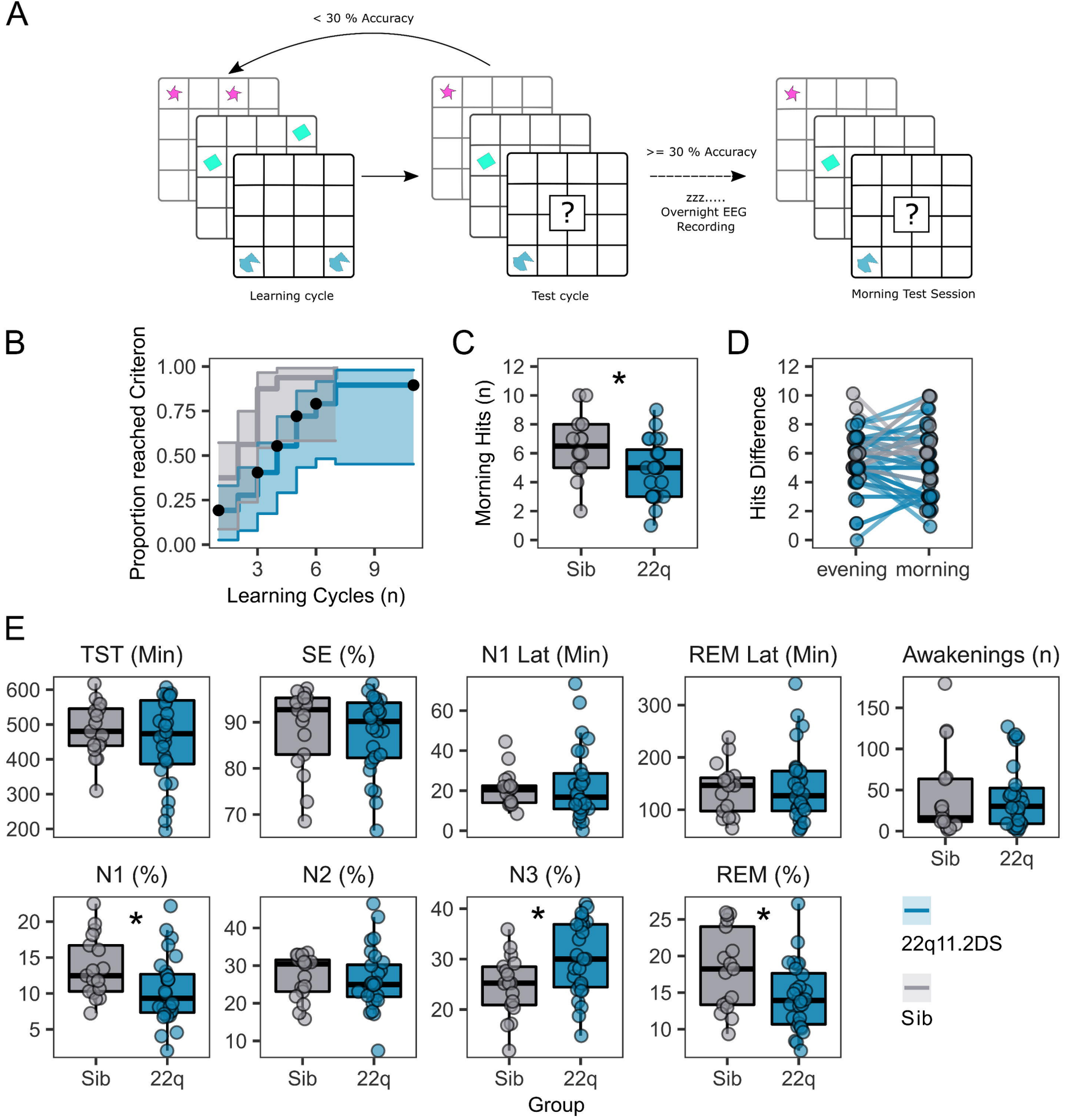
A
< 30 % Accuracy
>= 30 % Accuracy
zzz.....
Overnight EEG
Recording
Learning cycle
Test cycle
Morning Test Session
B
Proportion reached Criteron
Learning Cycles (n)
C
Morning Hits (n)
Sib
22q
D
Hits Difference
evening
morning
E
TST (Min)
SE (%)
N1 Lat (Min)
REM Lat (Min)
Awakenings (n)
N1 (%)
N2 (%)
N3 (%)
REM (%)
Group
22q11.2DS
Sib

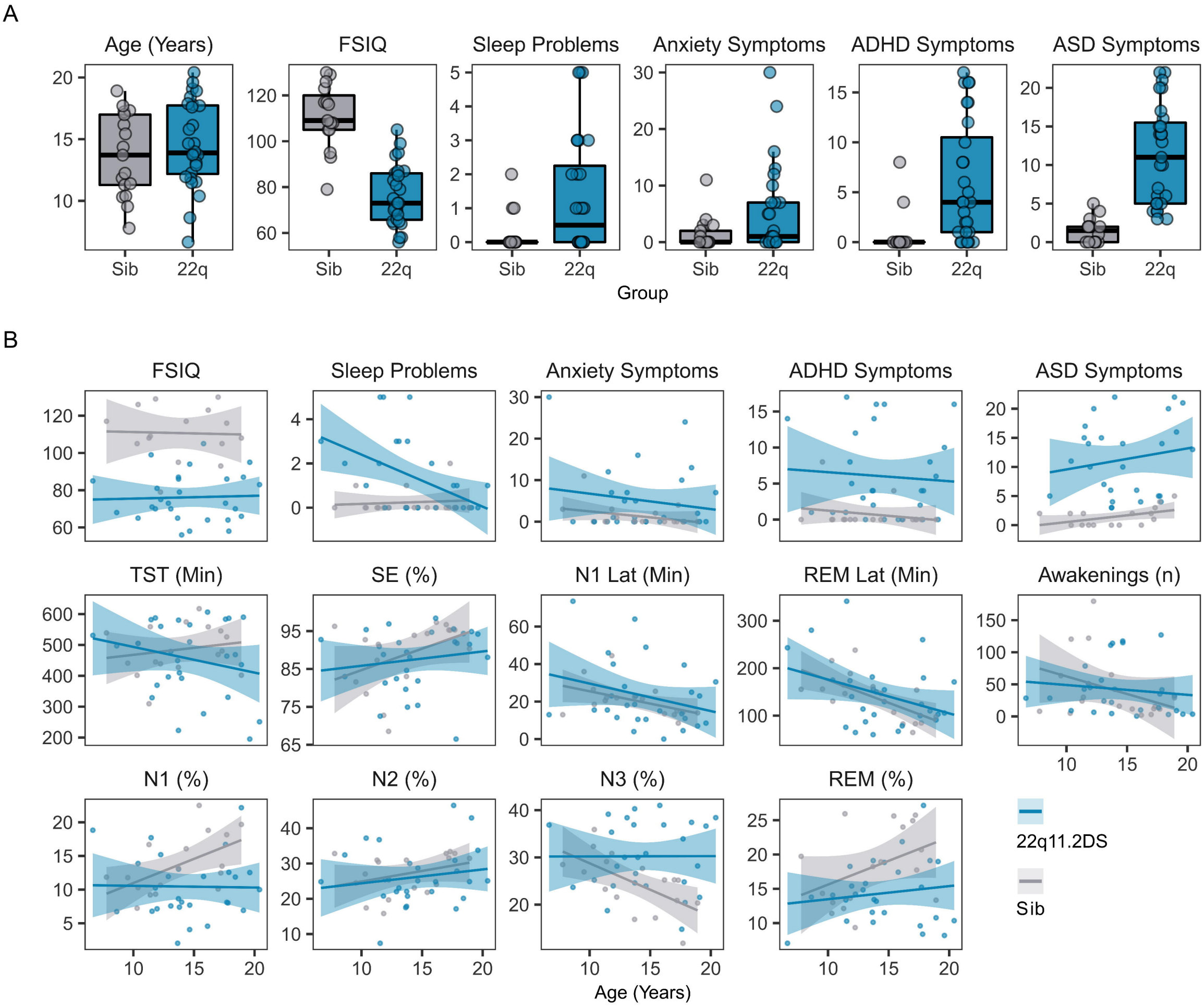
A
Age (Years)
FSIQ
Sleep Problems
Anxiety Symptoms
ADHD Symptoms
ASD Symptoms
Sib
22q
Group
B
FSIQ
Sleep Problems
Anxiety Symptoms
ADHD Symptoms
ASD Symptoms
TST (Min)
SE (%)
N1 Lat (Min)
REM Lat (Min)
Awakenings (n)
N1 (%)
N2 (%)
N3 (%)
REM (%)
Age (Years)
22q11.2DS
Sib

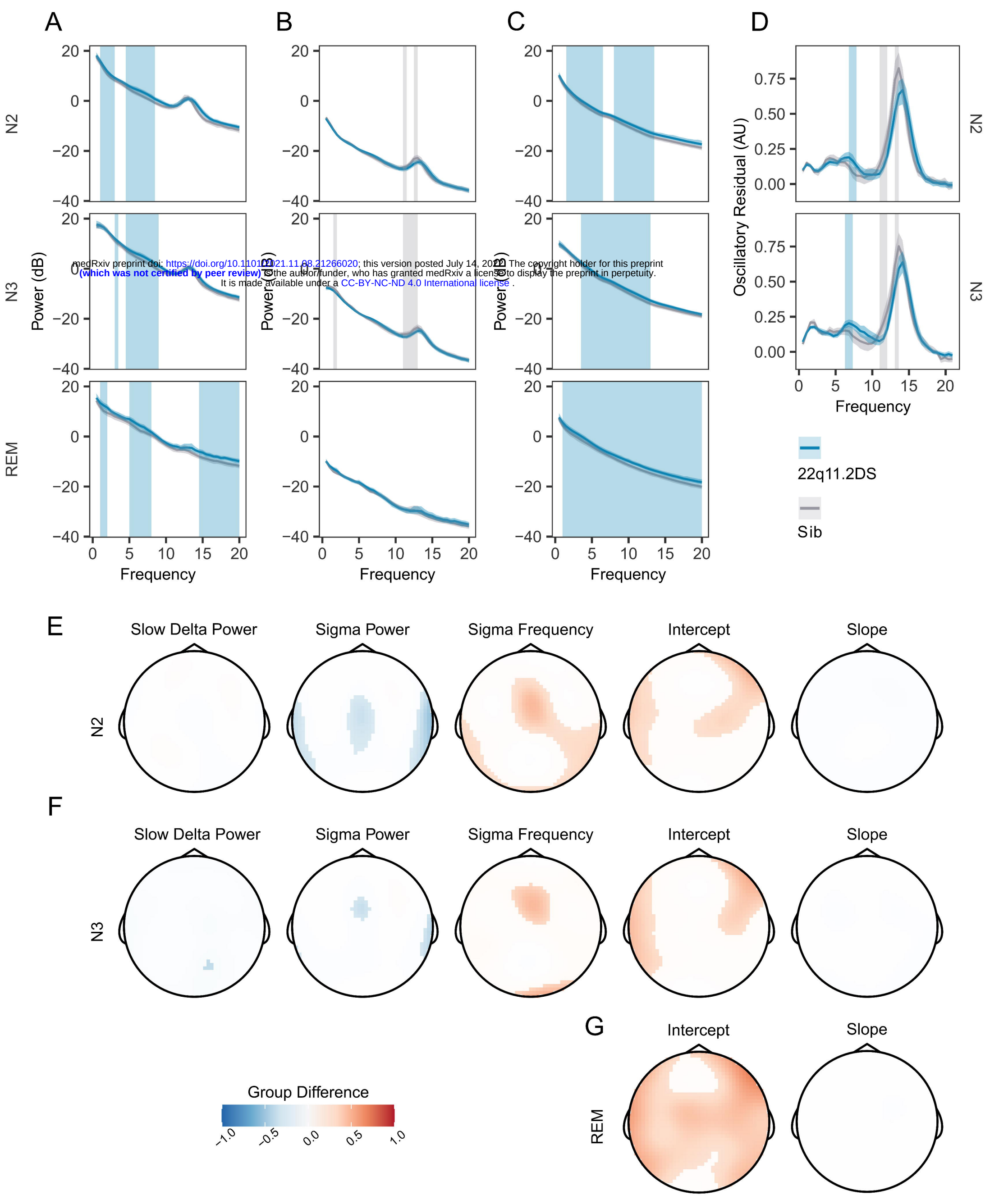

medRxiv preprint doi: https://doi.org/10.1101/2021.11.08.21266020; this version posted July 14, 2022 The copyright holder for this preprint (which was not certified by peer review) is the author/funder, who has granted medRxiv a license to display the preprint in perpetuity. It is made available under a CC-BY-NC-ND 4.0 International license .

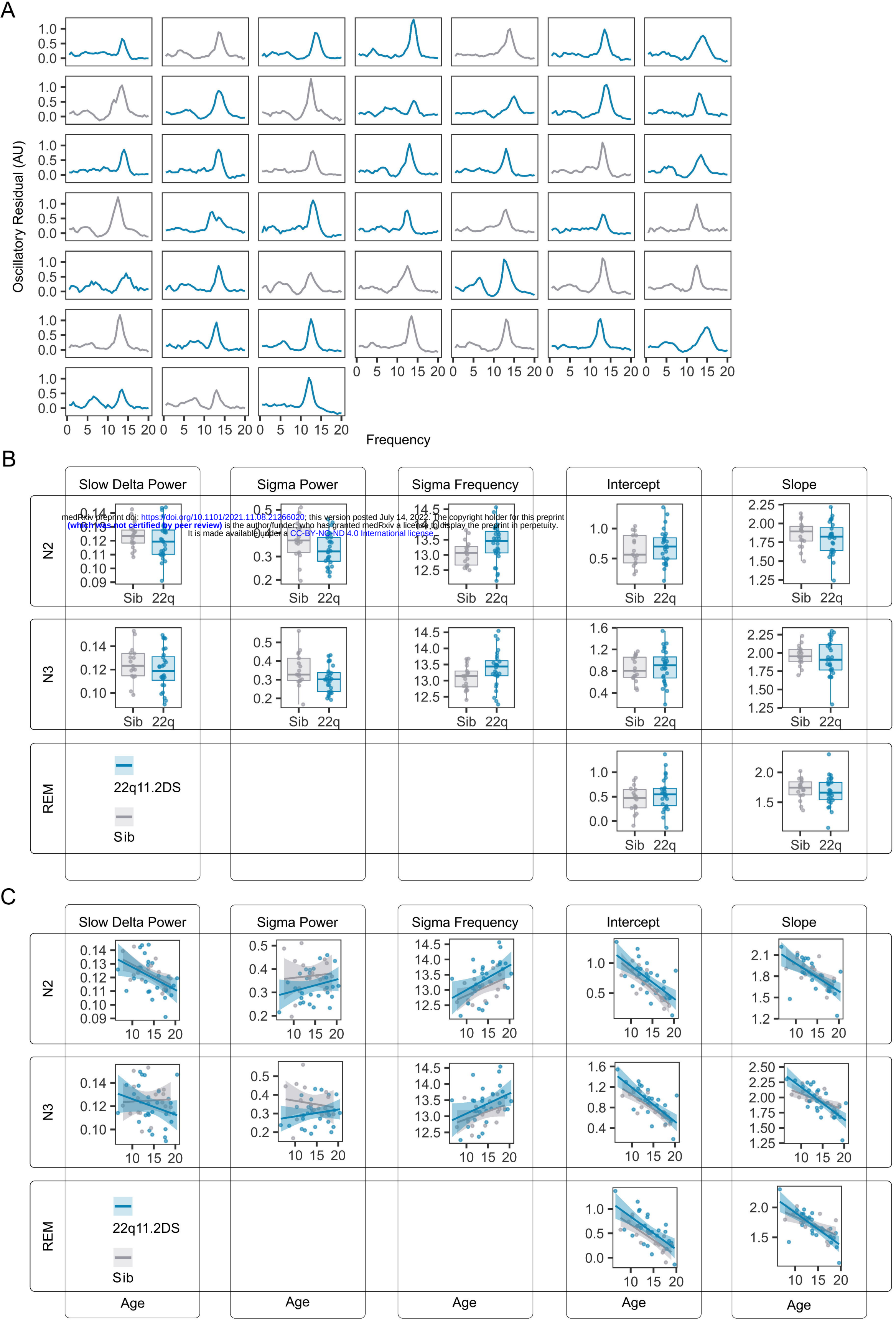

medRxiv preprint doi: https://doi.org/10.1101/2021.11.08.21266020; this version posted July 14, 2022. The copyright holder for this preprint (which was not certified by peer review) is the author/funder, who has granted medRxiv a license to display the preprint in perpetuity. It is made available under a CC-BY-NC-ND 4.0 International license.

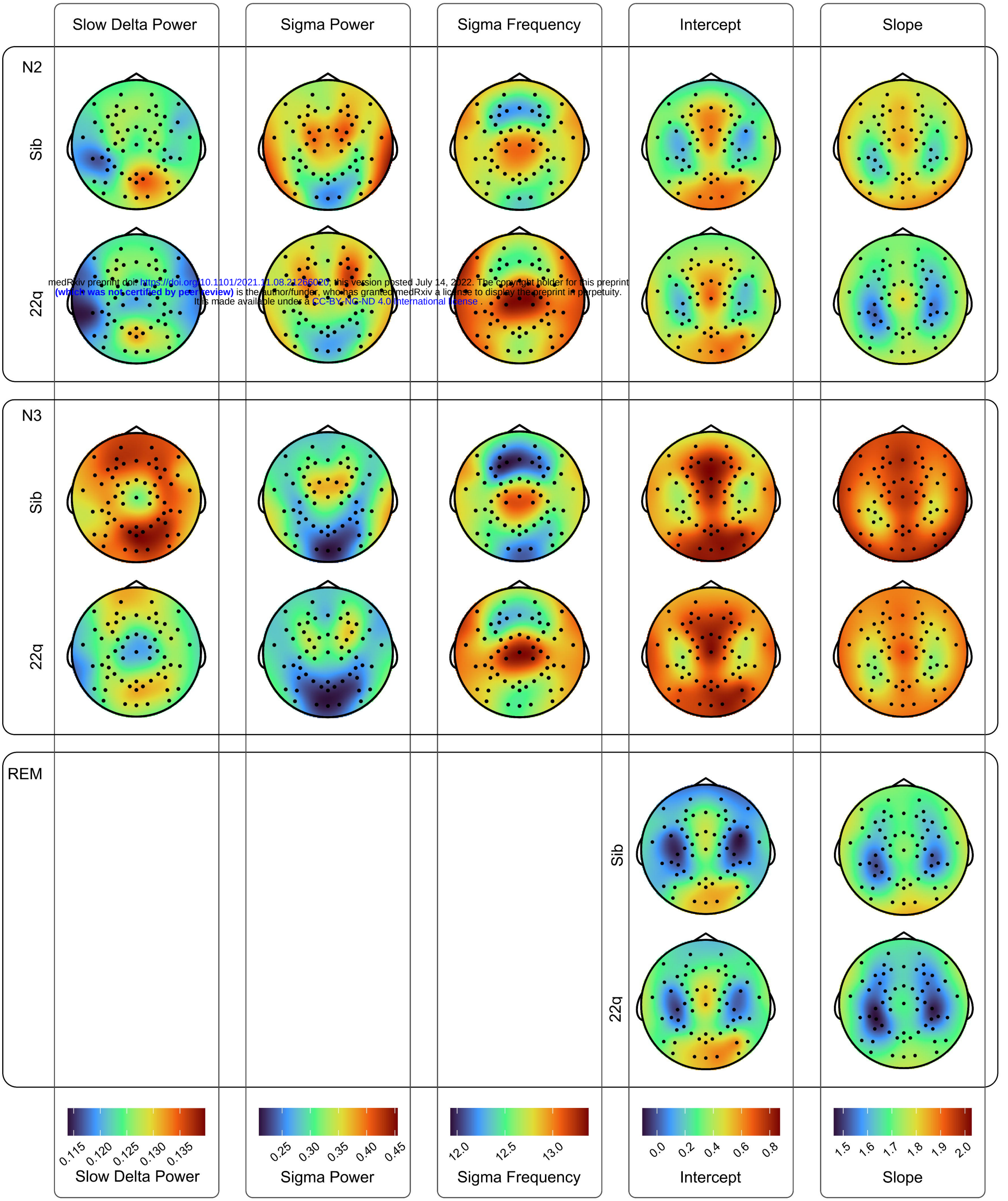

medRxiv preprint doi: https://doi.org/10.1101/2021.11.08.21266020; this version posted July 14, 2022. The copyright holder for this preprint (which was not certified by peer review) is the author/funder, who has granted medRxiv a license to display the preprint in perpetuity. It is made available under a CC-BY-NC-ND 4.0 International license .

medRxiv preprint doi: https://doi.org/10.1101/2021.11.08.21266020; this version posted July 14, 2022. The copyright holder for this preprint (which was not certified by peer review) is the author/funder, who has granted medRxiv a license to display the preprint in perpetuity. It is made available under a CC-BY-NC-ND 4.0 International license .

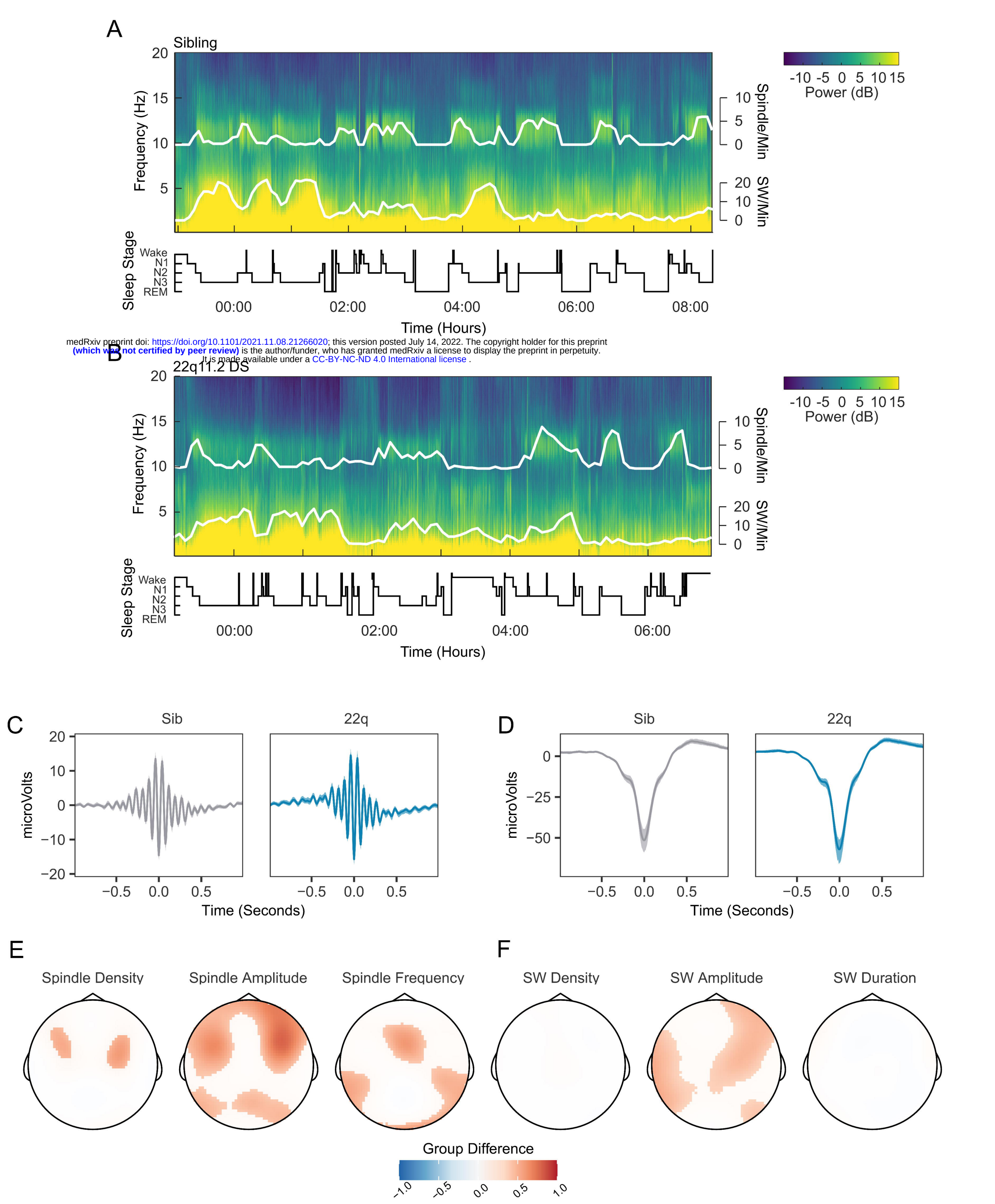

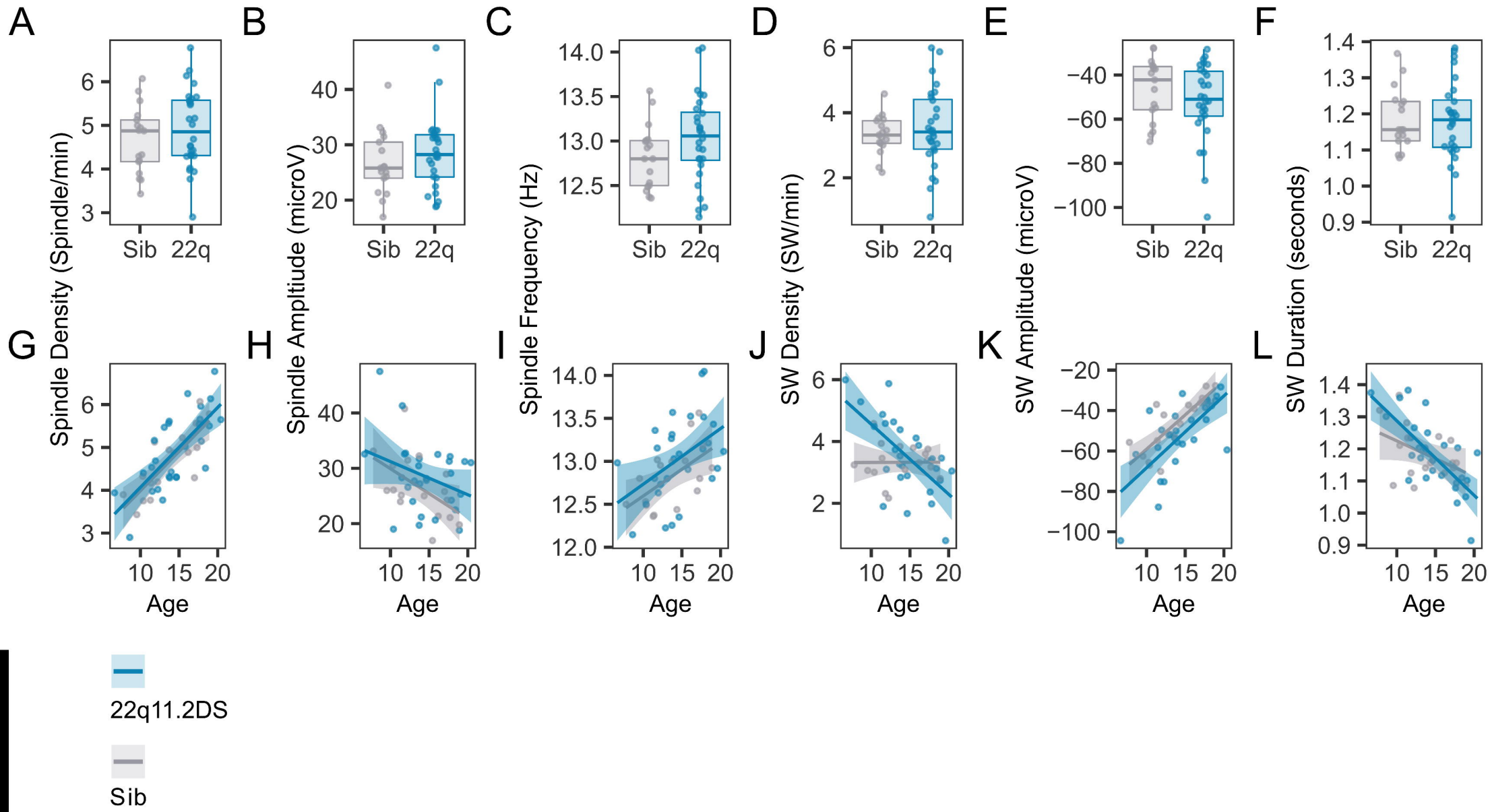
A
B
C
D
E
F
G
H
I
J
K
L
Spindle Density (Spindle/min)
Spindle Amplitude (microV)
Spindle Frequency (Hz)
SW Density (SW/min)
SW Amplitude (microV)
SW Duration (seconds)
Sib
22q
Age
22q11.2DS
Sib

medRxiv preprint doi: https://doi.org/10.1101/2021.11.08.21266020; this version posted July 14, 2022. The copyright holder for this preprint (which was not certified by peer review) is the author/funder, who has granted medRxiv a license to display the preprint in perpetuity. It is made available under a CC-BY-NC-ND 4.0 International license .

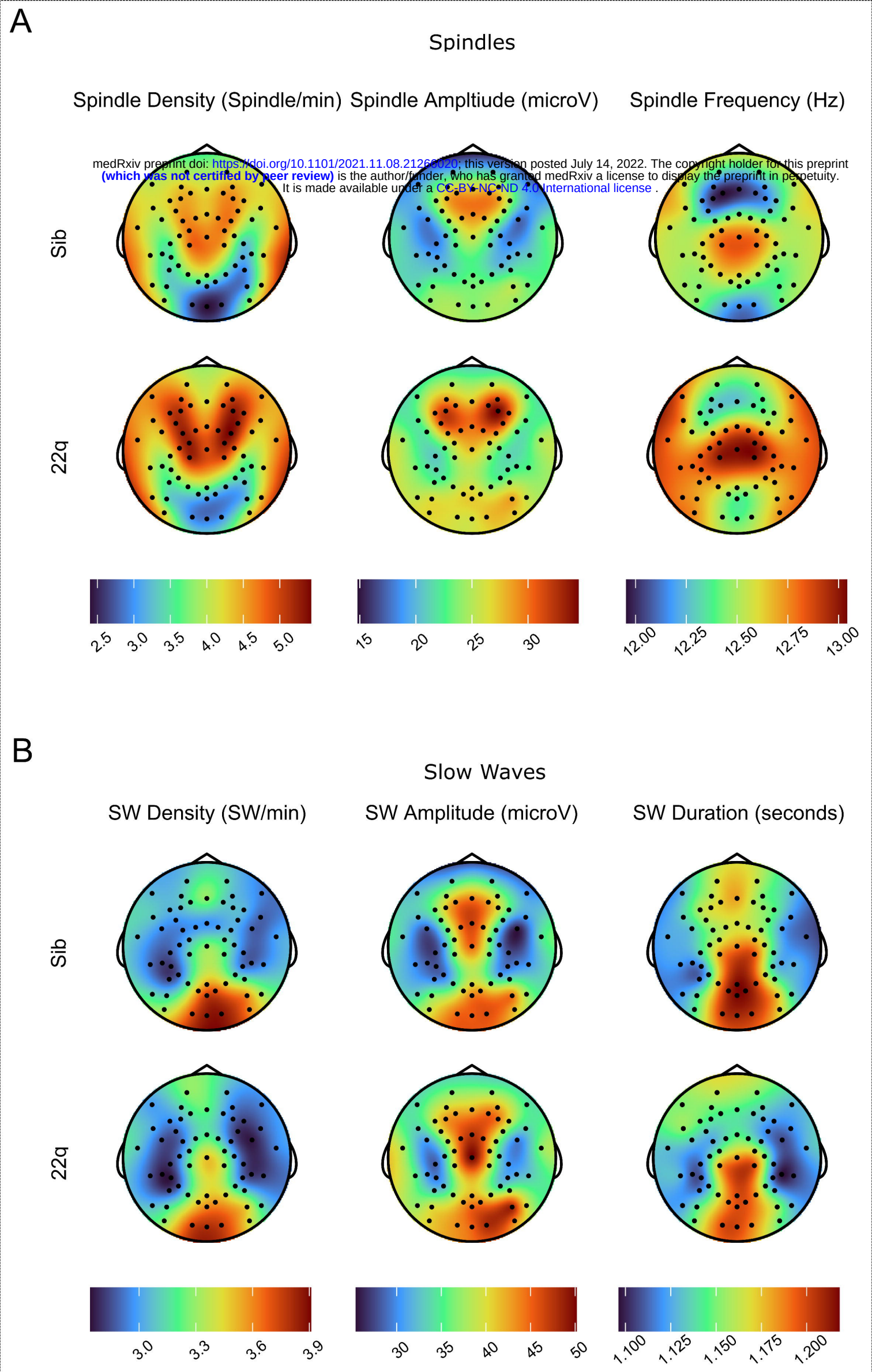

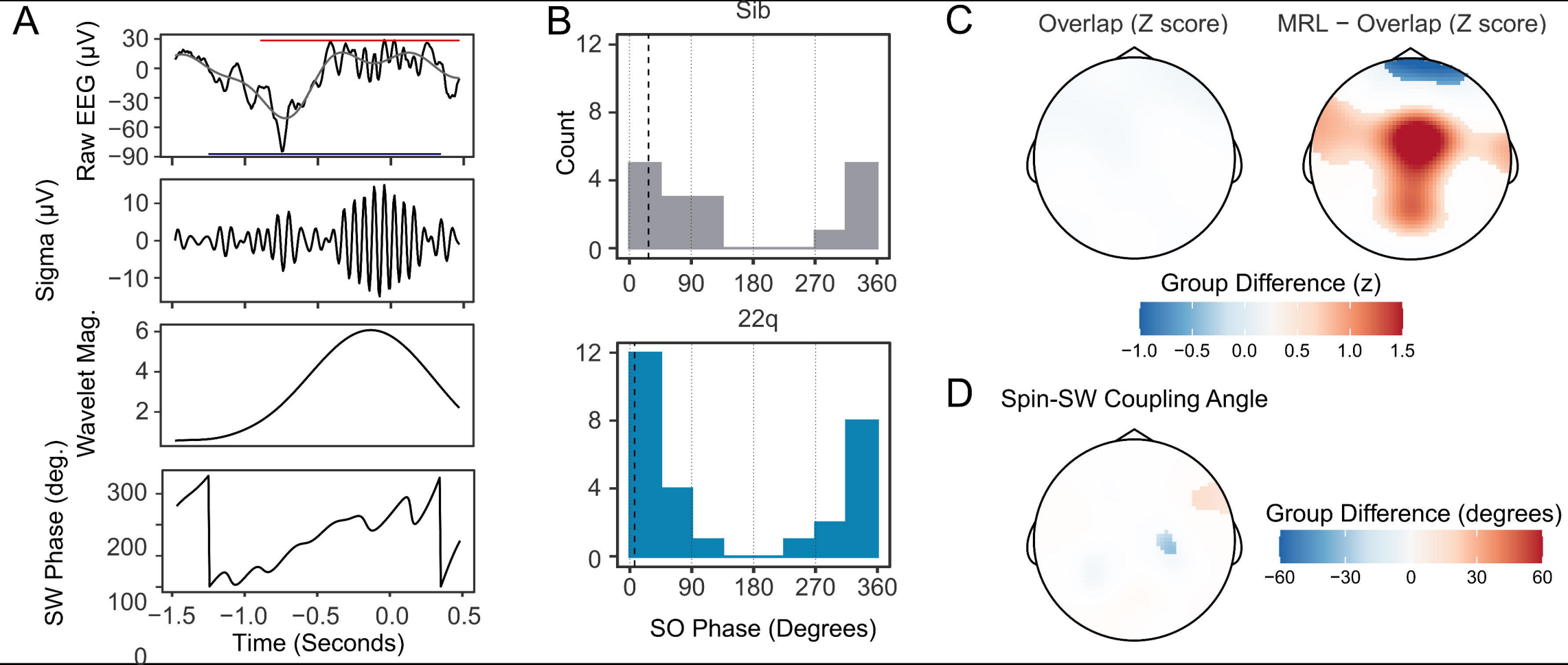
A
Raw EEG (µV)
30
0
−30
−60
−90
Sigma (µV)
10
0
−10
Wavelet Mag.
6
4
2
SW Phase (deg.)
300
200
100
0
−1.5
−1.0
−0.5
0.0
0.5
Time (Seconds)
B
Sib
Count
12
8
4
0
0
90
180
270
360
22q
12
8
4
0
0
90
180
270
360
SO Phase (Degrees)
C
Overlap (Z score)
MRL − Overlap (Z score)
Group Difference (z)
−1.0
−0.5
0.0
0.5
1.0
1.5
D
Spin-SW Coupling Angle
Group Difference (degrees)
−60
−30
0
30
60

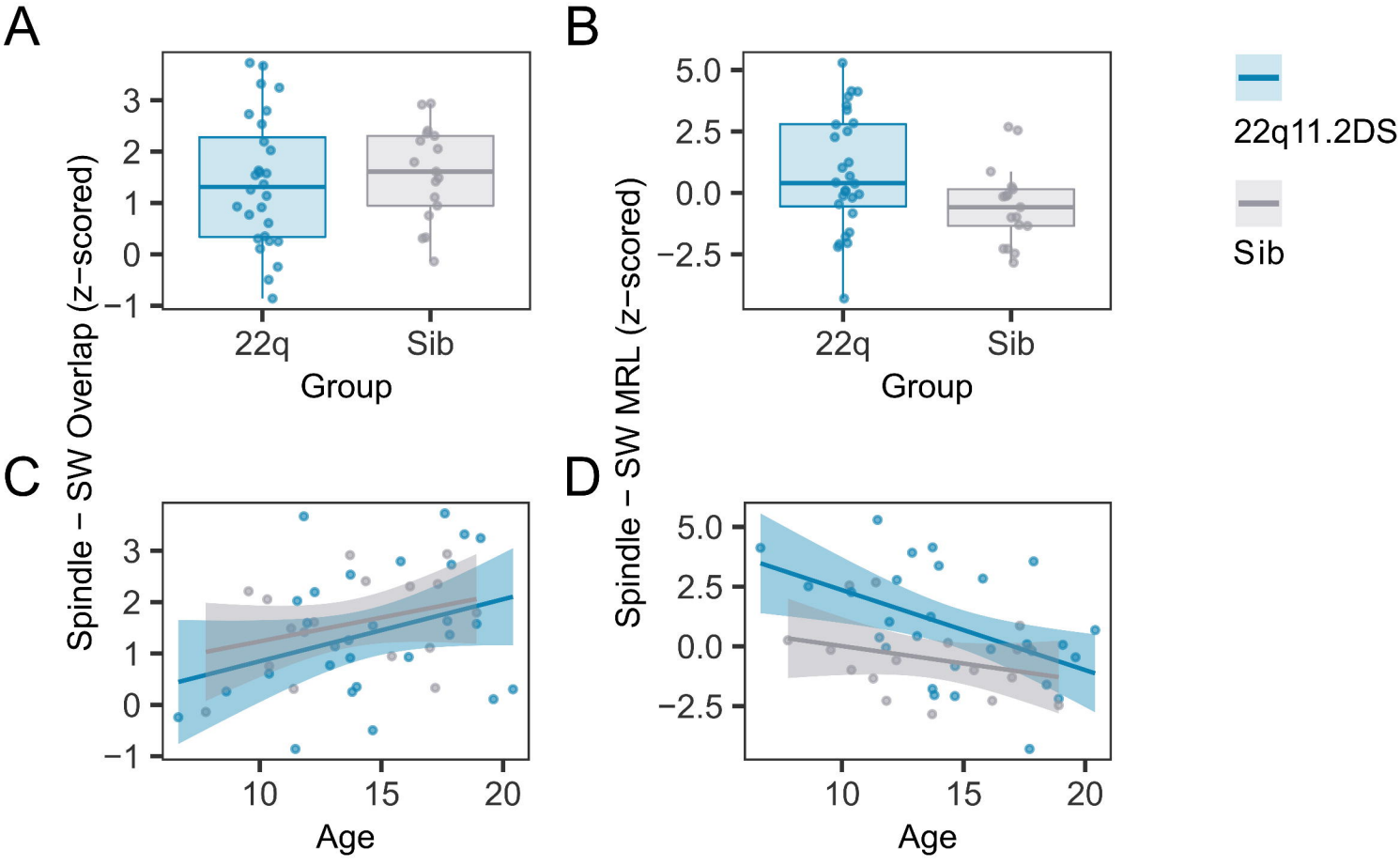
A
B
C
D
Spindle – SW Overlap (z−scored)
Spindle – SW MRL (z−scored)
3
2
1
0
−1
5.0
2.5
0.0
−2.5
22q
Sib
Group
10
15
20
Age
22q11.2DS
Sib

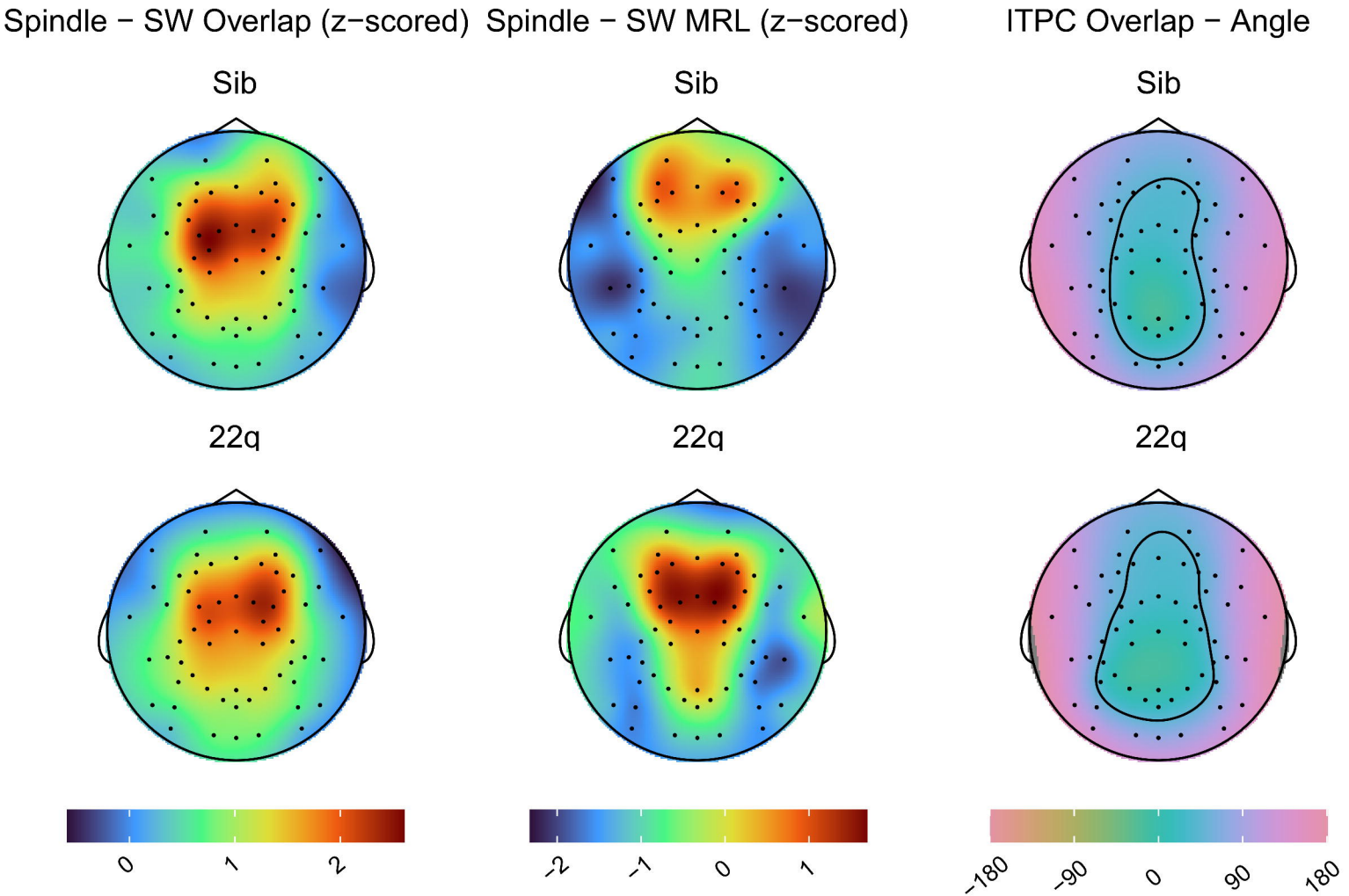
Spindle − SW Overlap (z−scored)
Spindle − SW MRL (z−scored)
ITPC Overlap − Angle
Sib
Sib
Sib
22q
22q
22q
0
1
2
−2
−1
0
1
−180
−90
0
90
180

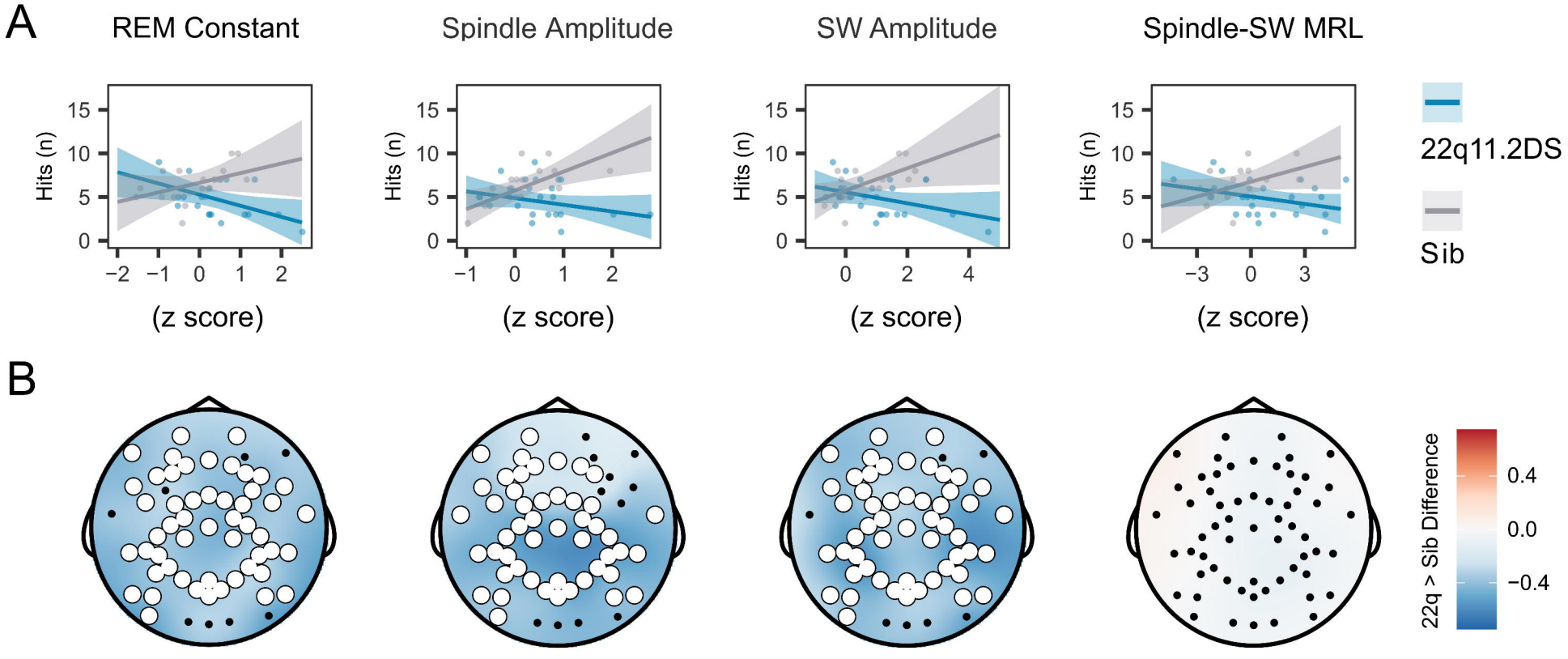
A
REM Constant
Spindle Amplitude
SW Amplitude
Spindle-SW MRL
Hits (n)
(z score)
22q11.2DS
Sib
B
22q > Sib Difference
0.4
0.0
−0.4

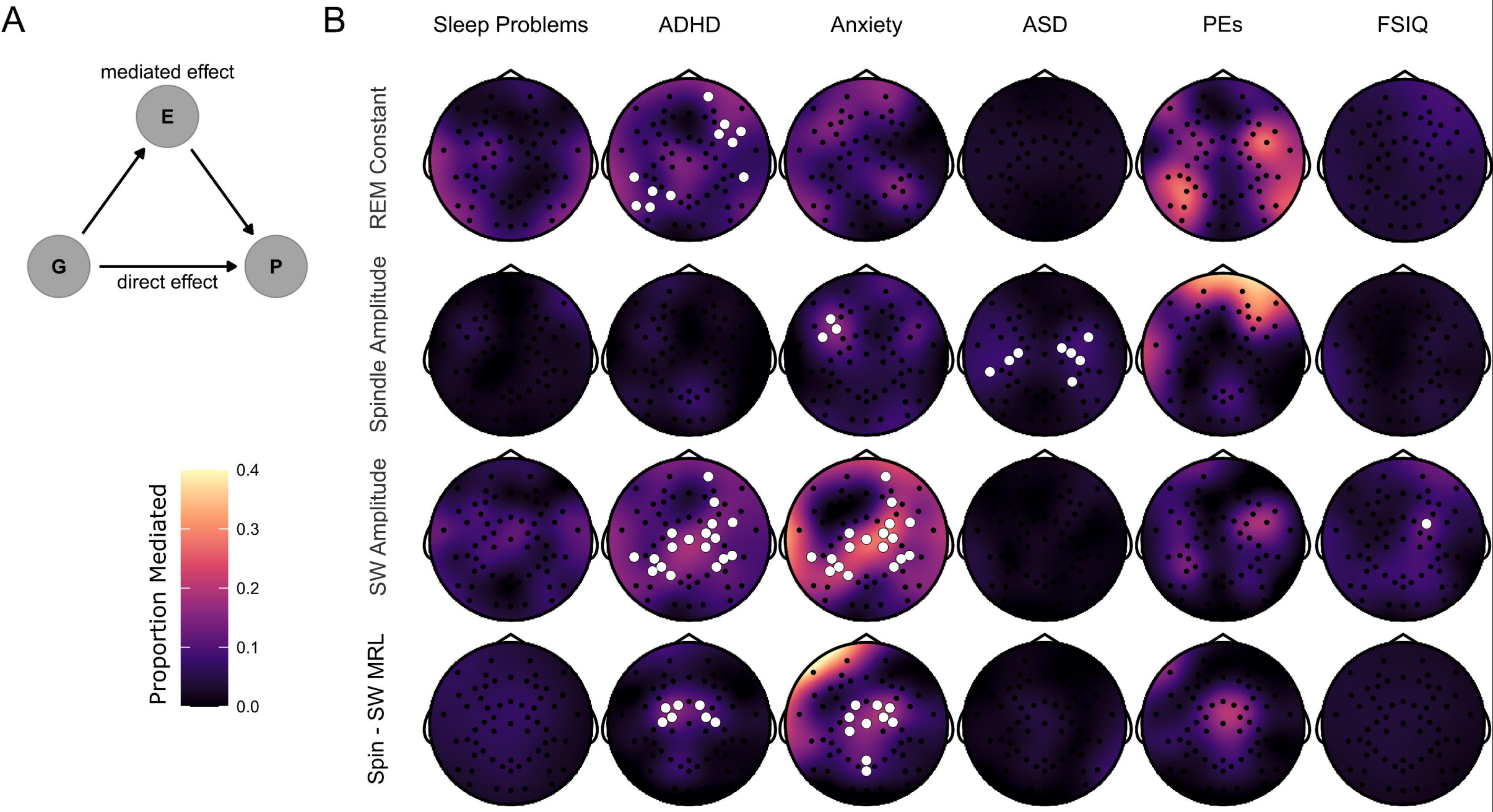
A
mediated effect
E
G
P
direct effect
B
Sleep Problems
ADHD
Anxiety
ASD
PEs
FSIQ
REM Constant
Spindle Amplitude
SW Amplitude
Spin - SW MRL
Proportion Mediated
0.4
0.3
0.2
0.1
0.0